

---

Report No. BDK75 977-32  
FINAL REPORT

Date: February 2012

Contract Title: Base Connections for Signal/Sign Structures  
UF Project No. 00087289  
Contract No. BDK75 977-32

---

**BASE CONNECTIONS FOR  
SIGNAL/SIGN STRUCTURES**

---

Principal Investigators: Ronald A. Cook, Ph.D., P.E.  
David O. Prevatt, Ph.D., P.E.

Graduate Research Assistant: Sadie A. Dalton, E.I.

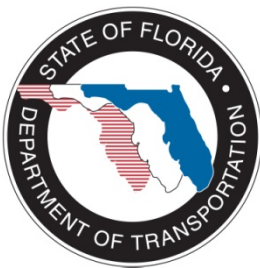
Project Manager: Andre Pavlov, P.E.

---

Department of Civil and Coastal Engineering  
College of Engineering  
University of Florida  
Gainesville, FL 32611

Engineering and Industrial Experiment Station

---



## DISCLAIMER

The opinions, findings, and conclusions expressed in this publication are those of the authors and not necessarily those of the State of Florida Department of Transportation.

## METRIC CONVERSION TABLE

SYMBOL	WHEN YOU KNOW	MULTIPLY BY	TO FIND	SYMBOL
<b>LENGTH</b>				
<b>in</b>	inches	25.4	millimeters	mm
<b>ft</b>	feet	0.305	meters	m
<b>yd</b>	yards	0.914	meters	m
<b>mi</b>	miles	1.61	kilometers	km

SYMBOL	WHEN YOU KNOW	MULTIPLY BY	TO FIND	SYMBOL
<b>AREA</b>				
<b>in<sup>2</sup></b>	square inches	645.2	square millimeters	mm <sup>2</sup>
<b>ft<sup>2</sup></b>	square feet	0.093	square meters	m <sup>2</sup>
<b>yd<sup>2</sup></b>	square yard	0.836	square meters	m <sup>2</sup>
<b>ac</b>	acres	0.405	hectares	ha
<b>mi<sup>2</sup></b>	square miles	2.59	square kilometers	km <sup>2</sup>

SYMBOL	WHEN YOU KNOW	MULTIPLY BY	TO FIND	SYMBOL
<b>VOLUME</b>				
<b>fl oz</b>	fluid ounces	29.57	milliliters	mL
<b>gal</b>	gallons	3.785	liters	L
<b>ft<sup>3</sup></b>	cubic feet	0.028	cubic meters	m <sup>3</sup>
<b>yd<sup>3</sup></b>	cubic yards	0.765	cubic meters	m <sup>3</sup>

NOTE: volumes greater than 1000 L shall be shown in m<sup>3</sup>

SYMBOL	WHEN YOU KNOW	MULTIPLY BY	TO FIND	SYMBOL
<b>MASS</b>				
<b>oz</b>	ounces	28.35	grams	g
<b>lb</b>	pounds	0.454	kilograms	kg
<b>T</b>	short tons (2000 lb)	0.907	megagrams (or "metric ton")	Mg (or "t")

SYMBOL	WHEN YOU KNOW	MULTIPLY BY	TO FIND	SYMBOL
<b>TEMPERATURE (exact degrees)</b>				
<b>°F</b>	Fahrenheit	5 (F-32)/9 or (F-32)/1.8	Celsius	°C

SYMBOL	WHEN YOU KNOW	MULTIPLY BY	TO FIND	SYMBOL
<b>ILLUMINATION</b>				
fc	foot-candles	10.76	lux	lx
fl	foot-Lamberts	3.426	candela/m <sup>2</sup>	cd/m <sup>2</sup>

SYMBOL	WHEN YOU KNOW	MULTIPLY BY	TO FIND	SYMBOL
<b>FORCE and PRESSURE or STRESS</b>				
<b>lbf</b>	pound force	4.45	newtons	N
<b>lbf/in<sup>2</sup></b>	pound force per square inch	6.89	kilopascals	kPa
<b>kip</b>	1000 pounds force	4.45	kilonewtons	kN
<b>kip-ft</b>	1000 pounds force - feet	1.36	kilonewton-meter	kN-m
<b>kip/in<sup>2</sup></b>	1000 pounds force per square inch	6.89	megapascals	MPa

TECHNICAL REPORT DOCUMENTATION PAGE

1. Report No.	2. Government Accession No.	3. Recipient's Catalog No.	
4. Title and Subtitle  Base Connections for Signal/Sign Structures		5. Report Date February 2012	
		6. Performing Organization Code	
7. Author(s) R. A. Cook, D. O. Prevatt, and S. A. Dalton		8. Performing Organization Report No. 00087289	
9. Performing Organization Name and Address University of Florida Department of Civil and Coastal Engineering 365 Weil Hall / P.O. Box 116580 Gainesville, FL 32611-6580		10. Work Unit No. (TRAIS)	
		11. Contract or Grant No. BDK75 977-32	
12. Sponsoring Agency Name and Address Florida Department of Transportation Research Management Center 605 Suwannee Street, MS 30 Tallahassee, FL 32301-8064		13. Type of Report and Period Covered Final Report April 2010 – February 2012	
		14. Sponsoring Agency Code	
15. Supplementary Notes			
16. Abstract <p>The Atlantic hurricane season of 2004 brought with it a series of four major hurricanes that made landfall across Florida within a six-week period. During this time, a number of cantilever sign structures along the state interstate system failed. As a result, the Florida Department of Transportation (FDOT) began a series of research initiatives to address this issue. The first research project determined the cause of the failures, the proper design procedure, and a retrofit option. A second suggested a load transfer system to eliminate anchor bolts from the foundation design. The current project suggests a way to also eliminate annular plates from the design of the base connection. The alternative chosen for testing after a literature review was the tapered bolted slip base design. This alternative consists of two main components: a slip joint and through-bolts. The slip joint is designed to transfer flexural loads while the through-bolts are responsible for transferring torsional loads from the upper pole to the lower pole. The selection of this alternative as a replacement for the anchor bolt and annular plate option has the potential to improve the AASHTO fatigue rating from an E or E' up to a B.</p> <p>The results of the test program give a detailed representation of the behavior of the base connection components. The data and observations during and after testing reveal how the load is transferred along the length of the slip joint and across the through-bolts. The tapered bolted slip base connection has been proven adequate for transferring both flexural and torsional loads as applied to a cantilever signal or sign structure. It is recommended that a number of field specimens be constructed and monitored to better determine the necessary design procedures and confirm the behavior of the base connection as predicted by the results of this test program.</p>			
17. Key Word  cantilever sign structures, slip joint, slip splice, telescoping splice, through-bolt, wind loads, base connection, annular plate, anchor bolt, anchors		18. Distribution Statement No restrictions	
19. Security Classif. (of this report) Unclassified	20. Security Classif. (of this page) Unclassified	21. No. of Pages 181	22. Price

## ACKNOWLEDGMENTS

The authors would like to acknowledge and thank the Florida Department of Transportation (FDOT) for funding this research initiative. This project represents a collaborative effort between the Department of Civil and Coastal Engineering at the University of Florida and the FDOT Research Management Center in Tallahassee, Florida. The personnel at the FDOT Marcus H. Ansley Structures Research Center provided tremendous support throughout the various stages of this research project: constructing the test apparatus, mounting all of the instrumentation, conducting tests, and collecting data. Their resourcefulness and dedication have helped make this research project a success.

## EXECUTIVE SUMMARY

The Atlantic hurricane season of 2004 brought with it a series of four major hurricanes that made landfall across Florida within a six-week period. During this time, a number of cantilever sign structures along the state's interstate system failed. As a result, the Florida Department of Transportation (FDOT) began a series of research initiatives focused on determining the cause of these failures as well as a variety of ways to improve the design of the base connection and the transfer of load from the superstructure to the foundation. The primary cause of the failures was identified as a concrete breakout in the foundation due to the large torsional loads being transferred to the concrete as a shear force on the anchors parallel to the edge of the foundation. The relevant design procedure for a shear force on anchors parallel to the edge of the concrete was identified in ACI 318 Appendix D. In addition, a retrofit option using carbon fiber reinforced polymer (CFRP) wrap around the concrete pedestal was developed to prevent failures of existing structures. Once the problem with the existing design was identified, a new and more effective load transfer system for the foundation was developed using an embedded pipe and plate assembly rather than anchor bolts. Having a more effective load transfer system within the concrete, the development of an alternative base connection above the foundation eliminating the annular base plate was the subject of this study.

The primary objectives of this research initiative were as follows:

- Design an alternate base connection for use with the embedded pipe and plate assembly from FDOT report BDK75 977-04.
- Eliminate annular plates from the base connection design.
- Improve the American Association of State Highway and Transportation Officials (AASHTO) fatigue rating of the base connection.

In order to fulfill these objectives, a number of alternatives to the anchor bolt and annular plate base connection system, some of which are identified in FDOT report BDK75 977-04, were

examined. A literature review to investigate the advantages and disadvantages of each base connection alternative was conducted. From the results of the literature review, a testing program was developed by considering the applicable design codes for each component.

The alternative chosen for testing was the tapered bolted slip base design. This alternative consists of two main components: a slip joint and through-bolts. Each component transfers a portion of the applied load from the mast arm and superstructure to the foundation. The slip joint transfers flexural loads while the through-bolts transfer torsional loads from the superstructure monopole to the pole embedded in the concrete as part of the new load transfer system. The AASHTO guidelines for slip joint connections can be used as a starting point for design, but detailed checks for localized buckling should be performed to make certain the slip joint length is adequate for the wall thickness of the section. The selection of this alternative as a replacement for the anchor bolt and annular plate option has the potential to improve the AASHTO fatigue rating from an E or E' up to a B, which allows the connection to be designed for a larger magnitude fatigue limit.

The test program was designed to determine if the tapered bolted slip base connection can be designed using existing code guidelines or if a new design procedure is required. The results of the test program provided a detailed representation of the behavior of the base connection components. The data and observations during and after testing gave some indication as to how the load is being transferred along the length of the slip joint and across the through-bolts. Based on this information, it was determined that the through-bolt design can be conservatively predicted using the existing AASHTO guidelines.

# TABLE OF CONTENTS

	<u>page</u>
DISCLAIMER .....	ii
METRIC CONVERSION TABLE.....	iii
TECHNICAL REPORT DOCUMENTATION PAGE .....	iv
ACKNOWLEDGMENTS .....	v
EXECUTIVE SUMMARY .....	vi
LIST OF FIGURES .....	xi
LIST OF TABLES.....	xv
CHAPTER	
1 INTRODUCTION .....	1
2 LITERATURE REVIEW .....	5
2.1 Summary of Previous Reports.....	5
2.2 Summary of Existing Base Connections .....	7
2.3 Alternate Base Connections.....	8
2.3.1 Bolted Plate Connection .....	9
2.3.2 Tapered Bolted Slip Base Connection.....	11
2.3.3 Grouted Slip Base Connection .....	14
2.3.4 Welded Sleeve Connection.....	17
2.3.5 Inverted Grouted Slip Base Connection .....	19
2.3.6 Prestressed Concrete Pole with Tapered Steel Monopole .....	21
2.4 Fatigue and Corrosion of Components .....	25
2.4.1 Bolt Fatigue .....	26
2.4.2 Weld Fatigue .....	28
2.4.3 Corrosion of Steel Elements.....	30
2.5 Selection of Base Connection.....	31
3 DEVELOPMENT OF TEST PROGRAM .....	36
3.1 Design Code Considerations.....	36
3.1.1 Slip Joint Splice Length.....	36
3.1.2 Bolted Connections .....	43
3.1.2.1 Nominal shear resistance.....	46
3.1.2.2 Bearing at bolt holes.....	47
3.1.2.3 Special consideration for through-bolting HSS members.....	48
3.1.3 Steel Pole Strength .....	49



3.1.3.1	Bending moment resistance .....	50
3.1.3.2	Shear resistance .....	51
3.1.3.3	Torsional resistance .....	53
3.1.3.4	Interaction of bending moment, axial load, shear, and torsion .....	53
3.2	Experimental Design .....	55
3.3	Equipment and Materials .....	57
3.3.1	Reinforced Concrete Block and Tie-downs .....	57
3.3.2	Reinforced Concrete Pedestal .....	59
3.3.3	Tapered Steel Poles .....	60
3.3.4	Threaded Rods .....	63
3.3.5	Lever Arm Assembly .....	65
3.3.6	Summary of Test Apparatus .....	66
4	IMPLEMENTATION OF TEST PROGRAM .....	68
4.1	Measured Material Properties .....	68
4.1.1	Concrete Foundation and Pedestal .....	68
4.1.2	Tapered Steel Poles .....	70
4.1.3	Threaded Rods .....	72
4.1.4	Summary of Test Apparatus .....	73
4.2	Instrumentation .....	75
4.2.1	Strain Gauges for Torsion .....	75
4.2.2	Strain Gauges for Bending .....	77
4.2.3	Displacement Gauges .....	79
4.2.4	Load Cell and Actuator .....	80
4.3	Testing Procedure .....	81
4.3.1	Prediction of Through-bolt Failure .....	81
4.3.2	Observation of Slip Joint Behavior .....	82
5	FINDINGS .....	84
5.1	Test Outcome .....	84
5.1.1	Predicted vs. Actual Failure .....	84
5.1.2	Failure Mode .....	85
5.1.3	Effects of Friction .....	86
5.2	Summary of Data .....	91
5.2.1	Flexural Strain Data .....	92
5.2.2	Torsional Strain Data .....	96
5.2.3	Deflection Data .....	103
5.2.4	Rotational Data .....	108
6	DISCUSSION .....	113
6.1	Constructability Concerns .....	113
6.1.1	Placement and Alignment of the Embedded Pole .....	113
6.1.2	Placement of the Upper Pole Section .....	115
6.1.3	Placement of Through-bolts in the Slip Joint .....	117

6.2	Maintenance Concerns.....	118
6.2.1	Fatigue Inspections.....	119
6.2.2	Corrosion Inspections.....	120
6.2.3	Repair of Base Connection.....	123
6.3	Design Guidelines.....	126
6.3.1	Slip Joint Splice Length Design.....	126
6.3.2	Through-bolt Design.....	127
7	CONCLUSIONS.....	129
	REFERENCES.....	133
<b>APPENDIX</b>		
A	DESIGN OF TAPERED BOLTED SLIP BASE CONNECTION.....	136
A.1	Capacity of Steel Pole Section.....	136
A.1.1	Analysis of the Flexural Capacity of the Pole Section.....	137
A.1.2	Analysis of the Torsional Capacity of the Pole Section.....	139
A.1.3	Analysis of the Interaction of Torsion and Flexure for the Pole Section.....	140
A.2	Capacity of Through-bolted Connection.....	143
A.2.1	Analysis of Shear Strength.....	143
A.2.2	Analysis of Bearing Strength.....	144
B	CONSTRUCTION DRAWINGS.....	147
C	INSTRUMENTATION.....	156
D	ACCOUNTING FOR FRICTION IN THE SLIP JOINT.....	162
D.1	Evaluation for Flexure.....	163
D.1.1	Flexural Analysis Assuming Concentrated Point Loads on Slip Joint.....	163
D.1.2	Flexural Analysis Assuming Distributed Loads along Slip Joint.....	164
D.2	Evaluation for Torsion.....	164
D.2.1	Predicted Shear Resistance of Through-bolts.....	165
D.2.2	Predicted Applied Load.....	165

## LIST OF FIGURES

<u>Figure</u>	<u>page</u>
1-1 Failed cantilever sign structure.....	1
1-2 Failed concrete foundation of cantilever sign structure.....	2
1-3 Typical cantilever sign structure.....	3
2-1 Transfer of wind load through cantilever structure to the foundation.....	6
2-2 Experimental result using ACI concrete breakout strength for anchors in shear.....	6
2-3 Embedded steel pipe and plate configuration in concrete foundation.....	7
2-4 Base plate connection shown with stiffeners.....	10
2-5 Tapered bolted slip base connection.....	12
2-6 Slip joint splice typical in monopole extensions.....	12
2-7 Grouted slip base connection.....	15
2-8 Welded sleeve connection.....	17
2-9 Inverted grouted slip base connection.....	20
2-10 Direct burial spun cast prestressed concrete base and steel superstructure.....	22
2-11 Spun cast prestressed concrete and steel connection shown with through-bolts.....	23
3-1 AASHTO slip joint splice.....	37
3-2 Concentrated loads on HSS.....	41
3-3 Confinement of the inner pole within a slip joint under concentrated load.....	43
3-4 Shearing reactions on through-bolts due to torsion in the poles.....	46
3-5 Reactions in HSS section at through-bolt due to an externally applied torsion.....	49
3-6 Forces induced on steel poles by the transfer of moment through a slip splice.....	50
3-7 Interaction of forces at the slip joint base connection.....	54
3-8 Reinforcement cage for the concrete block.....	58
3-9 Tie-down assemblies connecting the base of the test apparatus to the lab floor.....	58

3-10	Tapered steel poles manufactured by Valmont Structures .....	62
3-11	Lever arm assembly for test apparatus.....	66
4-1	Honeycomb around pedestal and repair of pedestal .....	69
4-2	Small burrs on the surface of pole (left) and fitted slip joint (right).....	72
4-3	Examples of unacceptable and acceptable threaded rod test specimens.....	73
4-4	Wiring schematic for torsional rosette strain gauge arrangement .....	76
4-5	Arrangement of rosette strain gauges along the length of the slip joint .....	76
4-6	Wiring for flexural strain gauge arrangement.....	77
4-7	Extreme bending behavior of loosely-fitted and tight slip joints.....	78
4-8	Arrangement of linear strain gauges for bending .....	79
4-9	LVDT arrangement at each of the four indicated locations along test apparatus.....	80
4-10	Load cell and actuator used for applying load to test apparatus .....	81
5-1	Pipe buckling near the access panel on the embedded pole.....	85
5-2	Bolt shear and kink in through-bolt .....	86
5-3	Contact of poles within slip joint region.....	87
5-4	Concentrated internal couple transferring applied load through slip joint .....	88
5-5	Distributed internal couple transferring applied load through slip joint.....	88
5-6	Frictional and bolt shear resistance to torsion.....	89
5-7	Plot of the impact of friction on predicted applied load .....	90
5-8	Plot of the applied load versus stroke after unloading times removed .....	91
5-9	Flexural strain gauges on compression face of outer pole along the slip joint .....	92
5-10	Flexural strain measured along the length of the slip joint.....	93
5-11	Oblong deformation at the base of the outer pole during loading .....	94
5-12	Scratches on the tension face of the inner pole.....	95
5-13	Plastic deformation on the tension face of the inner pole in slip joint region. ....	95

5-14	Rosette strain gauges located between bolt holes .....	97
5-15	Plot of shear strain measured along slip joint for select load cases .....	98
5-16	Plot of shear strain measured along slip joint for select load cases (limited view) .....	99
5-17	Rear view of the separation of pole surfaces during testing .....	100
5-18	Principal bend in each through-bolt.....	101
5-19	Cross-sections of slip joint during loading from a rear view of test apparatus.....	102
5-20	Section view of LVDT placement .....	104
5-21	Vertical displacements along the left edge of the test poles .....	104
5-22	Vertical displacements along the right edge of the test poles.....	105
5-23	Vertical displacements along the bottom edge of the test poles .....	106
5-24	Unaltered deflection data along the length of the test poles .....	106
5-25	Deflection along the length of test poles adjusted for pedestal displacements.....	107
5-26	Geometry of vertical displacements used to calculate section rotation .....	109
5-27	Plot of applied torsion versus the calculated rotation of the poles .....	110
5-28	Change in rotation between outer and inner poles across slip joint.....	110
5-29	Comparison of rotation in test poles with theoretical pole .....	111
5-30	Measured rotation along length of poles with the predicted angle of twist.....	111
6-1	Alignment rebar within pedestal and external bracing of embedded pole.....	114
6-2	Alternate embedment design.....	115
6-3	Placement of the upper pole for the test apparatus using an overhead lift. ....	116
6-4	A short I-beam for supporting the drilling equipment for placement of bolt holes.....	118
6-5	Longitudinal seam weld placed to the right of through-bolt holes .....	120
6-6	Rust on the surface of a pole and within the bolt holes. ....	122
A-1	Steel pole interaction curves for torsion and flexure .....	142
B-1	Top view of test apparatus .....	148

B-2	Side view of test apparatus .....	149
B-3	Front view of test apparatus .....	150
B-4	Section view through the concrete pedestal.....	151
B-5	Detail of the embedded pole with torsional and flexural plates.....	152
B-6	Detail of the outer pole member .....	153
B-7	Detail of the flange plate at the end of the tapered pole .....	154
B-8	Detail of the tie-down assembly .....	155
C-1	Diagram of rosette strain gauges on the right face of the slip joint .....	157
C-2	Diagram of rosette strain gauges on the left face of the slip joint .....	158
C-3	Diagram of linear strain gauges on the upper face of the slip joint .....	159
C-4	Diagram of linear strain gauges on the bottom face of the slip joint.....	160
C-5	Diagram of LVDT placement and orientation along test apparatus .....	161
D-1	Side view of test apparatus with select dimensions .....	162
D-2	Front view of test apparatus with slip joint section and dimensions .....	162
D-3	Concentrated internal couple transferring applied load through slip joint .....	163
D-4	Distributed internal couple transferring applied load through slip joint.....	164
D-5	Frictional and bolt shear resistance to torsion.....	165
D-6	Plot of the impact of friction on predicted applied load .....	166

LIST OF TABLES

<u>Table</u>		<u>page</u>
2-1	Summary of advantages and disadvantages for each design alternative .....	34
3-1	Typical HSS diameter-to-thickness ratios for FDOT cantilever sign structures .....	39
3-2	Summary of testing materials and minimum material strengths .....	67
3-3	Predicted failure loads with minimum specified material strengths.....	67
4-1	Measured concrete compressive strengths.....	69
4-2	Measured strengths of steel coupons .....	70
4-3	Measured tensile force and strength of threaded rod specimens .....	73
4-4	Specified materials for test apparatus with measured strengths .....	74
4-5	Predicted test failure loads based on actual material strengths.....	74
5-1	Measure of the approximate angle (degrees) of the bend in each through-bolt.....	100

## CHAPTER 1 INTRODUCTION

During the Atlantic hurricane season of 2004, four major hurricanes made landfall across the state of Florida within a six-week time period. During this time, a number of overhead cantilever sign structures along the interstate system failed during extreme wind load conditions (Figure 1-1). As a result, the Florida Department of Transportation (FDOT) began a series of research projects to investigate why these failures occurred and ways to improve the design of these structures. Two research projects on the subject have preceded this one and have prompted this third project.



Figure 1-1. Failed cantilever sign structure. Photo courtesy of FDOT.

The primary research project examining the failures of these sign structures was completed in August 2007 as FDOT report BD545-54, *Anchor Embedment Requirements for Signal/Sign Structures*. The objectives of that project were to determine the cause of the foundation failures, identify the proper design procedures to account for this failure mode, and establish a viable retrofit option for existing foundations. The report discusses the effects of torsional loading on



the anchor bolt group in the concrete foundation and identifies it as the primary cause of the failures of a number of cantilever sign structures (Figure 1-2).



Figure 1-2. Failed concrete foundation of cantilever sign structure. Photo courtesy of FDOT.

The second research project regarding the failures of the cantilevered sign structures was completed in August 2010 as FDOT report BDK75 977-04, *Alternative Support Systems for Cantilever Signal/Sign Structures*. This secondary program was initiated to identify a more effective alternative foundation system than the anchor bolt group for transferring the torsional load from the sign column to the foundation as well as a method to design for this new alternative. Of the nine alternatives investigated, an embedded steel pipe and plate configuration was deemed the best choice for testing.

As a result of the findings of the second research project, the column-to-base connection must be evaluated to accommodate this new configuration with a steel pipe protruding from the foundation. Currently, an annular plate, anchor bolt, and leveling nut base connection system is used for the majority of cantilever sign structures (Figure 1-3) and high-mast luminaire poles. A similar bolted flange plate connection in addition to other alternative base connection systems

were recommended in the previous report, *Alternative Support Systems for Cantilever Signal/Sign Structures*, for use with the embedded pipe and plate assembly.

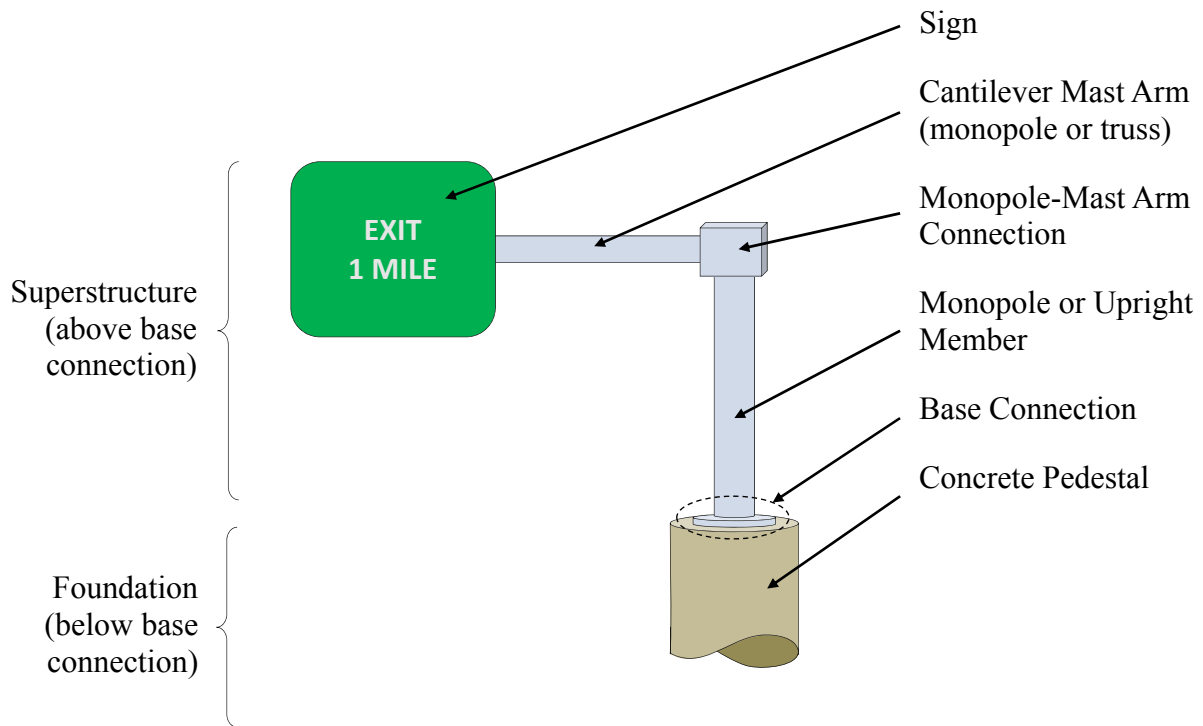


Figure 1-3. Typical cantilever sign structure

This research program begins by examining six design alternatives, four of which are suggested in the second report in this series, *Alternative Support Systems for Cantilever Signal/Sign Structures* by Cook and Jenner (2010). The first design is a double annular plate configuration where both the protruding steel pipe and monopole are fitted with welded base plates. Bolts and leveling nuts are then used to connect the two annular plates and level the structure. The next two designs are variations of a bolted slip base connection in which a monopole is placed over a section of pipe protruding from the foundation and secured by bolts extending through the diameter of the overlapping poles. The fourth design is a welded sleeve connection in which a segment of steel pipe is fitted over both the protruding foundation pipe

and the monopole. The fifth is based on an embedded casing foundation and the sixth combines directly embedded precast prestressed foundation poles with steel superstructures.

The main objective of this research program is to determine if a viable alternative base connection exists that will work in conjunction with the new foundation support system for cantilever signal and sign structures. In order to accomplish this, the alternative monopole-to-base connections are evaluated initially for fatigue to discard any problematic designs. Ideally, the new base connection will have a better AASHTO fatigue rating than the existing anchor bolt and annular plate system.

Although all of the proposed designs present similar concerns with respect to fatigue and strength, the second and third designs involving the bolted slip base connection have the addition of a failure mode that is distinct from the other alternatives. Since the monopole acts as a sleeve over a length of the tube protruding from the foundation, it may be possible to design the through-bolts to fail under torsional wind loading before any other structural failures occur. Ideally, this will release the superstructure allowing it to simply rotate around the foundation and not collapse. If this occurs, then the repair work should consist primarily of repositioning the sign and replacing the failed through-bolts. If this type of failure mode dictates the structural design, then this type of base connection may be most appealing as the alternative design choice. However, the plausibility of this feature must be explored.

## CHAPTER 2 LITERATURE REVIEW

The sections that follow include a detailed literature review for the various design alternatives considered for use with cantilever signal and sign structures. The literature review includes a summary of the research that led to this project and an investigation of the base connections currently in use. A number of alternative base connection options that eliminate anchor bolts and annular plates from the base connection design are explored. Each is considered for its advantages and potential to improve the fatigue rating of the base connection.

### **2.1 Summary of Previous Reports**

The directive for this research comes from two prior research reports focused on preventing the failure of overhead cantilever signal and sign structures. As a result, much of the literature review that follows originates from these reports and their respective references. Additional information specific to the objectives of this research program is also included as appropriate.

The initial research report, *Anchor Embedment Requirements for Signal/Sign Structures*, examines the failures of cantilever sign structures along Florida highways (Cook and Halcovage 2007). Heavy winds during the 2004 hurricane season created large torsional loads at the foundations of these structures, and ultimately led to some structural failures (Figure 2-1). The results of the program indicate that the foundations of these sign structures failed due to concrete breakout caused by shear forces directed parallel to the edge of the foundation by way of the anchor bolts. The appropriate design procedures for this failure mode were found to exist in ACI 318 Appendix D, and a test program was developed to test the applicability of the procedure to the design of cantilever sign structure foundations (Figure 2-2). The test data prove that the

provisions of ACI 318 Appendix D are appropriate for the design of cantilever sign foundations and should be considered for cantilever structure foundations.

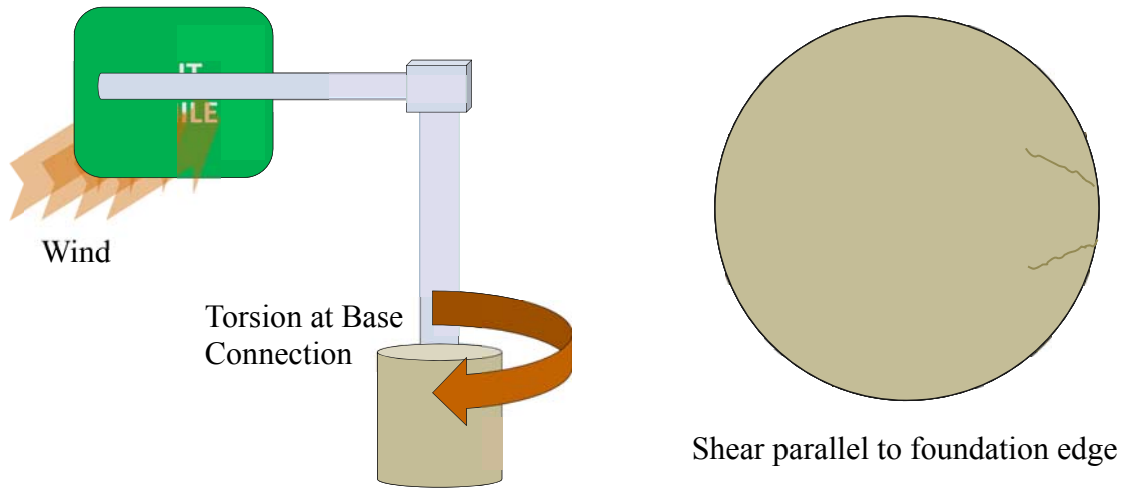


Figure 2-1. Transfer of wind load through cantilever structure to the foundation

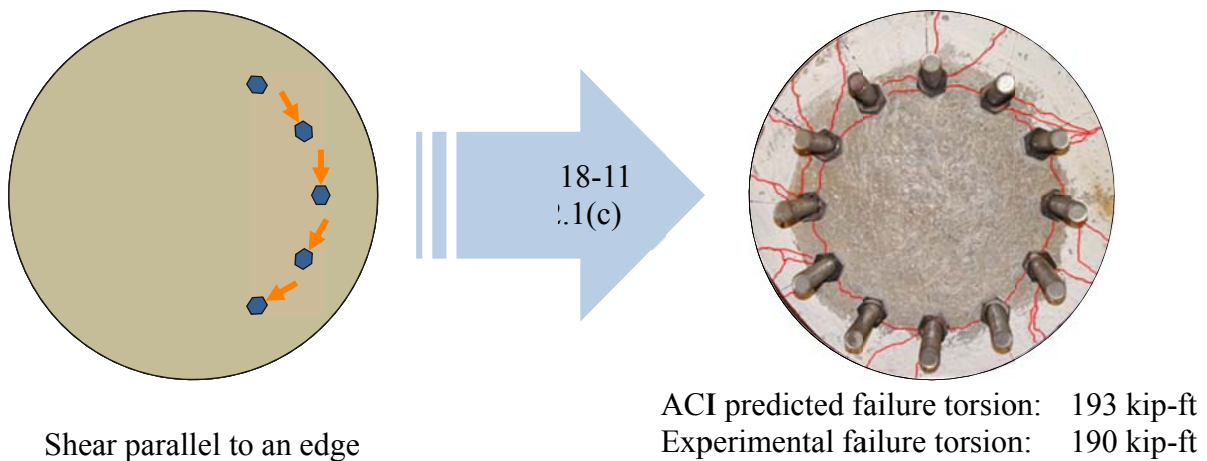


Figure 2-2. Experimental result using ACI concrete breakout strength for anchors in shear

The second research report regarding the failures of these cantilever sign structures, *Alternative Support Systems for Cantilever Signal/Sign Structures*, was established to identify an alternative foundation system that does not involve the use of anchor bolts for transferring the torsional and flexural loads from the sign column to the foundation (Cook and Jenner 2010). By first identifying how anchor bolts transfer loads from the monopole to the foundation, the researchers were able to identify potential problems of the design, which helped identify areas of

concern for alternate designs. Of all the alternatives considered, an embedded steel pipe and plate configuration was deemed the best choice for transferring the loads encountered by a cantilever support system from the steel monopole to the concrete foundation (Figure 2-3).

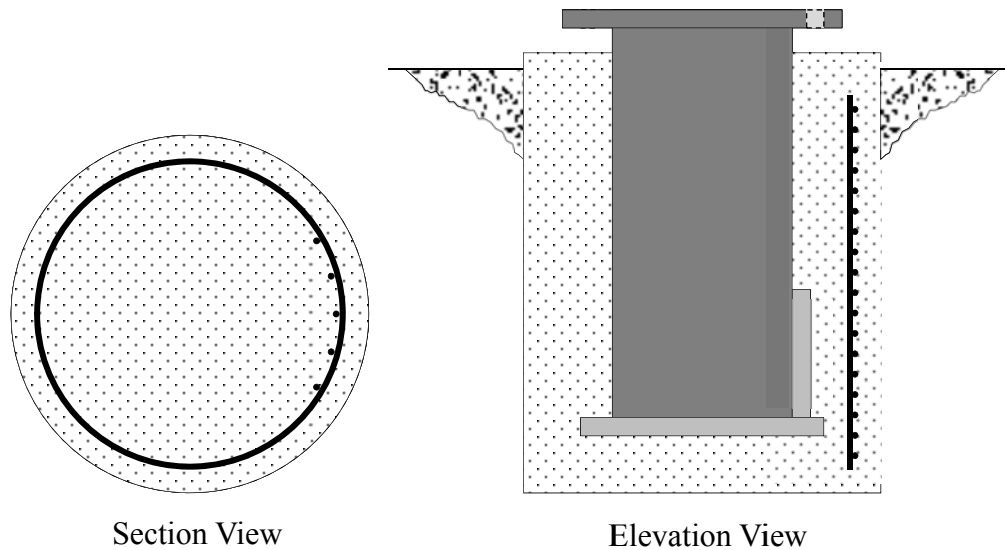


Figure 2-3. Embedded steel pipe and plate configuration in concrete foundation

The design of the test specimen incorporating the embedded pipe and plate assembly into the foundation was derived using ACI 318 Appendix D. The results of the test indicate that the assembly is an improvement over the anchor bolt system currently in use, because the design takes full advantage of the depth of the foundation in maximizing the concrete breakout cone. The results also indicate that the design procedure developed from ACI 318 Appendix D for the new load transfer system is able to accurately predict the possible foundation failure modes.

## 2.2 Summary of Existing Base Connections

A review of available standard specifications, plans, and drawings of state transportation departments confirms the results of the survey conducted for *National Cooperative Highway Research Program (NCHRP) Report 494: Structural Supports for Highway Signs, Luminaires, and Traffic Signals* (Fouad et.al. 2003) and summarized in *Alternative Support Systems for Cantilever Signal/Sign Structures* by Cook and Jenner (2010). The results indicate that the

majority of state transportation departments are primarily utilizing reinforced cast-in-place drilled shafts for overhead cantilever and similar structural support foundations with annular plates and anchor bolts at the monopole-to-concrete connection.

An investigation into alternate foundation designs and base connections in other industries is included in *Alternative Support Systems for Cantilever Signal/Sign Structures* (Cook and Jenner 2010). Further review into industry designs confirms that the transmission line and wind turbine industry both have similar anchor bolt base connections as those used by the state departments of transportation. However, both of these industries share a similar technique for extending the height of their structures by the use of a telescopic slip joint splice (Tempel and Shipholt 2003; Chan 2003). The slip joint splice is also mentioned briefly in the AASHTO *Standard Specifications for Structural Supports for Highway Signs, Luminaires and Traffic Signals* (2009) as a method of extending the height of a monopole structure.

The transmission line industry has also used bolted flanges, which is similar to the anchor bolt base connection, to connect multiple sections of tubing to generate the required height for their monopoles (Chan 2003). Similar to how this industry has adapted the anchor bolt base connection for an extension purpose, it may be possible to adapt the slip joint splice as a viable base connection for cantilever structures. The wind turbine industry uses the slip joint as a method of saving time during installation of offshore wind turbines, although there are some concerns regarding the design that are addressed in the following sections (Tempel and Shipholt 2003).

### **2.3 Alternate Base Connections**

The purpose of this research directive is to find an alternate base connection design for use with the embedded pipe and plate assembly developed in FDOT report BDK75 977-04 by Cook and Jenner (2010). As a result, the focus for the alternate base connection designs below is not

only to eliminate anchor bolts in the foundation, but also to incorporate the new embedded pipe and plate assembly as the primary structural element for transferring flexural and torsional loads from the superstructure to the foundation. The second objective is to improve the overall fatigue rating of the connection.

Most of the base connections described in the following sections incorporate the embedded steel pipe with welded plates that was tested during the previous research program, *Alternative Support Systems for Cantilever Signal/Sign Structures* (Cook and Jenner 2010). The new embedded steel pipe system has been tested and proven effective in transferring torsional and flexural loads from the monopole to the concrete foundation. As such, the base connections discussed in the sections below are intended to accommodate this alternate embedded pipe design, and thus make the primary benefit of each connection the elimination of both the anchor bolt group and preferably the annular plate from the foundation design.

The first four base connection designs in the following sections were initially presented as possible alternative base connections in *Alternative Support Systems for Cantilever Signal/Sign Structures* (Cook and Jenner 2010). The fifth design alternative is a variation of a design described in *Design of Steel Transmission Pole Structures* (ASCE 2006). The final design, which does not incorporate the use of the embedded pole assembly, was suggested for consideration by representatives of the Florida Department of Transportation.

### **2.3.1 Bolted Plate Connection**

The bolted plate design is most nearly akin to the current annular plate and anchor bolt design (Figure 2-4). The design of annular base plates has been studied extensively in recent decades and details on these studies can be found in *Annular Base Plate Design Guidelines* (Reid 2003), *Design Guidelines for Annular Base Plates* (Cook and Bobo 2001), and *Design Procedure for Annular Base Plates* (Cook et al 1995). Additional studies and finite element



analysis models of the behavior of annular base plates can be found in *Deflection Calculation Model for Structures with Annular Base Plates* (Cook et al 1998) and *Analysis of Annular Base Plates Subjected to Moment* (Beese 1995).

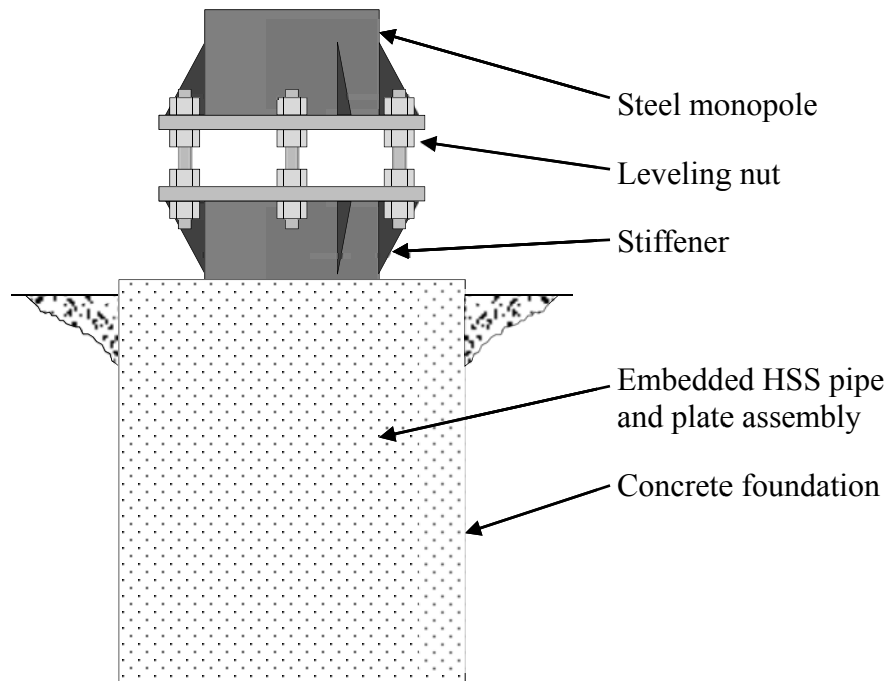


Figure 2-4. Base plate connection shown with stiffeners

In the design of the annular plate for the embedded pipe assembly, plates are welded to both the top of the steel pipe stub extending from the concrete foundation and the base of the monopole. The plates are then joined by bolts allowing space for leveling nuts in between. This design can be modified to include stiffeners at the base of the monopole, if necessary. Due to its similarity to the current annular plate and anchor bolt system, this design was initially recommended for the incorporation of the embedded pole assembly presented in *Alternative Support Systems for Cantilever Signal/Sign Structures* (Cook and Jenner 2010).

The advantage of this alternative is that it is similar to the current connection design, which should result in a smooth transition for those doing the installation of signal and sign structures. Only the foundation construction varies, while the monopole-to-base connection is essentially

the same. Similar dual-plate construction can be found in smaller monopole structures, such as break-away street signs and lamp posts, but does not appear to have been adapted to overhead cantilever sign structures in any quantifiable numbers.

Unfortunately, the design of the bolted plate connection includes all the same concerns as the current anchor bolt system, except for the anchorage-in-concrete interaction. Both designs incorporate plates, bolts, and welds to transfer loads from the monopole to the foundation. Therefore, the same concerns involving fatigue and corrosion apply for both designs and there is no improvement in its fatigue rating. Also, if a complete failure occurs in either the bolts or welds, it is likely that a collapse of the structure will occur much as in the cases of the foundation failures during the 2004 hurricane season. For these reasons, the bolted plate connection does not meet the objectives of the current research, but is included here only because it was recommended for use with the embedded pipe and plate assembly in the design guidelines of *Alternative Support Systems for Cantilever Signal/Sign Structures* (Cook and Jenner 2010).

### **2.3.2 Tapered Bolted Slip Base Connection**

In this option, the base connection is made between the steel pipe and plate assembly embedded in the foundation and the monopole. Both pieces share the same taper so as to fit snugly together and are secured by bolts extending through the diameter of the sleeved connection (Figure 2-5).

The above slip base design is similar to the slip joint splice seen in the transmission line, wind turbine, and lighting industries. The slip base design connects the monopole to the foundation, whereas the slip joint splice is typically used to join two sections of a monopole to extend the overall height of the structure. Based on AASHTO (2009) and industry standards for a slip joint splice, the length of the splice should be at least 1.5 times the diameter of the pipe

(Figure 2-6). This specification is explored further in a section on the slip joint splice in Chapter 3.

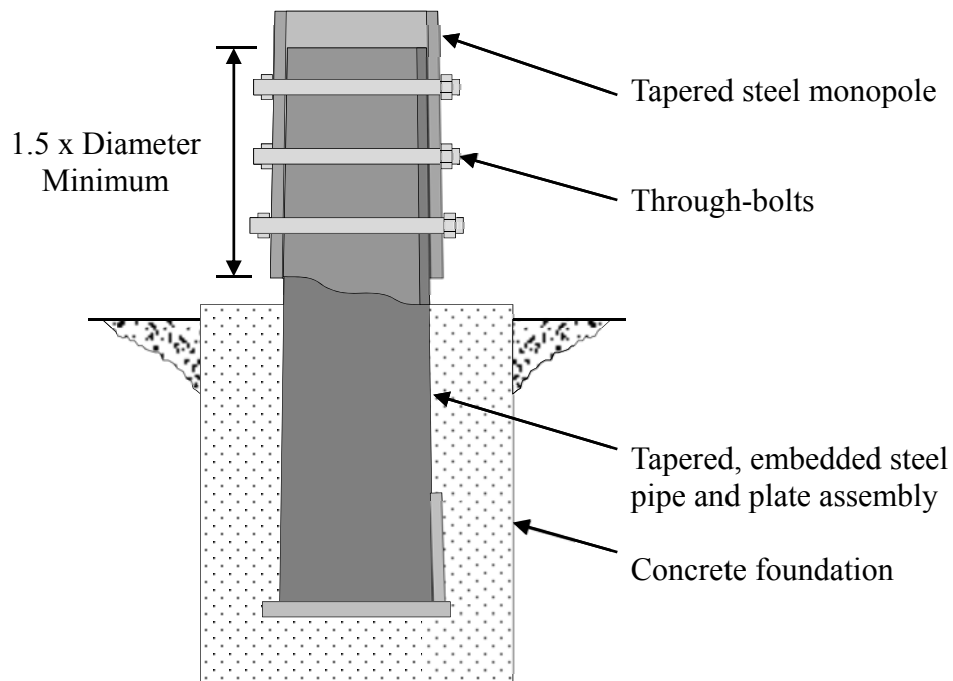


Figure 2-5. Tapered bolted slip base connection

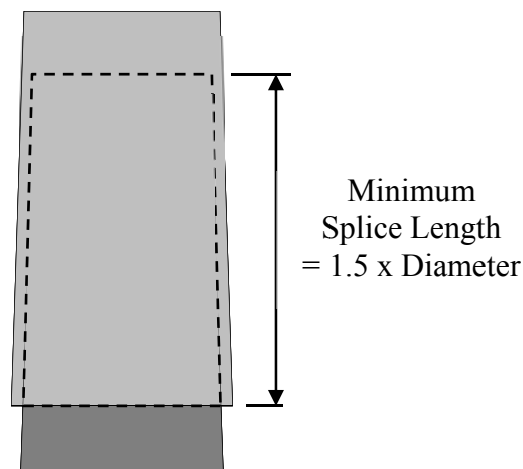


Figure 2-6. Slip joint splice typical in monopole extensions

The design elements to be considered for this connection are primarily in the bolted connections. The bolts must be designed for shear strength to transfer the torsional wind load from the monopole to the foundation. Friction between the spliced poles may help transfer the torsional loads, but likely provides negligible resistance to the bolt shear in round sections

(Tempel and Shipholt 2003). The results of the test program contradict this statement and are discussed in greater detail later. The bolt holes must also be designed for bearing strength to ensure the proper thicknesses of the two poles. Current guidelines for the design of the slip joint splice length are minimal and further investigation into the proper design procedure is needed.

One favorable aspect of the slip base connection is the stability given to the monopole by the segment of embedded pipe protruding from the foundation. Perhaps the main consequence of the previous cantilever sign foundation failures is that the structures completely collapsed to the ground, causing road hazards that could potentially lead to injury or death for travelers. By designing the bolts in the base connection to fail before the concrete foundation or steel poles, it may be possible to prevent the collapse of the sign structure. Given the amount of overlap between poles in the spliced connection, it may be possible for the portion of the pipe protruding from the foundation to support the weight of the cantilever sign during extreme wind conditions. In these conditions, if the bolts fail and the structure remains upright, then repairing these structures could be as simple as correcting the position of the sign and replacing the bolts.

However, there are some shortcomings to this base connection. As mentioned by Cook and Jenner (2010), the availability of these tapered sections may be problematic during construction. The sections need to match up closely and have the same degree of taper where they overlap. Also, the bearing strength of the bolts on the monopoles as well as normal loads transferred through the slip joint may require a greater wall thickness. The process of manufacturing these pieces may be time intensive and costly. The other major concern regarding construction is alignment of the connection. The anchor bolt connection uses leveling nuts to achieve alignment, but the slip base does not have these. Aligning the base of the monopole

flush with the concrete foundation may work in some instances, but not if a standoff from the base is required.

Fatigue is a major area of concern for all structures, and this connection design may be susceptible. As with the anchor bolts, the bolts securing the splice connection may be vulnerable to fatigue, but the impact in this case should be minimal. Anchor bolts are loaded in tension, which is why they have a poor fatigue rating, while other bolted connections loaded in shear have better fatigue ratings. In addition, tapered pipe sections have been shown to experience vertical fatigue cracks originating at the bottom of the splice, particularly where longitudinal welds exist in multi-sided sections (Chan 2003; Dexter and Ricker 2002). These fatigue cracks may impact the bearing capacity of bolted connections and reduce the stability of the structure in the event of a bolt failure.

Corrosion may be another area of concern for this tapered bolted slip base connection since it may have small gaps between the poles. Transmission line monopoles in which large gaps exist between the male and female sections of the splice-joint are usually the result of fabrication or assembly errors (Chan 2003). The existence of a gap in the splice-joint at the base of the structure may result in an accumulation of water and debris, which can ultimately lead to corrosion of the steel sections and bolts. Perhaps by locating the base of the slip joint well above the concrete, the buildup of debris can be minimized.

### **2.3.3 Grouted Slip Base Connection**

In this option, the base connection is made between the steel pipe and plate assembly embedded in the foundation and the steel monopole. The embedded steel pipe is prismatic while the monopole is tapered and placed over the portion of the embedded steel pipe protruding from the foundation. Bolts extending through the diameter of the overlapped sections secure the

connection. The void space between the prismatic and tapered monopole sections is then filled with high-strength grout (Figure 2-7).

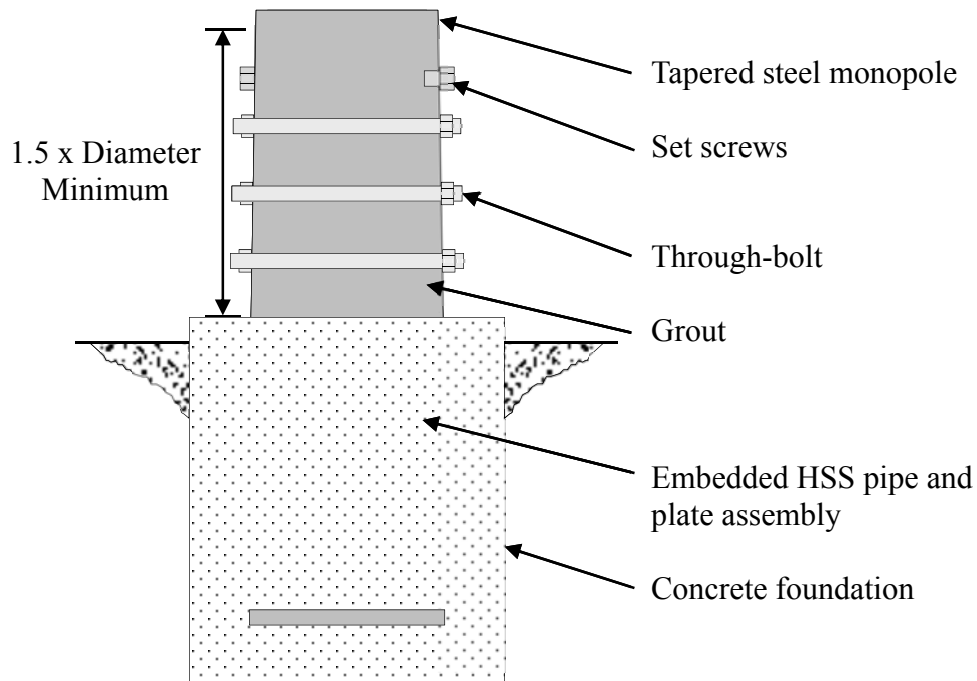


Figure 2-7. Grouted slip base connection

Similar to the tapered bolted slip base connection, the design elements to be considered are primarily in the bolted connections and the calculations should be relatively straight-forward. The bolts must be designed for shear and bearing strength to transfer the torsional load from the monopole to the foundation. The bolt holes must also be designed for bearing strength to ensure the proper thicknesses of the two poles. As previously mentioned, the current guidelines for the design of the slip joint splice length are minimal and further investigation into the proper design procedure is needed.

One advantage of this design over the tapered bolted slip base connection is that the embedded steel pipe is more easily obtainable due to its more standard prismatic cross-section. Fabrication of the steel pipe with welded-on plates as well as its placement in the concrete foundation is simpler. Another shared aspect of this design and the tapered bolted slip base

connection is the stability given to the monopole by the segment of embedded pipe protruding from the foundation. By designing the bolts in the base connection to fail before the concrete foundation, it may be possible for the sign structure to simply rotate around the protruding foundation pipe rather than collapse. If the bolts fail and the structure remains upright, then repairing these structures merely involves correcting the position of the sign and replacing the through-bolts.

This design also shares some unfavorable characteristics with the tapered bolted slip base connection. The bearing strength of the bolts on the monopoles and the normal forces from the transfer of flexural load through the slip joint may require a greater wall thickness, which make the pieces more costly. The other major concern regarding construction is alignment of the connection. Without the availability of leveling nuts to achieve alignment, there is little tolerance for error in aligning the bolt holes across the diameter of the section. One possibility to improve the alignment is to take advantage of the void space between pole sections and the addition of set screws to the slip joint prior to placing grout.

A potential drawback unique to this design is the complication of adding high-strength grout. The placement of grout between the two sections may prove difficult with little to no space at the bottom of the slip joint. Additional holes may have to be drilled in the outer pole above the slip joint to allow for a tube to place the grout. It may also require the use of an additional construction crew to visit the installation site. Whereas contractors currently send a crew to pour the foundation and a second to place the superstructure, a third crew would be required to return to the site to place the grout after the superstructure is erected and aligned. On the other hand, grout may assist the through-bolts in transferring loads from the monopole to the concrete foundation and could help minimize the effects of corrosion.

### 2.3.4 Welded Sleeve Connection

In this alternative, the base connection is established between the protruding section of the embedded steel pipe and the monopole by using a third segment of steel pipe as a sleeve to join the two pieces. Once in place, the sleeve is welded to both the monopole and embedded pipe around the circumference of the two pole segments to secure the connection (Figure 2-8).

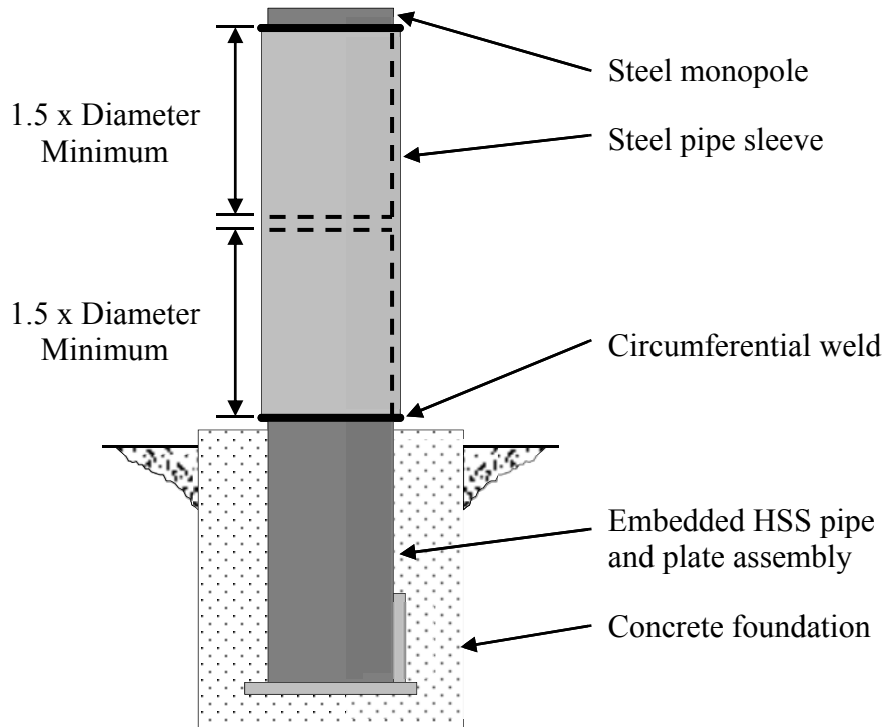


Figure 2-8. Welded sleeve connection

This is a relatively simplified design that eliminates the use of annular plates and bolts from the connection, thus eliminating related concerns regarding fatigue and corrosion of these components. However, the circumferential welds become the only component to transfer the torsional loads from the monopole to the embedded steel pipe. The design calculations for the weld are likely simple, but ensuring that the weld and sleeve can handle the torsional and flexural loads from the sign structure may be more challenging.



In terms of constructability, the welded sleeve connection may pose some challenges. There is currently no known AASHTO or industry standard for this type of structural connection, and the slip joint splice mentioned in Section 2.3.2 appears to be the closest match. In the slip joint splice, the standard requires the length of the splice to be at least 1.5 times the diameter of the pipe (AASHTO, 2009). Within the connection, the two joining steel poles meet in the center of the sleeve, either butted against each other or separated by a spacer. In order to maintain structural stability and secure the connection, it may be necessary to make the full length of the sleeve at least three times the diameter of the steel pipe, which allows a minimum coverage length of 1.5 times the diameter of the pipe for each of the joined sections. The simplicity of the design makes the fabrication of the welded sleeve easy, but the increased length may increase the material cost.

The closest match to a welded sleeve connection is used by the transmission line industry for repairing dented tubular poles. A set of reinforcing plates made of the same grade steel with a thickness equal to or greater than the tubular pole thickness are fabricated to match the size and shape of the existing pole. The two half-shell reinforcing plates are positioned over the damaged area and welded into place. Grooves are cut into the plates to allow for plug welds while the edges of the plates are sealed and fillet welded to the original structure. A protective paint coating then covers the entire area of the reinforcing plates and welds (Chan 2003). The principal difference between this repair process and the proposed base connection is that the reinforcing plates surround an intact structure, except for maybe a hole in the location of the dent. The welded sleeve in the proposed base connection, on the other hand, must be able to conjoin two entirely separate pieces of tubing.

Fatigue in the welds is another area for concern. If improperly fabricated, notches can form that create high-stress areas and may initiate cracks within the weld. Therefore, the need for a skilled welder at the installation site may add cost to the construction of the sign structure. Corrosion also becomes an issue with the welded sleeve connection since it is entirely comprised of steel. The welding process burns away any protective coatings already on the steel, such as paint or galvanization, and needs to be replaced (Chan 2003).

### **2.3.5 Inverted Grouted Slip Base Connection**

A design found commonly in the transmission line industry is the embedded casing foundation. This type of connection between the foundation and the superstructure is discussed in *Design of Steel Transmission Pole Structures*, a document published by the American Society of Civil Engineers (ASCE) in conjunction with the Structural Engineering Institute (SEI). In this design, either a round or polygonal steel tube is placed directly in the ground and serves as the foundation for the superstructure. These steel caissons can be prismatic or tapered depending on the foundation requirements and method of installation. Once the casing is embedded, the steel superstructure is installed by one of two methods. One type of connection uses a base plate on both the embedded casing and the superstructure pole so the two can be bolted together. The other type of connection is a type of inverted, loosely-fitted slip joint, in which the steel pole for the structure is placed inside the top portion of the steel casing and secured with set screws. The annular space between the two members is then filled with grout or concrete depending on how large the void space is between them (ASCE 2006).

In a typical embedded casing foundation, the embedment length of the casing is responsible for transferring all structural loads to the soil. However, in order to use the embedded pipe and plate assembly developed by Cook and Jenner, modifications to the direct embedment of the caisson must be made. This alternate design uses the embedded pipe and plate

assembly in a typical concrete foundation. However, instead of oversizing the steel pole for the superstructure to fit over the embedded pipe, the embedded pipe is oversized so that the steel superstructure pole will fit down inside of it. The concrete on the inside of the embedded pipe serves as the base on which the superstructure pole rests. Set screws hold the superstructure plumb while grout is poured into the annular space between the two steel members. Through-bolts may still be required to transfer the torsional load from the superstructure to the base considering the substantially larger torsional loads likely experienced by a cantilever signal or sign structure as compared to a transmission pole (Figure 2-9).

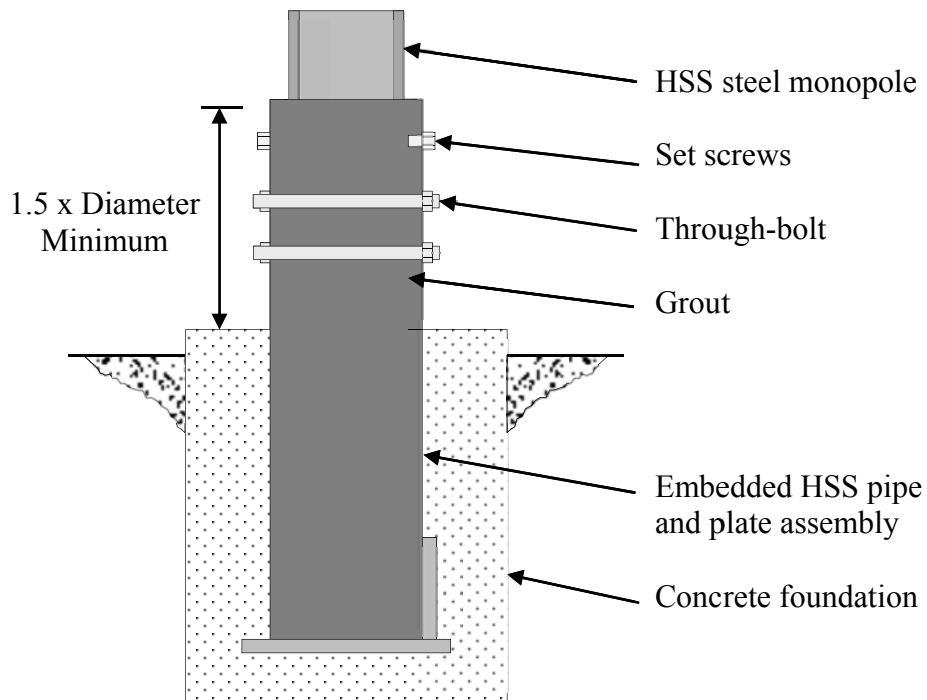


Figure 2-9. Inverted grouted slip base connection

The advantage of this alternative is that there are some standards already in place for how to approach the design. Since the inverted slip joint does not require that the inner and outer poles fit snugly together, typical hollow structural sections (HSS) sections can be used and the space between them filled with grout. This also means that the inner pipe can be placed after the concrete foundation has cured around the embedded outer pipe. Doing this means that the base

of the superstructure pole can rest on the concrete while it is being aligned and the grout cures. This differs from the typical slip joint in which the base of the joint is well above ground level and may require jacking forces to fit the poles snugly together.

There are also some concerns associated with this design. Since this is an inverted slip joint, the exposed edge of the slip joint faces up towards the sky and can possibly catch and hold water and debris if the grout is not properly placed or sealed. If water is allowed to soak into the grout, then it may lead to corrosion of the two pole sections if proper drainage is not provided. As with the other design options, the alignment of the upright pole may be challenging. In this instance, the upright pole does not fit snugly inside the lower pole, and may require set screws to maintain alignment while the through-bolts and grout are being placed. Also, if a torsional failure occurs in the slip joint, then the repair could simply require replacement of both the grout and the through-bolts.

### **2.3.6 Prestressed Concrete Pole with Tapered Steel Monopole**

This design alternative is similar to the previously described slip base connections in sections 2.3.2 and 2.3.3, but with one key difference. In this design alternative, unlike all the other proposed designs, there is no embedded steel tube component. Instead, a tapered spun cast prestressed concrete pole protrudes from ground level, so that the steel monopole can slip directly over the concrete (Figure 2-10). The steel monopole can be either round or sixteen-sided. As previously mentioned, the length of the splice should be at least 1.5 times the diameter of the pipe based on AASHTO (2009) and industry standards. However, that length specification is based on tests of steel-to-steel connections and may have to be modified to account for steel-to-concrete connections. In addition, the spun cast prestressed concrete pole should be manufactured and tested to meet the specification of ASTM C1089 for spun cast prestressed poles (2006).

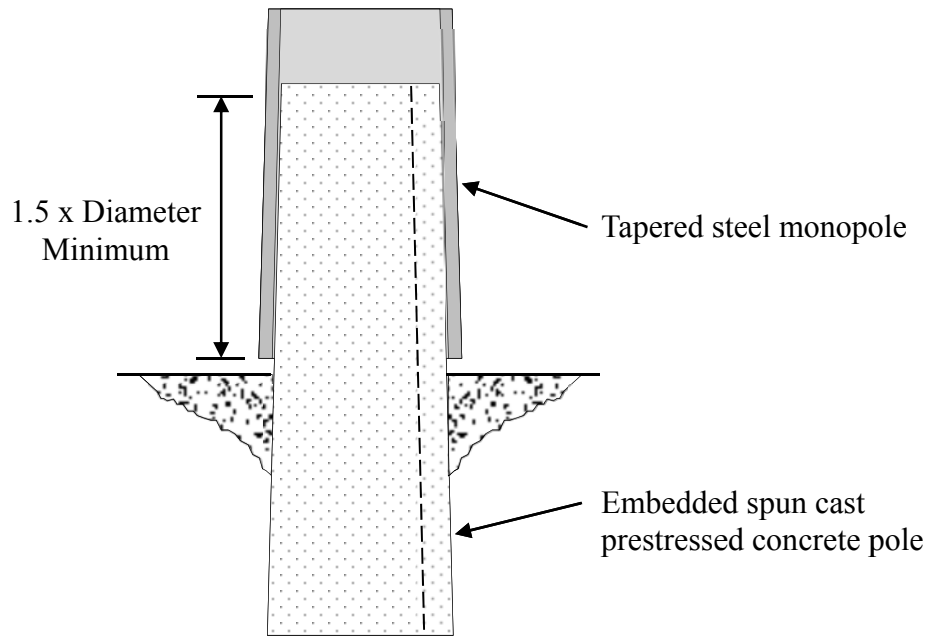


Figure 2-10. Direct burial spun cast prestressed concrete base and steel superstructure

This design alternative is perhaps the most simplified of all the proposed options, because it eliminates the embedded steel tube altogether and does not require any annular plates or anchor bolts to make the monopole-to-foundation connection. The base connection as shown in Figure 2-10 consists of only two primary elements: the concrete foundation and the steel superstructure. Friction between the concrete and steel in the splice provides the only resistance to torsion, which may not be quantifiable for design purposes if any localized crushing of the concrete occurs. Determining the normal force created between the steel and concrete sections presents one challenge, while any gaps between the members present another challenge. Since the torsional capacity of the connection is of vital importance to the design, it may be necessary to insert bolts through the cross-sections of the two poles to resist rotation about the concrete substructure (Figure 2-11).

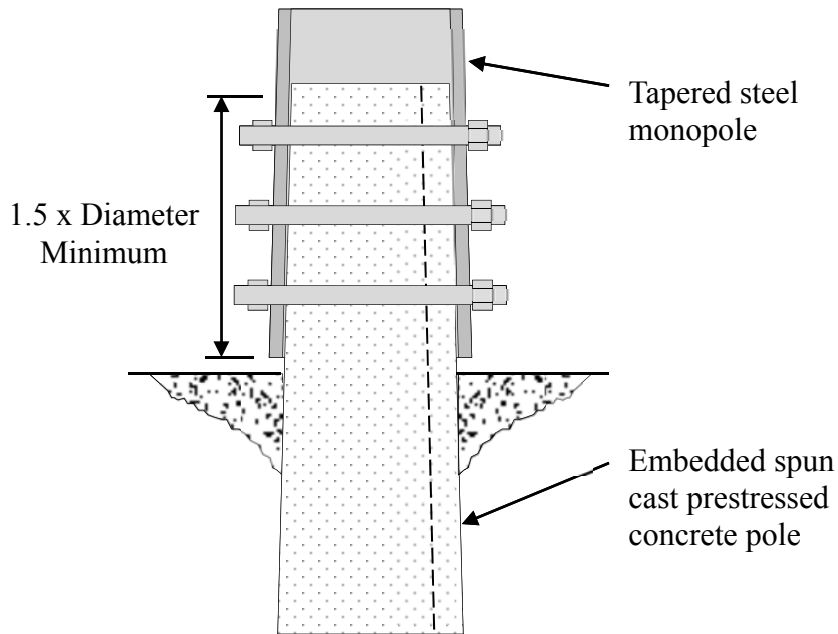


Figure 2-11. Spun cast prestressed concrete and steel connection shown with through-bolts

Comparable to the slip base alternatives, the slip joint connection in this design provides added stability to the monopole by means of the segment of embedded concrete pipe protruding from the ground. However, there are some shortcomings to this base connection. The availability of tapered concrete and steel sections may be problematic during construction. The sections need to match up closely and have the same degree of taper where they overlap. Most likely the two members will have to be manufactured by different companies, which could make matching the tapers more difficult or complicate the collaboration of fabrication schedules for special orders. Concerns unique to this design alternative relate to the alignment of the superstructure and design of the concrete sections for torsion. In terms of alignment, some of the other base alternatives can possibly be aligned using set screws and high-strength grout or leveling nuts. Unfortunately, these are not likely options in the case of the spun cast concrete. The alignment must begin during embedment of the lower section, which needs to be plumb as it protrudes from ground level. Perhaps the most troubling aspect of this design is accounting for the torsional wind loads. These types of poles are typically implemented as supports for small

cantilever arms, such as luminaries, and wire spun traffic signals. These types of applications do not experience the large torsional loads that overhead cantilever signal and sign structures endure, and so designing the embedded portion of concrete to transfer these large torsional loads raises questions.

Although the foundation design is not the primary objective of this project, a few design parameters should be considered in order for this base alternative to become a feasible option. The torsional capacity of a smooth, round concrete pole in soil must be confirmed to be able to withstand the torsional loads of large cantilever sign structures. One option for embedment of the concrete pole is to cast it in a surrounding poured concrete foundation, so that the foundation will meet the requirements depicted in index 11310 of the 2010 FDOT design standards. However, ensuring a strong bond between the precast and poured concrete is another issue to address. A second option might be to directly embed the concrete section by jacking the precast member into the ground. Unfortunately, this method often greatly disturbs the surrounding soil and may make alignment difficult and cause unwanted settlements of a structure this size (McVay et al 2009). A third possibility might be to auger a hole in which to place the concrete pole. This method does not disturb the soil surrounding the structure, but properly backfilling the hole around the concrete pipe is essential to maintain proper alignment. For the purposes of evaluating this alternative design in this report, the foundation and appropriate soil interactions are assumed to have been previously designed for all geotechnical requirements.

Fatigue may only play a minor role in this proposed base connection, because it contains few parts. However, tapered, multi-sided pipe sections have been shown to experience vertical fatigue cracks originating at the bottom of the splice (Chan 2003; Dexter and Ricker 2002). These sections alone also may not provide enough frictional resistance to withstand the torsional

wind loads because of their limited contact with a round concrete pole. This could potentially lead to slight to severe rotations of the structure about the base in extreme wind conditions. As a result, it is still imperative to conduct regular inspections of this base connection. Round sections, though less susceptible to fatigue, still may not provide adequate frictional resistance and may require through-bolts to sustain extreme wind loads.

Corrosion in this design is also expected to be of minimal concern. The steel monopole is most likely to experience corrosion, but the effects can easily be curbed by common anti-corrosive techniques, such as galvanization. The main concern for this design might be the accumulation of debris along the base of the connection. If a round steel section is used, then a sealant should suffice to prevent debris and water and from finding its way into the slip joint. However, if a multi-sided steel section is used over a round concrete section, then it may be imperative to include high-strength grout or a sealant in the joint to prevent debris from accumulating in the gaps between multi-sided steel and round concrete sections.

#### **2.4 Fatigue and Corrosion of Components**

Fatigue and corrosion of structures has always been a concern in the United States, but this concern has been amplified in recent years with the increasing attention given to the nation's aging infrastructure. As noted in *The Falling Sky* (Ward 2009), the effects of fatigue and corrosion may soon wreak havoc as structures that have been in service for many decades, some near the end of their expected service lives, may begin to experience structural failures. Of particular interest to this report are proper inspection, maintenance, and repair techniques being utilized with high-mast light towers, traffic signal supports, and overhead sign structures.

The AASHTO *Standard Specifications for Structural Supports for Highway Signs, Luminaires, and Traffic Signals* (2009) specifies fatigue stress limits for cantilevered support structures based on constant-amplitude fatigue limits (CAFL). The current annular base plate



system in use with cantilever signal and sign structures falls into an AASHTO stress category of E or E' depending on the type of weld used to join the pole to the transverse plate. Anchor bolts have only a slightly higher stress category of D. The sections below discuss concerns of fatigue and corrosion as they relate to specific elements of the proposed base connection designs.

#### **2.4.1 Bolt Fatigue**

Bolts typically must be adequately pretensioned to prevent them from carrying the full applied load and experiencing fatigue. When bolts are properly pretensioned, friction between the faying surfaces on the joined pieces should carry most of the applied load. However, when the bolts are loose, the faying surfaces may not remain in contact and be able to slide freely such that the bolts are the only components transferring load from one member of the structure to the next (FHWA 2005). The impact of the bolts transferring loads repeatedly through the structure results in fatigue and shortens the useful life of the bolts. Due to this possibility, shear fatigue is a potential concern for the slip base connection designs utilizing through-bolts as well as the bolted plate connection alternative.

The potential concern for bolt fatigue in the alternatives that utilize a slip joint to transfer flexure is related to cyclic galloping loads more so than extreme wind loading conditions. The through-bolts are oriented in the slip joint so that they are not influenced by the flexural loads resulting from wind, which positions them parallel to the mast arm. However, this places them directly in line with the cyclic bending moments associated with galloping loads, which when they occur cause the mast arm to vibrate vertically as opposed to the horizontal motion associated with wind loading. Even though the slip joint is responsible for transferring bending moments, it is still possible that the swaying motion of the upper pole section could impact the through-bolts if they are not pretensioned to some degree. Without pretensioning, slip may occur allowing the through-bolts to transfer moment from the galloping loads to the inner pole.

The shear strength of any bolt depends proportionally on its available cross-sectional shear area. The shear strength is already less than the tensile strength for bolts. Unfortunately, any imperfections in the bolt, such as a notch or fretting from corrosive effects, may further reduce the available shear area of the bolt. These defects and subsequent reductions in shear area can cause stress concentrations in those particular places and increase the propagation of fatigue cracks on the bolts (Kulak et al 2001).

On the other hand, though, care must be taken not to place excess tension on the bolts placed through the diameter of the poles. If too much tension is applied to the bolts, the pole sections may distort under the excessive loading. This could create undue internal stresses in the monopole and foundation pipe, which could impact the effectiveness of the structure (Chan 2003). Therefore, it is important to follow the standards for the various bolt tightening methods. For instance, the AISC (2005) specification does not allow for any pretensioning of through-bolts in hollow structural sections (HSS). Fortunately, this exclusion of pretensioned and slip-critical bolts from the proposed base connection designs should have minimal impact, because cyclic galloping loads that induce bending moments are carried by the slip joint splice rather than the bolts.

Related to shear fatigue in the bolted connection is bearing strength and fatigue. The bearing strength of the round sections is vital in maintaining the connection once the bolts loosen from their initial tightening. Care should be taken not to place bolt holes too near to longitudinal welds in multi-sided sections, since these welds are susceptible to fatigue cracking.

In general, AASHTO places bolted connections using steel materials in stress categories ranging from B to D. For bolted connections that place the fasteners in tension, such as with anchor bolts, the stress category is D. In other connections that use fully tightened, high-strength

bolts, the stress category is considered a B (AASHTO 2009). Therefore, from a bolting standpoint, the use of through-bolts rather than anchor bolts is an improvement to the design of the base connection.

#### **2.4.2 Weld Fatigue**

The fatigue life of welds can be greatly impacted by the presence of defects in the weld joints that can cause stress concentrations and ultimately lead to premature failure of the weld and structure. Defects can be caused by the inclusion of slag in the weld joint, incomplete fusion along the contact surfaces of the weld metals, pockets of gas trapped within the weld joint, and the development of an undercut, or a groove in the base metal next to the edge of the weld. In a study on AH36 plate steel, researchers found that fatigue cracks began forming between 90,000 and 170,000 load cycles. They also noted that the initiation of fatigue cracks began sooner in the base metal than in the weld metal, which is likely attributable to differences in the material strengths (Lee et al 2000).

Base plate welds have been known to fail due to fatigue in cantilever sign structures. The cyclic loads produced by galloping caused the failure of an overhead cantilever sign near Rancho Cucamonga, California, in 1999. In this case, investigators identified the failure to have occurred at the toe of the fillet weld along the pole-to-base plate connection. Due to the nature of galloping, the fatigue cracks appeared to spread from the area of the weld directly under the mast arm as well as the area directly opposite the mast arm. (Dexter and Ricker 2002) The development of the fatigue cracks along the toe of the weld corroborates the findings of Lee et al (2000).

This evidence of weld fatigue in cantilever sign structures raises concerns for the welded sleeve connection described in Section 2.3.4. The proposed design relies entirely on welds to maintain the connection between monopole and foundation, so weld fatigue could be potentially

devastating in this design option. It also raises concern for the bolted plate connection discussed in Section 2.3.1, since it relies on welds and bolts to secure the connection between monopole and foundation pipe.

Aside from base plate welds, weld fatigue can be found in the longitudinal joints of tapered, multi-sided tubular poles. Ward (2009) identified these vertical welds running the full length of tubular support posts as one of the many cases of fatigue that can lead to structural failures of high-mast light towers. Dexter and Ricker also noted that tapered poles appear to be more susceptible to fatigue than others (2002).

The presence of fatigue cracks in the vertical joints of tapered pole sections is cause for concern with respect to the two slip base connection designs in Sections 2.3.2, 2.3.3, and 2.3.6 as all three incorporate tapered monopole supports. Given the likelihood of galloping and vortex shedding on cantilever sign structures, galloping is very rare in cantilever structures and, in accordance with AASHTO Table 11-1, vortex shedding is not considered in design. If vertical fatigue cracks develop, they may cause the monopole to loosen from the foundation pipe and negatively impact the effectiveness of the bolted portion of the connection. However, the use of perfectly round cross-sections that do not require numerous welded joints along their length may eliminate some concern for vertical fatigue cracks in these design alternatives.

Based on AASHTO's categorization of fatigue details for cantilevered support structures, welded details and connections typically range in stress categories from B' to E'. The assignment of the various stress categories vary based on the type of weld and its application. Fillet-welded connections are limited to E and E' stress ratings while groove-welded connections fall into stress categories of B', D, E, and E'. Of particular interest is the longitudinal seam weld

in elements with the welds parallel to the direction of applied stress, which is rated as a B' (AASHTO 2009).

### **2.4.3 Corrosion of Steel Elements**

Corrosion is another major concern for the lifespan of steel structures. With regard to overhead cantilever signal and sign structures, the connections and joints are most at risk to the damaging effects of corrosion due to the methods and designs used to construct them. Corrosion can accelerate the impact of fatigue loading on the structure and further reduce the usefulness of steel structures, which is why it is so important to protect the steel from corrosion.

The destruction of protective coatings and galvanization is a primary concern with regard to corrosion of steel elements. Hot-dip galvanizing, which involves submerging pieces into a vat of molten zinc, typically provides better protection than a mechanical galvanizing process, which includes tumbling pieces with glass beads and zinc powder as a means of building up the zinc coating, by providing a heavier coating for longer protection of the steel (FHWA 2005). The application of zinc primer and paint is another common method to prevent corrosion (USDA 2008). The disintegration of painted surfaces and galvanization can occur naturally over time, but there are also other factors to consider. Defects in the protective coatings can occur during transportation, assembly, or field alterations to the components. Any defects or joints at risk of deterioration should be addressed in the field by repairing or adding a protective coating to prevent corrosion (Chan 2003).

Pack rust is a form of corrosion often formed between built up steel sections, because in traditional slip joints used in high-mast lighting towers the accumulation of pack rust increases pressure and leads to vertical seam weld cracks in geometric tubular sections (Ward 2009). Wind loads and wind-induced movement generated from galloping and vortex shedding can accelerate the process of cracking in seam welds. Pack rust can be a major concern in slip joint

connections where water can be drawn between the contact surfaces of the two poles by capillary action (FHWA 2005). A similar phenomenon can be found in bolted connections between the plates and washers, for example. The proximity of the alternative base connections to the ground may increase exposure to debris and moisture, which can in turn amplify the development of pack rust.

Field welds can also lead to corrosion of steel elements. The thermal energy required for welding is capable of melting galvanized metal and burning through protective paint layers, which exposes the connection to environmental corrosion (Chan 2003). Since welds are the primary method of unification in the welded sleeve connection, it is necessary to address the impact of these welds on the corrosiveness of the structure. If corrosion of the welded joints leads to gaps along the base of the sleeve, then the sleeve connection becomes vulnerable to pack rust in the same way as the slip base connections.

To prevent failure of signal and sign structures due to corrosion, it is imperative to provide protection against oxidization. In the case of the slip joint, sealing the base of the connection after assembly is complete and then painting the connection delays any corrosive effects (FHWA 2005). Similarly, welded connections need to be galvanized or painted to ensure the weld and base metals are protected from corrosion. As for bolted connections, the bolts can be galvanized or covered with a protective sealant to help fill in the spaces of the bolt holes and prevent any moisture or debris from corroding the connection.

## **2.5 Selection of Base Connection**

The selection of alternative base connection designs for testing at the FDOT Marcus H. Ansley Structures Research Center is based on the literature review presented above. Taking into consideration the pros and cons of each design alternative, the list of six proposed designs can be reduced to one preferred alternative for testing (Table 2-1). Ultimately, the steel-to-steel

tapered bolted slip base connection is selected for testing as an alternative to anchor bolts and an annular plate.

One of the most appealing aspects of this base connection alternative is the improvement in fatigue ratings based on the AASHTO (2009) system. The tapered bolted slip base connection consists of three main elements to consider in terms of fatigue. The first is the slip joint, which when designed with a minimum splice length of 1.5 times the diameter of the poles falls into the B stress category. The second component to consider is the through-bolt group. The through-bolts in the connection experience shear and not tension, and are likely made of high-strength material. This type of a bolted joint also falls in the B stress category. The third component to consider is the tapered poles that make up the slip joint. Tubes with longitudinal seam welds fall into the stress category of B'. Overall, these components of the tapered bolted slip joint connection are much improved compared to the stress categories of D and E' associated with anchor bolts and annular plates, respectively. In terms of the constant-amplitude fatigue limits this increases the value from 2.6 ksi for the anchor bolt and annular plate system to at least 12 ksi for the tapered bolted slip joint connection (AASHTO 2009).

The tapered bolted slip base connection is a variation of a commonly used slip joint connection seen in many different applications. The use of the slip joint in different industries proves that it is versatile, but the lack of information regarding its behavior and design makes it an ideal candidate for testing. For the purposes of applying the tapered bolted slip base connection for use in cantilever signal and sign structures, it is important to ensure that it is capable of transferring both torsional and flexural loads associated with extreme wind conditions. An understanding of how the connection transfers these loads is also essential to

developing proper design procedures. In addition, the construction and maintenance of this type of base connection is examined for field applications.



Table 2-1. Summary of advantages and disadvantages for each design alternative

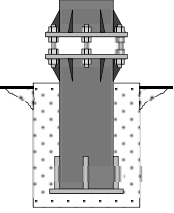
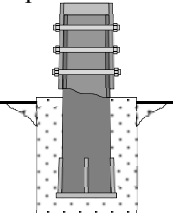
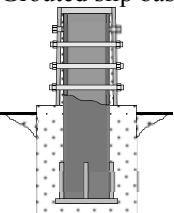
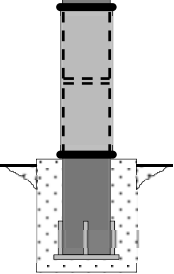
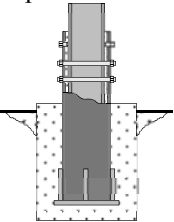
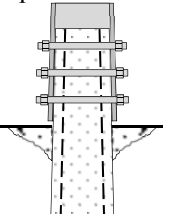
Design alternative	Above grade load transfer	Design considerations	Pros	Cons*
<p>Bolted plate</p> 	<p>Flexure: Bolts (axially) Torsion: Bolts (shear)</p>	<p>Bolt strength in tension and compression Bolt shear strength Number of bolts required Bearing strength of plates</p>	<p>Similar to existing construction Alignment (leveling nuts) No anchor bolts Bolts transfer flexure and torsion</p>	<p>Similar to existing construction Bolt, plate, and weld fatigue Bolts carry axial and shear load AASHTO fatigue rating of D for bolts in tension Loosening of nuts Entrapment of debris between plates causing corrosion If bolts fail, structure may collapse</p>
<p>Tapered bolted slip base</p> 	<p>Flexure: Splice Torsion: Bolts (bearing on steel wall)</p>	<p>Splice length (AASHTO)** Bolt shear strength Bearing strength of steel Number of bolts required</p>	<p>Splice transfers flexure Repair of through-bolt failure Structure may not collapse if bolts fail Few structural design elements Does not require welds AASHTO fatigue rating of B for splice and bolts</p>	<p>Alignment Bearing strength of wall Matching taper of poles Bolt fatigue Gaps in slip-joint trap debris causing corrosion</p>
<p>Grouted slip base</p> 	<p>Flexure: Splice Torsion: Bolts (bearing on steel wall)</p>	<p>Splice length (AASHTO)** Bolt shear strength Bearing strength of steel Number of bolts required</p>	<p>Splice transfers flexure No taper matching Ease of repair of through-bolt failure Structure may not collapse if bolts fail Grout may help resist corrosion</p>	<p>Alignment using set screws Bearing strength of wall Inserting grout and sealant Bolt fatigue Ability to monitor corrosion within splice</p>

Table 2-1. Continued

Design alternative	Above grade load transfer	Design considerations	Pros	Cons*
<p>Welded sleeve</p> 	<p>Flexure: Splice (2x) Torsion: Weld</p>	<p>Weld strength Splice length per section (AASHTO)**</p>	<p>Splice transfers flexure Weld transfers torsion No annular plates</p>	<p>Alignment On-site welding, fabrication Sleeve cost, length and thickness Weld fatigue and corrosion AASHTO fatigue rating of E or E' for welds</p>
<p>Inverted grouted slip base</p> 	<p>Flexure: Splice Torsion: Bolts (bearing on steel wall)</p>	<p>Splice length (AASHTO)** Bolt shear strength Bearing strength of steel Number of bolts required</p>	<p>Splice transfers flexure No taper matching Ease of repair of through-bolt failure Structure may not collapse if bolts fail Grout may help resist corrosion</p>	<p>Alignment using set screws Bearing strength of wall Inserting grout and sealant Bolt fatigue Ability to monitor corrosion within splice</p>
<p>Prestressed concrete and tapered steel</p> 	<p>Flexure: Splice Torsion: Bolts</p>	<p>Splice length (AASHTO)** Bolt shear strength Number of bolts required Bearing strength of steel Bearing strength of concrete</p>	<p>Splice transfers flexure Simplified connection – no annular plates or welds Fatigue and corrosion limited</p>	<p>Alignment Matching taper Bolt fatigue Foundation design of spun cast concrete and reinforcement not tested Debris along base of slip-joint may cause corrosion Spun-cast embedment requirements</p>

\* All designs implement the use of round cross-sectional members. If a tapered, multi-sided cross-section is used for design, then vertical fatigue cracks along the longitudinal welds of the monopole may be likely (Dexter and Ricker 2002).

\*\* Splice lengths will be designed based on AASHTO standards that call for a slip-joint splice length at least 1.5 times the diameter of the cross-section.

## CHAPTER 3 DEVELOPMENT OF TEST PROGRAM

The sections that follow discuss the considerations for the design of a test program to determine the feasibility of utilizing a tapered bolted slip base connection for use with cantilevered signal and sign structures. For each structural component within the connection, the appropriate design code specifications are considered. In addition, the components of the test apparatus are described and discussed in detail, including the types of materials being specified for each one.

### **3.1 Design Code Considerations**

A number of structural code considerations have to be taken into account when designing the tapered bolted slip base connection for testing and use in field applications. Each component of the connection must be analyzed to determine if it has adequate strength to transfer the loads from the mast arm to the foundation. The tapered bolted slip base connection consists of three main components that must be designed: the slip joint splice length, the through-bolted connection, and the steel poles. The sections that follow discuss the design considerations for these components, and sample calculations pertaining to the design of the tapered bolted slip base connection are located in Appendix A.

#### **3.1.1 Slip Joint Splice Length**

The slip joint splice is a feature seen in many of the proposed alternate base connection designs, including the design chosen for testing. The slip joint splice is commonly found in structures where the required height cannot be obtained by a single length of material, as is the case with high mast lighting poles. The use of the slip joint splice allows a telescoping of members to achieve the desired height. The length of overlap of adjoining members is an essential part of the connection. A splice with insufficient length is unstable and unable to

maintain the connection, particularly if the applied loads induce moments to be transferred over the connection. A splice length that is too long does not present any major structural implications, but does present a concern with regard to unnecessary increases in material costs.

To determine the appropriate length of the slip joint, a review of the 2009 AASHTO *Standard Specifications for Structural Supports for Highway Signs, Luminaires and Traffic Signals* was conducted. In Section 5 on steel design, the specification for slip type field splices is proved in article 5.14.3, which states “the minimum length of any telescopic (i.e. slip type) field splices for all structures shall be 1.5 times the inside diameter of the exposed end of the female section” (Figure 3-1). Also, Section 11 on fatigue design includes a table of common details for various connection types that includes the slip joint splice where the length of the splice is equal to or greater than 1.5 times the diameter of the pole. Further investigation within the commentary for this section reveals that this connection detail and others come from a review of state departments of transportation standard specifications as well as manufacturers’ guidelines for various types of connections associated with cantilever support structures.

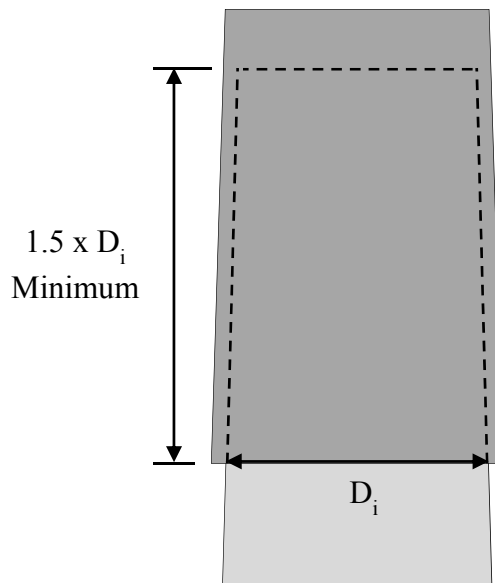


Figure 3-1. AASHTO slip joint splice

An examination of the FDOT *2010 Design Standards for Design, Construction, Maintenance, and Utility Operations on the State Highway System*, specifically index number 17502 for high mast lighting structures, further supports the AASHTO specification. However, reviewing the pole design tables included in the index initially suggested that perhaps the FDOT requires a splice length of approximately 2.0 times the diameter of the pole structure. Further investigation into this requirement reveals that the specification as implemented by the FDOT is more specifically 1.5 times the diameter of the pole plus an additional six inches to account for galvanization thickness (FDOT 2007a).

An investigation into the origins of the specification for minimum required slip joint splice length led to two empirical studies testing the failure loads for various splice length-to-diameter ratios. The first study was conducted by the Japanese steel pole manufacturer Sumitomo Metal Industries, Ltd. in 1970. The study was based on a limited number of experiments using octagonal, tapered poles and found that the predominant type of slip joint failure is caused by local buckling under flexural loading. The manufacturer also recommends a splice length of at least 1.7 times the diameter of the section, but noted that reinforcing the cross-sections could reduce the splice length to as little as 1.0 times the diameter of the section (Kai and Okuto 1974).

The details of the test program raise some questions as to the applicability of the results directly for use with poles commonly used in the United States. Information regarding the taper and width-to-thickness ratios of the test specimens can be found in an unpublished report that was mailed to the American Society of Civil Engineers (ASCE) Structural Division (K. Okuto, May 31, 1977). The taper used in most of the test specimens is 0.3 inches per foot, which is a little more than twice the amount of taper specified for use in FDOT applications. The report also indicates width-to-thickness ratios of 80 for the multi-sided sections, which comes from a

wall-to-wall diameter of approximately 20 inches and wall thickness of 0.25 inches. The diameter-to-thickness ratio for an HSS 16x0.375 section is approximately 43, much lower than the ratio in the Sumitomo study (Table 3-1). This might indicate that the recommendation of a minimum splice length of 1.7 times the diameter is higher than required for a typical HSS section to prevent plastic deformations within the slip joint region.

Table 3-1. Typical HSS diameter-to-thickness ratios for FDOT cantilever sign structures

Outer diameter (in)	Wall thickness (in)	Diameter-to-thickness ratio
12.75	0.375	34.0
14.00	0.375	37.3
16.00	0.375	42.7
18.00	0.438	41.1
20.00	0.500	40.0
24.00	0.375	64.0
24.00	0.562	42.7
24.00	0.688	34.9
30.00	0.500	60.0
30.00	0.625	48.0

The second study on the strength of slip joint splices was funded by the Electric Power Research Institute (EPRI) to further explore the capacity of slip joints under flexural loading. The results of this study are presented by Donald D. Cannon, Jr. in “Strength and Behavior of Slip Splices in Tapered Steel Poles,” an unpublished report to be referenced in the upcoming edition of ASCE standard 48. For the experiments, slip joint splices constructed of dodecagonal cross-sections with varying taper and width-to-thickness ratios were tested until failure. Most of the sections had tapers of 0.3 inches per foot while a few of the test cases had tapers of 0.15 inches per foot, which is most similar to the 0.14 inches per foot taper used by the FDOT. The width-to-thickness ratios of the tested specimens were varied between 25.5, 29.4, and 34.8. These ratios are much lower than those tested in the Sumitomo study and are also slightly lower in some cases than the range of diameter-to-thickness ratios for the typical round sections

specified by the FDOT in its Cantilever Overhead Sign program (2007b). The graphical results of the test program indicate that in order for the ultimate moment and allowable moment of the section to equal one another, a splice length of at least 1.5 times the diameter of the pole should be used.

The most information pertaining to the design of slip joint splices can be found in ASCE Standard 48-05, *Design of Steel Transmission Pole Structures* (2006). Within the standard, information on the design, fabrication, and assembly of slip joints can be found. Regarding the strength design of the slip joint, the standard requires that it be able “to resist the maximum forces and moments at the connection” and also should be able to resist at least 50 percent of the moment capacity of the weaker pole used for assembly of the connection. Fabrication of the poles should take into account any tolerances for the manufacturing process and the established minimum and maximum allowable splice length. Rather than specify a required minimum splice length, the standard indicates a range of 1.42 to 1.52 times the diameter of the pole as having proven acceptable in field applications and only requires that the splice length be long enough to meet strength requirements for the connection and short enough not to exceed overall structure height limitations.

None of the above-mentioned specifications refer to the required wall thickness for use in slip joint connections. The AASHTO (2009) specifications define width-to-thickness ratios for round and multisided tubular sections with respect to local buckling in compression members and allowable bending stresses, but not specifically from concentrated forces perpendicular to the wall of the pole section. One possible source for determining the required wall thickness of the pole sections making up the slip joint splice comes from the *AISC Hollow Structural Sections (HSS) Connections Manual* (1997). The manual provides guidelines for designing HSS

with concentrated loads either transversely or longitudinally on the face of the section (Figure 3-2).

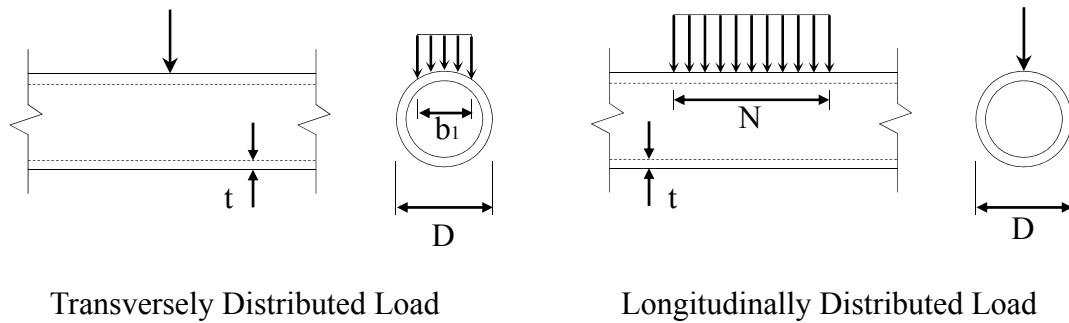


Figure 3-2. Concentrated loads on HSS (figure adapted from ASIC 1997)

To gauge the acceptability of the normal forces within the slip joint, the AISC *Hollow Structural Sections Connections Manual* (1997) may be referred for determining the value of acceptable concentrated forces on the face of the HSS. Within the specifications and commentary of the appendix, there are details on how to determine the design strength of unstiffened HSS subjected to concentrated loads. The case most similar to the loads acting on the slip joint is for concentrated loads perpendicular to the face of the HSS and distributed across some bearing length.

The first case presented is for concentrated loads distributed transversely over the perimeter of the cross-section. This case is discussed in Section 8.1 of the specification and is given as:

$$R_n = \frac{5F_y t^2}{1 - 0.81 b_1/D} Q_f \quad (3-1)$$

where

- $R_n$  = strength at locations of concentrated loads on unstiffened HSS, kip
- $F_y$  = yield stress of the pole, ksi
- $t$  = wall thickness, in
- $b_1$  = width of the load, in
- $D$  = outside diameter of round HSS, in
- $Q_f$  = 1 for tension in the HSS
- =  $1 - 0.3 f/F_y - 0.3(f/F_y)^2 \leq 1$  for compression in the HSS



$f$  = magnitude of maximum compression stress in HSS due to axial and bending at the location of concentrated force, ksi

The second case presented is for concentrated loads distributed longitudinally over some length of the member. This case is discussed in Section 8.2 and is given in the specification as follows:

$$R_n = 5F_y t^2 \left( 1 + 0.25 \frac{N}{D} \right) Q_f \quad (3-2)$$

where

- $R_n$  = strength at locations of concentrated loads on unstiffened HSS, kip
- $F_y$  = yield stress of the pole, ksi
- $t$  = wall thickness, in
- $N$  = bearing length of the load along the length of HSS, in
- $D$  = outside diameter of round HSS, in
- $Q_f$  = 1 for tension in the HSS  
 $= 1 - 0.3 f/F_y - 0.3(f/F_y)^2 \leq 1$  for compression in the HSS
- $f$  = magnitude of maximum compression stress in HSS due to axial and bending at the location of concentrated force, ksi

Both equations can be modified to account for concentrated point loads by setting the respective load width or bearing length to zero. Since point loads are applied over infinitesimally small areas, the results of simplifying both equations are the same. By substituting zero for  $b_1$  in Equation (3-1) and zero for  $N$  in Equation (3-2) both equations simplify to the same expression applicable to point loads on the face of the HSS:

$$R_n = 5F_y t^2 Q_f \quad (3-3)$$

where

- $R_n$  = strength at locations of concentrated loads on unstiffened HSS, kip
- $F_y$  = yield stress of the pole, ksi
- $t$  = wall thickness, in
- $Q_f$  = 1 for tension in the HSS  
 $= 1 - 0.3 f/F_y - 0.3(f/F_y)^2 \leq 1$  for compression in the HSS
- $f$  = magnitude of maximum compression stress in HSS due to axial and bending at the location of concentrated force, ksi

These considerations in the *HSS Connections Manual* (AISC 1997) specify concentrated force distributions along a length of wall of a single HSS section. This is commonly associated

with stiffeners and flanged sections that connect to a single section of HSS. When a single cross-section experiences pipe buckling, the pole wall may flare out on the sides as the face being loaded collapses inward toward the center of the cross-section. In the case of the slip joint, however, there are two cross-sections that make up the connection. The outer pole section provides confinement to the inner pole section, allowing it to resist pipe buckling under similar loading conditions (Figure 3-3).

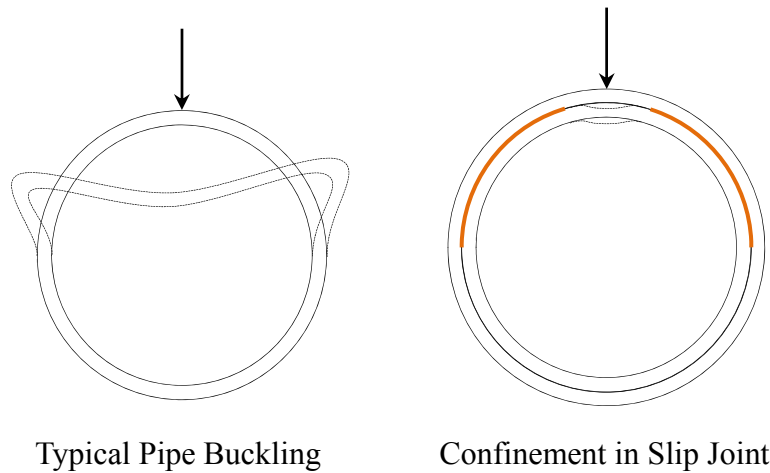


Figure 3-3. Confinement of the inner pole within a slip joint under concentrated load

Preliminary calculations using Equation (3-3) indicate that a wall thickness much greater than the typical 0.375 inches associated with a 16”-diameter pole is required to prevent pipe buckling. It is not expected that a wall thickness approximately three times that specified will be required, because of the confinement the outer pole section provides to the inner pole section. This confinement will allow the pole sections to resist a larger load than the equation predicts for the 0.375”- wall thickness. As a result, the equations for concentrated loads on the walls of HSS are not applicable to the scenario involving pipe buckling within a slip joint.

### 3.1.2 Bolted Connections

In the tapered bolted slip base connection, the slip joint is primarily responsible for transferring bending moments and the through-bolts are designed to transfer torsional loads from

the superstructure to the foundation. Therefore, the bolted connection in the slip joint must be designed to withstand the torsional loads produced by wind load on the signs connected to the cantilever mast arm. In order to determine the number of bolts needed in the connection, both the output from the FDOT Cantilever Sign Program, version 5.1 (2007) for the appropriate size upright members and the design capacities of the steel poles are reviewed. As such, the requirements for bolted connections set forth by AASHTO (2010) and AISC (2005) are considered. The test specimen is loaded until structural failure occurs, so it must be determined if the bolted portion of the connection can be designed to withstand as much or more torsion as the steel poles within the limited space of the slip joint splice.

One source for determining possible torsional loads to be carried through the base connection is the FDOT Cantilever Sign Program, version 5.1 (2007). The design variables considered were the height of the sign, wind location, wind speed, sign panel size, and sign position on cantilever. In addition, changes to the truss, web members, and chord members were made. The only variables left unchanged were those pertaining to the footing properties, which were set at the default program settings. Running various scenarios through the design program and focusing efforts on 16-inch diameter monopoles provides us with a possible maximum design torque of about 132 kip-ft. The output values of the design program are only intended to provide a point of comparison with the design values obtained from the AASHTO and AISC design specifications. If the bolted connection can be designed to exceed the output values from the software program, then the through-bolts are a feasible part of the connection design.

The monopole for the superstructure of the test apparatus was made of a round, tapered steel pole. Since the bolts in the proposed base connection are through-bolts and are required to carry the torsional loads from wind on the cantilever portion of the superstructure, the torsional

loads need to be converted to a shear load parallel to the circumference of the monopole in order to determine the appropriate loads to be carried by the bolts. In other words, whatever torsion value is determined to be appropriate for design of the connection needs to be adjusted so that the equivalent shear load is applied along the shear plane between the two pole sections.

The type of bolted connection needs to be taken into consideration when designing the through-bolts. A snug-tight connection is typical when bolts are in direct bearing and the plies to be connected are in firm contact. Pretensioned connections have a greater degree of slip-resistance and are common in joints that experience cyclic and fatigue loads. Slip-critical connections are used when slippage at the faying surfaces is considered to be a failure. In other words, the applied load is greater than the frictional resistance between the surfaces (AISC 2005). Although the monopole of the superstructure should not freely rotate about the embedded pole, small slips of the monopole bearing on the bolts should not be considered a failure in this design. Careful consideration should be given to the type of bolted connection to be specified, because the walls of HSS and presumably tapered poles tend to be too flexible to resist any pretensioning of bolts (AISC 2005). If it is assumed that tapered poles are equally as flexible as a comparable HSS member, then snug-tightening of the through-bolts has to be sufficient for use in the slip joint.

The two design codes to be considered for designing the bolted portion of the proposed alternate base connection for overhead cantilever signs are the *Standard Specifications for Structural Supports for Highway Signs, Luminaires and Traffic Signals* (AASHTO 2009) and the *Steel Construction Manual* (AISC 2005). It should be noted that the AASHTO specification for structural supports refers designers to the *LRFD Bridge Design Specifications* (AASHTO 2010) for the design of bolted of connections. For the purpose of highway signs, the AASHTO

specifications dictate the actual design, but for the purpose of designing the test program both AASHTO and AISC specifications were examined. The sections that follow describe the design equations outlined by these specifications for each applicable failure mode of the bolted connection.

### 3.1.2.1 Nominal shear resistance

It should be noted that since the bolts pass through the diameter of the steel pipe, each bolt contributes two shear reactions to the connection (Figure 3-4). Therefore, the number of through-bolts is half the value used for fasteners in many of the following equations from both AISC and AASHTO. The AISC equations for bolted connections come from Chapter J of the specification. In AISC Section J3.6, equation J3-1, the shear strength is provided per bolt per shear plane between two flat plates. The equation as it is shown below is slightly modified to include variables to account for multiple fasteners and shear planes as necessary:

$$R_n = F_{nv}A_b n N_s \quad (3-4)$$

where

- $R_n$  = nominal shear strength, kip
- $F_{nv}$  = nominal shear stress in bearing-type connections, ksi
- $A_b$  = nominal unthreaded body area of the bolt or threaded part, in<sup>2</sup>
- $n$  = number of bolts (assuming a flat plate connection)
- $N_s$  = number of shear planes per bolt

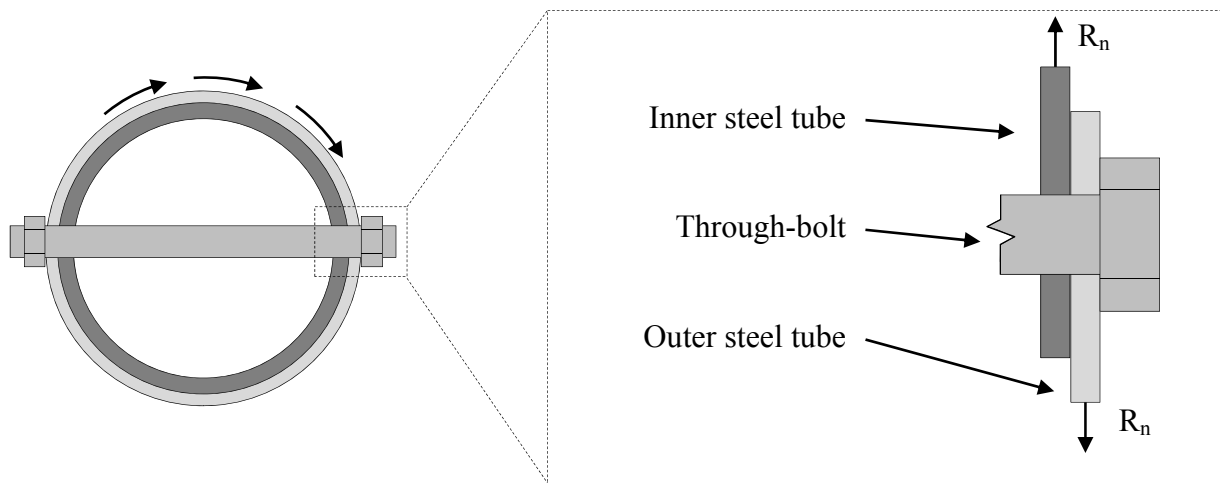


Figure 3-4. Shearing reactions on through-bolts due to torsion in the poles

The AASHTO design equations for bolted connections are found in Section 6.13.2 of the 2010 *LRFD Bridge Design Specifications*, in which shear resistance is specified in article 6.13.2.7. The shear resistance of a single high-strength bolt in a joint consisting of flat plates can be determined from equation 6.13.2.7-2 for the case when threads are included in the shear plane. The equation as it is given below has been modified to include a term to account for multiple fasteners:

$$R_n = 0.38nA_bF_{ub}N_s \quad (3-5)$$

where

- $R_n$  = nominal shear strength, kip
- $F_{ub}$  = specified minimum ultimate tensile strength of the bolt, ksi
- $A_b$  = area of the bolt at the nominal diameter, in<sup>2</sup>
- $n$  = number of bolts (assuming a flat plate connection)
- $N_s$  = number of shear planes per bolt

### 3.1.2.2 Bearing at bolt holes

In section J3.10 of the AISC specification, the design equation for bearing strength at bolt holes can be found. For a bolt in a connection with standard holes when deformation at the bolt hole at service load is a design consideration, equation J3-6a is used:

$$R_n = 1.2L_c t F_u \leq 2.4dt F_u \quad (3-6)$$

where

- $R_n$  = nominal bearing strength, kip
- $F_u$  = specified minimum tensile strength of connected material, ksi
- $L_c$  = clear distance in the direction of force between edges of adjacent holes or the edge of the material, in
- $t$  = thickness of the connected material, in
- $d$  = nominal bolt diameter, in

The bearing resistance at the bolt holes in a connection is discussed in article 6.13.2.9 in the 2010 AASHTO *LRFD Bridge Design Specifications*. In this case, the specifications in the AASHTO code match those from the requirements of the AISC specification given in Equation (3-6) above. The appropriate equations for this scenario is equation 6.13.2.9-1 and 6.13.2.9-2 in the AASHTO specification, which calls for bolts spaced at a clear distance between bolt holes

and the member end no less than two times the diameter of the bolt. As noted in the commentary, the nominal bearing resistance of the connected member can be taken as the sum of the resistances of each bolt hole in the connection.

### 3.1.2.3 Special consideration for through-bolting HSS members

In Section J3.10(c) as well as in Part 7 of the AISC *Steel Construction Manual* (2005), the specification describes special considerations for through-bolting to HSS members. In Part 7 of the manual, it explains that the flexibility of the walls of HSS members preclude the use of pretensioned bolts. Another important note is that the bolts are designed for static shear in the specification rather than torsion as in the base connection. The connection should be designed for bolt bearing under static shear using equation J7-1:

$$R_n = 1.8nF_yA_{pb} \quad (3-7)$$

where

$R_n$	=	nominal bearing strength, kip
$F_y$	=	specified minimum yield stress of connected material, ksi
$A_{pb}$	=	projected bearing area of the bolt on the connected material, in <sup>2</sup>
$n$	=	number of fasteners

As noted above, this consideration in the AISC specification is specific to through-bolts in static shear rather than torsion as is the case of the through-bolts in the tapered bolted slip base connection (Figure 3-5). What this might possibly mean is that the number of bolts required to maintain a given shear resistance is only half of the value obtained when solving for  $n$ . This is also seen in the shear resistance and bolt bearing equations above where each bolt contributes two shear reactions along the line of action of the applied force.

Another point to consider is that neither AASHTO specification appears to have a design consideration for this particular scenario of through-bolting HSS members to transfer torsion. The specifications appear to focus on through-bolting as a way to secure two adjacent members together, rather than connect two overlapping members. An examination of the sections on steel

HSS design in the *LRFD Bridge Design Specifications* (AASHTO 2010), the *Standard Specifications for Structural Supports for Highway Signs, Luminaries and Traffic Signals* (AASHTO 2009), as well as the *Hollow Structural Sections Connections Manual* (AISC 1997) did not reveal any guidelines specifically for this type of through-bolted connection.

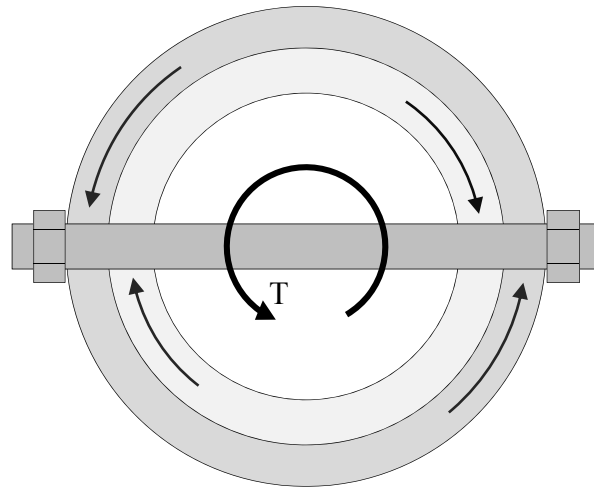


Figure 3-5. Reactions in HSS section at through-bolt due to an externally applied torsion

### 3.1.3 Steel Pole Strength

Current base connections used most frequently involve an annular base plate welded to the base of the monopole, which is then connected to the foundation with anchor bolts. With a slip joint connection, a steel pole overlaps another pole section protruding from the foundation. This configuration results in new, induced force interactions between the members of the two pole sections making up the slip joint connection (Cook et al 2003). These interactions need to be checked against the strength of the steel pole members to prevent any localized failures (Figure 3-6). Although the poles being tested are tapered, the same approach for determining the strength of hollow structural sections (HSS) can be used in this experiment.



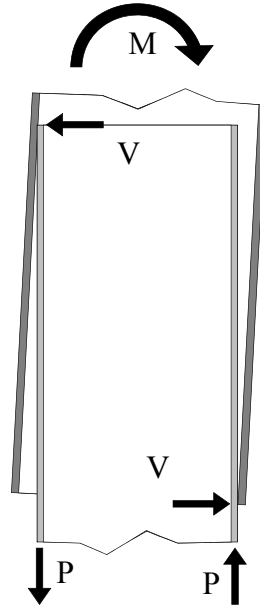


Figure 3-6. Forces induced on steel poles by the transfer of moment through a slip splice

### 3.1.3.1 Bending moment resistance

When calculating bending moment resistance for HSS members, both the AISC and AASHTO codes specify a limiting width-to-thickness ratios for the classification of steel sections with regard to local buckling. In both codes, HSS16x0.375 members with a minimum specified yield strength of 55 ksi meet the requirements for compact sections, which indicates that they will develop their plastic moment in bending before the onset of premature buckling (AASHTO 2009; AISC 2005). Therefore, the following calculations apply to compact sections as appropriate.

In the AISC specification, the nominal flexural strength is selected as the minimum value obtained from the evaluation of the limit states of yielding and local buckling. Since the section has already been determined to be compact, the limit state of local buckling can be ignored as per Section F.8.2(a). From Section F8.1, the yield moment can be calculated from equation F8-1 as:

$$M_n = F_y Z \quad (3-8)$$

where  $M_n$  = nominal flexural strength, kip-in

$$F_y = \text{specified minimum yield stress of material, ksi}$$

$$Z = \text{plastic section modulus, in}^3$$

The information in Section 6.12.2.2.3 of the 2010 AASHTO *LRFD Bridge Design Specifications* yields the same equation and results for a compact section as the AISC code. However, the 2009 AASHTO *Standard Specifications for Structural Supports for Highway Signs, Luminaries and Traffic Signals* uses an allowable stress design approach to arrive at an allowable bending stress with an included factor of safety of 1.5 for round hollow members. The equation for compact sections comes from AASHTO (2009) Table 5-3:

$$F_b = 0.66F_y \quad (3-9)$$

where

$$F_b = \text{allowable bending stress, ksi}$$

$$F_y = \text{specified minimum yield stress of material, ksi}$$

### 3.1.3.2 Shear resistance

As can be seen in Figure 3-6 above, the use of a slip joint splice to transfer bending moments creates localized shear forces on the walls of the steel tubing. This induced shear must be checked against the nominal shear strength of the member. The AISC code provides the design considerations for shear in Section G6 for round HSS members. The AISC commentary acknowledges that there is little information available with regard to round HSS members subjected to transverse shear and references to studies of torsional tests on the local buckling of cylinders as the chosen method of deriving the shear equations. Equations G6-1, G6-2(a), and G6-2(b) determine the nominal shear strength with respect to shear yielding and shear buckling as follows:

$$F_{cr} = \text{maximum} \left[ \frac{1.60E}{\sqrt{\frac{L_v}{D} \left(\frac{D}{t}\right)^{5/4}}}, \frac{0.78E}{\left(\frac{D}{t}\right)^{3/2}} \right] \leq 0.6F_y \quad (3-10)$$

$$V_n = \frac{F_{cr} A_g}{2} \quad (3-11)$$

where

- $V_n$  = nominal shear strength, kip
- $A_g$  = gross area of HSS section based on design wall thickness, in<sup>2</sup>
- $D$  = outside diameter, in
- $L_v$  = distance from maximum to zero shear force, in
- $E$  = modulus of elasticity, ksi
- $F_y$  = specified minimum yield stress of material, ksi
- $t$  = design wall thickness, in

The note in Section G6 explains that shear buckling typically controls for diameter-to-thickness ratios over 100, high-strength steels, and long lengths. Since the HSS used for this experiment and in the field does not meet these restrictions, the shear yielding condition controls, so that  $F_{cr} = 0.6 F_y$ .

The AASHTO allowable stress for support structures is also based on elastic torsional buckling of long, cylindrical tubes (2009). Therefore, there is not a separate consideration for the allowable torsional stress of round tubular members. The design calculations for shear come from Section 5.11.1, equations 5-11 and 5-12, which include a factor of safety of 1.75:

$$\text{When } \frac{D}{t} \leq 1.16 \left( \frac{E}{F_y} \right)^{2/3}$$

$$F_v = 0.33 F_y \quad (3-12)$$

otherwise

$$F_v = \frac{0.41 E}{\left( \frac{D}{t} \right)^{3/2}} \quad (3-13)$$

where

- $F_v$  = allowable shear stress, ksi
- $D$  = outside diameter, in
- $E$  = modulus of elasticity, ksi
- $F_y$  = specified minimum yield stress of material, ksi
- $t$  = design wall thickness, in

### 3.1.3.3 Torsional resistance

As mentioned before, the AASHTO code does not provide a separate provision for the analysis of torsional strength of HSS members used as structural supports for signal and sign structures. However, the AISC specification provides equations H3-1, H3-2(a), and H3-2(b) in Section H3.1 for calculating the nominal torsional strength of round HSS. As in the other cases, the limit state of yielding and buckling are taken into consideration by the following equations:

$$T_n = F_{cr}C \quad (3-14)$$

$$F_{cr} = \text{maximum} \left[ \frac{1.23E}{\sqrt{\frac{L}{D} \left(\frac{D}{t}\right)^{5/4}}}, \frac{0.60E}{\left(\frac{D}{t}\right)^{3/2}} \right] \leq 0.6F_y \quad (3-15)$$

where

- $T_n$  = nominal torsional strength, kip-in
- $C$  = torsional constant, in<sup>3</sup>
- $F_y$  = specified minimum yield stress of material, ksi
- $D$  = outside diameter, in
- $E$  = modulus of elasticity, ksi
- $L$  = length of member, in
- $t$  = design wall thickness, in

### 3.1.3.4 Interaction of bending moment, axial load, shear, and torsion

As with any support member being exposed to a variety of forces, the interaction of the simultaneous application of these forces must be taken into consideration when the structure is being designed (Figure 3-7). In the AISC code, section H3.2 defines the conditions for which equation H3-6 should be used. When the required torsional strength of an HSS member exceeds 20 percent of the available torsional strength, the AISC code calls for the interaction of torsion, shear, flexure, and/or axial force to be limited by the following relationship:

$$\left(\frac{P_r}{P_c} + \frac{M_r}{M_c}\right) + \left(\frac{V_r}{V_c} + \frac{T_r}{T_c}\right)^2 \leq 1.0 \quad (3-16)$$

where

- $P_r$  = required axial strength using applicable load combinations, kip
- $P_c$  = applicable design tensile or compressive strength, kip

- $M_r$  = required flexural strength using applicable load combinations, kip-in
- $M_c$  = applicable design flexural strength, kip-in
- $V_r$  = required shear strength using applicable load combinations, kip
- $V_c$  = applicable design shear strength, kip
- $T_r$  = required torsional strength using applicable load combinations, kip-in
- $T_c$  = applicable design torsional strength, kip-in

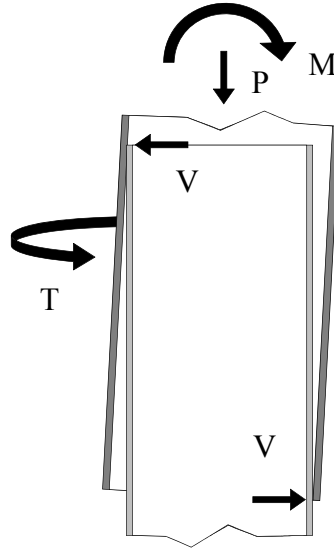


Figure 3-7. Interaction of forces at the slip joint base connection

The 2009 AASHTO code specifies a similar interaction relationship for vertical, cantilever pole supports subjected to combinations of bending, shear, compression, and torsion. Section 5.12.1 provides the interaction equation for the allowable combination of stresses on the member. In this equation, as mentioned in previous sections, the shear term applies for both shear and torsion under the AASHTO guidelines:

$$\frac{f_a}{0.6F_y} + \frac{f_b}{C_A F_b} + \left(\frac{f_v}{F_v}\right)^2 \leq 1.0 \quad (3-17)$$

- where
- $f_a$  = computed axial stress, ksi
  - $F_y$  = specified minimum yield stress of the material, ksi
  - $f_b$  = computed bending stress, ksi
  - $C_A$  = coefficient for amplification to account for secondary moments
  - $F_b$  = allowable bending stress, ksi
  - $f_v$  = computed shear stress, ksi
  - $F_v$  = allowable shear stress, ksi

### 3.2 Experimental Design

The experimental program for testing the tapered bolted slip base connection has been designed so that much of the test apparatus from the previous two research projects related to this topic, FDOT reports BD545-54 and BDK75 977-04, can be utilized again. As in the previous cases, the test apparatus must provide a fixed-base support to simulate the foundation of a typical cantilevered sign or signal structure. The load applied to the test apparatus must also generate both a large flexural and torsional response in the system. For these reasons, a test apparatus similar to the ones used previously is beneficial for this testing program. It also allows another opportunity to test the embedded pipe with welded plate assembly that is proposed to replace anchor bolts in FDOT report BDK75 977-04.

The basis for the test apparatus was first established in FDOT report BD545-54. It was originally designed to be a half-scale model of one of the cantilever sign specimens that failed along Interstate 4 near Orlando, Florida during the hurricane season of 2004. Staying in line with this intent, the following test program also made use of this half-scale model with variations as appropriate. Taking into consideration the purposes of those test programs, which in both cases ultimately involved failing the concrete foundation, modifications can again be made to the design of the test apparatus to meet the needs of the current test program.

Unlike the two previous projects, which focused primarily on the interactions happening within the concrete foundations of cantilever signal and sign structures, the intent of this project is to examine how the base connection above the concrete is able to transfer flexural and torsional loads. As such, it is imperative that the concrete foundation not fail during testing. To ensure this, the design procedure developed by Cook and Jenner (2010) to calculate the strengths for various concrete failure modes using the embedded pipe and plate assembly is used to determine the appropriate diameter of the reinforced concrete pedestal to be constructed for

testing. By increasing the capacity of the concrete pedestal and eliminating all other failure modes, the concentration of the testing efforts were centered on the interactions with the through-bolts and tapered poles along the length of the slip joint.

A summary of the components for the test apparatus, which applies both flexural and torsional loads simultaneously to the slip joint connection, is as follows:

- A reinforced concrete block (6' x 10' x 2'-6") provides the fixed support at the base of the concrete pedestal. The design for the concrete block is the same as used in the previous projects.
- Two tie-down assemblies made of C12x30 channels and flat plates secure the reinforced concrete block to the floor. These assemblies are the same ones used for the previous testing programs.
- A reinforced concrete pedestal (3' in diameter and 3' deep) extends out from the large face of the reinforced concrete block.
- One tapered steel pole (16" in diameter at the largest point, 3/8" thick, 8'-4" long, and 0.14" diameter per 1' length taper) is embedded 24" into the reinforced concrete pedestal. The embedded portion of this pole is welded with four torsional stiffener plates (1" x 1" x 7") and a flexural stiffener, or annular, plate (20" outer diameter, 1" thick) to match the embedded pipe and plate assembly used in FDOT report BDK75 977-04.
- One tapered steel pole (16" diameter at the largest point, 3/8" thick, 8'-4" long, and 0.14" diameter per 1' length taper) is slipped over the embedded steel pole. The small end of this pole is welded to an annular plate (24" outer diameter, 1" thick) with 12 – 1 3/4" diameter bolt holes to connect to the lever arm assembly.
- Five bolt holes (1 5/16" diameter, spaced 4" apart) drilled through the overlapping portion of the two steel poles that makes up the slip joint connection.
- Three A307, grade 60 threaded rods (1 1/4" diameter, 20" long) and associated nuts and washers through-bolt the two tapered steel poles together in the first test.
- Five A193, grade B7 threaded rods (1 1/4" diameter, 20" long) and associated nuts and washers through-bolt the two tapered steel poles together in the second test.
- One lever arm assembly (HSS16x0.500, 10' long) attaches to the annular plate on the second tapered steel pole. This assembly is the same one used in the previous test programs.
- Twelve A490 bolts (4.5" long, 1.5" diameter) and associated nuts and washers connect the second tapered pole and the lever arm assembly.

### **3.3 Equipment and Materials**

In order to ensure the test apparatus would perform as desired, each of its components was carefully designed to preclude unwanted failures. As previously mentioned, the test program is designed to examine the behavior of the slip joint connection that is located above the concrete foundation. Therefore, the concrete components, in addition to the steel poles and lever arm assembly, must not fail during testing. The construction drawings detailing the various components of the test apparatus are located in Appendix B.

#### **3.3.1 Reinforced Concrete Block and Tie-downs**

The reinforced concrete block and tie-down assemblies provide a fixed support for the base of the cantilever system. The reinforced concrete block, as previously designed according to the American Concrete Institute (ACI) specifications, provides ample capacity for this test program and was reconstructed for use. To recap Cook and Halcovage (2007), the design of the block takes into consideration both the strut-and-tie model as well as beam theory to provide adequate reinforcement (ACI 2008). The reinforcement within the block consists of two main parts. First, the concrete block includes six No. 8 reinforcement bars spaced 9" apart with 12" hooks at each end. These No. 8 bars, three each in the top and bottom faces of the block once it is placed in position for testing, are situated along and run parallel to the long edge of the block. Second, there are two reinforcement cages constructed of No. 4 reinforcement bars in the front and back faces. These reinforcement cages provide a 9.5" x 11" grid in the vertical planes of the block when in position for testing (Figure 3-8).

In order to ensure that the concrete block can resist any overturning moments generated during testing, two tie-down assemblies hold the reinforced concrete block against the floor. As with the block, the tie-downs were previously designed for FDOT report BD545-54 and used again in FDOT report BDK75 977-04. The tie-downs are assembled from C12x30 steel channels



and ½”-thick steel plates. They are then connected to the floor using 1 ½”-diameter threaded rods (Figure 3-9). It is also important to note that in addition to the overturning moment, the bearing capacity of the reinforced concrete block was checked to prevent any localized crushing failures where the tie-downs are in contact with the block.

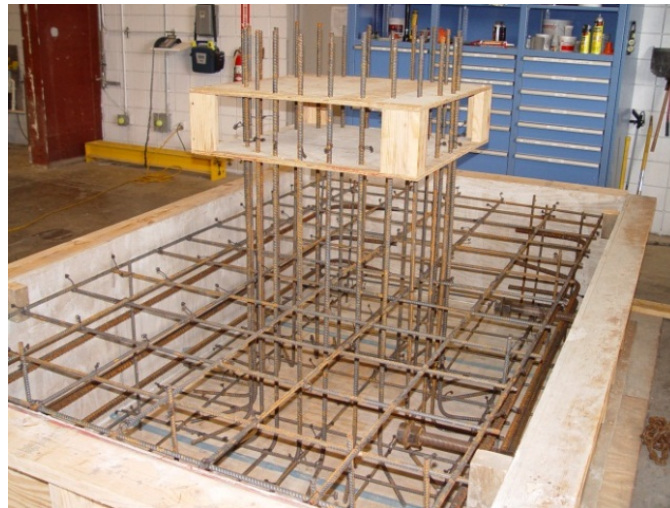


Figure 3-8. Reinforcement cage for the concrete block. Photo courtesy of FDOT.



Figure 3-9. Tie-down assemblies connecting the base of the test apparatus to the lab floor. Photo courtesy of FDOT.

### **3.3.2 Reinforced Concrete Pedestal**

The reinforced concrete pedestal provides the foundation for the steel pole assembly and is connected to the reinforced concrete block. In the original half-scale model presented in FDOT report BD545-54, the pedestal diameter was determined to be 30 inches. However, in that test and the tests completed for FDOT report BDK75 977-04, the pedestal was designed purposefully to fail under the applied loads. For this testing program, it is imperative that the pedestal not fail before any component of the bolted slip joint connection. Therefore, the pedestal diameter is enlarged to 36" to increase the capacity of the pedestal to exceed that of the steel poles used in the connection.

The reinforcement for the concrete pedestal includes both longitudinal and hoop steel. The longitudinal reinforcement consists of 24 No. 5 bars that originate within the reinforced concrete block. They are evenly spaced within the 32"-diameter hoop steel arrangement. There are also 11" hooks at the end of each longitudinal reinforcement bar, which are placed in the concrete block on the outer face of the rear reinforcement cage. The hoop steel is constructed of No. 3 bars, spaced 2" on center, about a 32" diameter. This provides 2" of cover around the circumference of the pedestal and at least 5" of clearance between the longitudinal reinforcement and embedded pole assembly at the widest point where the annular plate is located.

The design of the reinforced concrete pedestal is based on the method developed by Cook and Jenner (2010) in Appendix B of FDOT report BDK75 977-04, because the end of the steel pole, which is modified to include torsional and flexural stiffener plates, is embedded in the concrete pedestal. Using this method, the capacity of the pedestal is examined by taking into consideration the transfer of load from the embedded pole assembly and the strength of the reinforced pedestal. The following predictions are made assuming a minimum compressive concrete strength of 5,500 psi.

Examining the concrete capacity with respect to the embedded pole assembly, which includes torsional and flexural stiffener plates, four failure modes must be considered when both torsional and flexural loads are being applied. The torsional stiffener plates have an equivalent torsional concrete breakout from shear parallel to an edge of 507 kip-ft. They also have an equivalent torsional concrete breakout due to side face blowout of 713 kip-ft. According to the method, the annular plate can be divided into four distinct flexural stiffener plate areas. These flexural stiffener plates are determined to have an equivalent flexural concrete breakout from shear parallel to an edge of 390 kip-ft. There is also an equivalent flexural concrete breakout due to side face blowout of 506 kip-ft.

In addition, the capacity of the reinforced concrete pedestal should be evaluated with respect its flexural and torsional strengths. The flexural strength of the pedestal is evaluated by taking into consideration the longitudinal reinforcement and using the ACI 318 (2008) stress block. The flexural capacity is determined to be approximately 448 kip-ft. The torsional capacity of the pedestal is determined for three stages of loading. The threshold torsion is calculated to be 57 kip-ft followed by a cracking torsion of 226 kip-ft. Finally, the designed failure torsion for the pedestal is calculated as 444 kip-ft.

### **3.3.3 Tapered Steel Poles**

In order to create the bolted slip base connection, tapered poles were chosen to eliminate the need for high-strength grout and set screws. This simplifies the connection design as well as the construction. Slip joints are commonly found in various field applications and are detailed in the FDOT design standards for high mast lighting, Index 17502, and cantilever mast arm assemblies for traffic signals, Index 17745. In each case, the slip joint is made between two tapered sections. The typical taper for various signal and sign structures is 0.14 inches in

diameter per 1 foot of length of the pole and can be found in these design standards as well as the design standard for steel strain poles, Index 17723 (FDOT 2010).

The diameter and thickness of the tapered poles were chosen initially in accordance with the aforementioned half-scale model implemented in the previous test programs, which used a typical AISC hollow structural section (HSS) of HSS16x0.500. This section was chosen for its strength to prevent failure of the steel pole before the concrete foundation in those tests. However, for the purpose of the current tests, a more common section was chosen to duplicate those poles used in field applications. By choosing to keep a 16"-diameter section and adjust the thickness, the overall design of the test apparatus from the half-scale model can still be utilized. Starting with the FDOT Cantilever Sign Program, it was determined that the wall thickness of a typical 16"-diameter pole is 0.375" when using HSS sections for the upright member. Since this is a typical section size, it is the starting point for calculating the strength required of a similar tapered section.

The lengths of the two steel poles were initially chosen to provide a flexure-to-torsion ratio that matches the ratio of 8:9 used in the previous projects. The lower pole was intended to be a minimum of 6'-6" long with a 16" base diameter. In conjunction with a 7'-5" long upper pole, the theoretical length of the slip joint could be predicted to equal 1.5 the diameter of the pole section plus 6" to allow for slip assuming that the two pole sections are perfectly circular and fit together seamlessly. However, discussions with representatives of the manufacturer, Valmont Structures, Inc., revealed that the lengths and diameters of the two pole sections should be the same. The primary reason is to make certain the lower pole is long enough to allow for adequate slip length without interference from the access panel when placing the upper pole. Secondly, manufacturing poles of the same dimensions makes machining the sections simpler and also

results in a longer theoretical slip joint. This is beneficial, because any imperfections in the shape of the poles as well any added wall thickness from galvanization hinders slip and decreases the slip joint length. The longer theoretical slip joint length could also allow extra room for the placement of the necessary number of through-bolts. As a result, the final design length of each pole section is 8'-4" and the diameter is 16" at the large end (Figure 3-10). The actual length of the slip joint was determined during assembly and adjustments to the location and placement of through-bolts made as necessary.



Figure 3-10. Tapered steel poles manufactured by Valmont Structures. Photo courtesy of FDOT.

In order to design a steel pole, the type of material and its strength must be known. Initially, in accordance with the FDOT specifications Index 17310 for the upright members of cantilever sign structures, the minimum specified yield strength was chosen as 42 ksi. However, it was noted that the minimum specified yield strength of upright members used in high mast lighting applications ranges from 50 ksi to 65 ksi as indicated by Index 17502 (FDOT 2010). After speaking with representatives at Valmont Structures, the manufacturer of the tapered steel poles used for testing, it was determined that the most common structural material used in the manufacture of tapered steel poles for use in Florida is ASTM A572 grade 55, which has a minimum yield strength of 55 ksi (ASTM 2007).

Using the AISC and AASHTO specifications, an HSS16x0.375 section can be evaluated for bending, torsion, shear, and axial forces. Using a minimum yield strength of 55 ksi and the equations discussed previously in section 3.1.3, the capacity of a similar tapered pole can be estimated. Both the AISC and the AASHTO specifications first examine the diameter-to-thickness ratio of hollow sections to determine if particular failure modes must be included in the design process. The section chosen for testing is classified as compact, so local buckling should not be a concern. An HSS section with these material properties has a nominal flexural capacity of 392 kip-ft, torsional capacity of 360 kip-ft, and a shear capacity of 234 kip when evaluated independently of one another. For this test program, the axial load on the test specimen is negligible, since the pole is oriented horizontally, and the shear load was largely ignored since the applied load at the end of the lever arm results in a relatively small shear on the test pole relative to its capacity. The interaction of flexure and torsion being applied concurrently to a steel pole, the capacities are reduced to 288 kip-ft and 185 kip-ft, respectively.

#### **3.3.4 Threaded Rods**

The through-bolts for the tapered bolted slip base connection were shorter segments cut from continuously threaded rods. The threaded rod was cut into 20" sections that allowed a minimum of 2" on either end for the placement of washers and nuts. The threaded rod for use in the first test were made of ASTM A307, grade A steel with a zinc-plated, anti-corrosive coating. This grade of A307 steel has a minimum specified tensile strength of 60 ksi and no specified yield strength (ASTM 2003a). The threaded rod for use during the second test was to be made of ASTM A193, grade B7 steel with a zinc-plated, anti-corrosive coating. This grade of A193 steel has a minimum specified yield strength of 105 ksi and a minimum specified tensile strength of 125 ksi (ASTM 1993a), which is comparable to commonly used ASTM A325 structural bolts (ASTM 2002a).

For the purposes of testing, a 1.25"-diameter bolt is chosen for the through-bolted connection within the slip joint region. This diameter was chosen because it is similar in size to the diameter of anchor bolts used in the half-scale model for FDOT report BD545-54, and it also minimizes the number of bolts needed in the connection. This size bolt also limits the mode of bolt failure to a shear failure, whereas a larger diameter through-bolt would be susceptible to a bearing failure. Using the AASHTO and AISC design specifications, the nominal shear strength and nominal bearing resistance of a bolted connection using each material is determined. Since each through-bolt contributes two bolt reactions, one at each end of the through-bolt, the total AASHTO shear resistance per through-bolt provided for each type of material is 56 kips for A307 and 117 kips for A193.

Ultimately, the goal of including the through-bolts in the connection is to successfully resist normal torsional loads encountered by cantilevered signal and sign structures, but to fail under unusually high torsional loads before another component of the structure is in danger of failing. In order to determine if this is feasible, the through-bolts in the slip joint connection must be tested to determine if they will fail in accordance with the AASHTO specifications currently in use. It is expected that three 1.25"-diameter A307 through-bolts on a 16" diameter shear plane will experience failure controlled by a nominal shear reaction equivalent to 112 kip-ft of applied torsion while five A193 through-bolts have a capacity of 389 kip-ft of applied torsion. Given the assembled length of the slip joint and the real location of the through-bolts, the actual average shear plane diameter along the tapered slip joint can be determined to calculate a more accurate applied torsion load required to cause failure of the through-bolts.

In addition to the threaded rods used to make the through-bolts, a type of structural washer and heavy hex nut is also required to complete the connection. The structural washer chosen for

use in the test apparatus is a mechanically galvanized structural washer made of ASTM F436 steel (ASTM 2003b). The heavy hex nut selected for use with the A307 threaded rods is made from ASTM A563, grade A material designed for rods with 7 threads per inch (ASTM 2000). Since the A139 B7 threaded rods have 8 threads per inch, a nut made of ASTM A194, grade 2H steel and is cadmium plated for corrosion resistance is selected (ASTM 1993b). Each through-bolt is fitted with a structural washer and heavy hex nut at each end to fasten it to the sections of steel pole that form the slip joint.

### **3.3.5 Lever Arm Assembly**

The lever arm assembly allows both a torsional and flexural load to be applied to the bolted slip base connection at once. A point load at the end of the lever arm simulates the type of load associated with horizontal wind loads on cantilevered signal and sign structures. Since at no point is it desirable for the lever arm to fail during testing, it is designed using an HSS16x0.500 section that has a larger wall thickness and capacity than the 0.375" thick poles used to build the slip joint connection. The same lever arm used in the previous project testing was used for this test program. The lever arm was constructed using steel with a minimum yield strength of 42 ksi.

The lever arm was previously designed in FDOT report BD545-54 and has been determined to be adequate for use in this testing program. The lever arm measures 10' on its longest edge and roughly 8'-8" on its shortest edge. The HSS section is welded to a metal plate at 45 degrees and a second shorter section of HSS to create an elbow that allows the arm to connect to the tapered test poles by way of an annular plate (Figure 3-11). The applied load is located 6" from the free end of the lever arm, which creates a torsional arm of 9' from the point of load application to the longitudinal axis through the center of the slip joint.



Based on AASHTO and AISC design standards, the lever arm has a nominal flexural capacity of 392 kip-ft. The lower yield strength and greater wall thickness of the lever arm assembly is offset by the higher yield strength and lesser wall thickness of the slip joint pole assembly, which is why both have a similar calculated flexural capacity. The flexural reaction of the lever arm translates into a torsional reaction in the poles of the slip joint assembly, which has been calculated to be 360 kip-ft. Therefore, the flexural capacity of the lever arm well exceeds the torsional capacity of the slip joint assembly. The nominal torsional capacity of the HSS16x0.500 is 359 kip-ft, and so the smaller side of the lever arm elbow has a capacity that roughly matches that of the slip joint assembly.

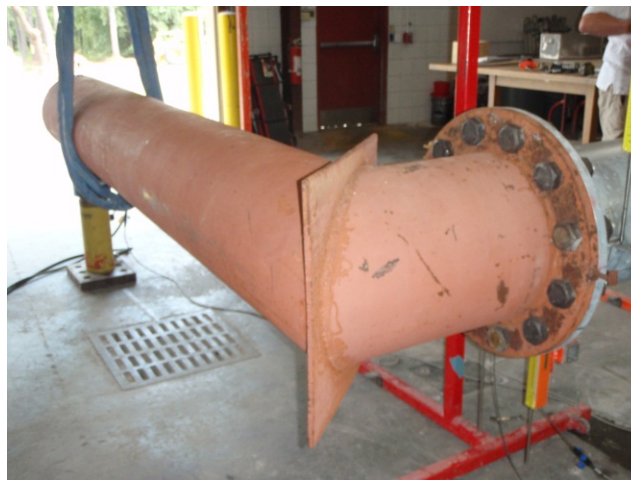


Figure 3-11. Lever arm assembly for test apparatus. Photo courtesy of S. Dalton.

### **3.3.6 Summary of Test Apparatus**

The components of the test apparatus have been specified to meet the structural requirements of the experiments to be conducted. The details of each design are found in the respective sections above and a summary of the major components is in Table 3-2. In an attempt to ensure that each test would perform as desired and that the appropriate failure modes occurred, each component of the test apparatus was designed to exclude unwanted failure modes (Table 3-3). Appendix A includes an example of this procedure, but uses the actual material strengths.

Table 3-2. Summary of testing materials and minimum material strengths

Item	Material grade	Minimum specified strength
Concrete	Class IV	5,500 psi
Tapered steel poles	ASTM A572, gr. 55	55 ksi (yield)
Threaded rods		
Test 1	ASTM A307, gr. 60	60 ksi (tensile)
Test 2	ASTM A193, gr. B7	125 ksi (tensile)
Washers	ASTM F436	
Nuts		
Test 1	ASTM A563, gr. A	
Test 2	ASTM A194, gr. 2H	

Table 3-3. Predicted failure loads with minimum specified material strengths

Failure mode	Predicted failure moment (kip-ft)	Predicted failure load* (kip)
Concrete block test frame (5,500 psi concrete)		
Strut-and-tie torsion	451	50.1
Strut-and-tie moment	705	50.1
Embedded pipe and stiffeners (5,500 psi concrete)		
Equivalent torsion from shear parallel to an edge	507	47.9
Equivalent torsion from side face blowout	713	67.3
Equivalent flexure from shear parallel to an edge	390	23.7
Equivalent flexure from side face blowout	506	30.7
Circular shaft - 36" (5,500 psi concrete)		
Threshold torsion**	57	-
Cracking torsion**	226	-
Torsion (rebar)	444	49.3
Flexure (rebar – assume 17 bars yield)	448	32.0
Lever arm - HSS16x0.500 (42 ksi steel)		
Torsion	359	39.9
Flexure	392	43.6
Steel poles - 16" x 0.375" (55 ksi yield)		
Torsion only	360	40.0
Flexure only	392	28.0
Interaction torsion	185	20.6
Interaction flexure	288	20.6
Through-bolts - AASHTO shear resistance		
3 - 1.25"-diameter ASTM A307 (60 ksi tensile)	112	12.5
5 - 1.25"-diameter ASTM A193 (125 ksi tensile)	389	43.3

\* The predicted failure load assumes a torsion arm of 9 feet and moment arm of 14 feet.

\*\* Not a failure mode.

## CHAPTER 4 IMPLEMENTATION OF TEST PROGRAM

The following sections include a discussion of the implementation of the test program. This includes a description of the process involved in gathering the actual material strengths for the components of the test apparatus as well as refining calculations for the design of the test apparatus based on these values. A detailed explanation regarding the instrumentation required to monitor the behavior of the tapered bolted slip base connection while transferring both torsional and flexural loads is also included. Finally, a description of the tests to be performed and their respective goals concludes the chapter.

### **4.1 Measured Material Properties**

During the preliminary design of the test program, minimum material strengths were used to estimate the capacities of the various components. In order to refine these predictions, samples of the various materials were tested and the results are summarized below.

#### **4.1.1 Concrete Foundation and Pedestal**

Preliminary calculations of the strength of the test apparatus were done using a minimum concrete compressive strength of 5,500 psi. To refine the calculations, cylinder tests conducted two days before the test of the base connection determined the actual compressive strength of the concrete. The results of three 6" x 12" test cylinders were averaged for each of the pours of concrete required to construct the base and pedestal of the test frame.

The reinforced concrete block was constructed with two separate batches of concrete due to an unexpected problem with the formwork during the initial pour. The set of cylinders from the first pour, which was done on May 4, 2011, had an average compressive strength of 7,939 psi (Table 4-1). The set of cylinders from the second pour of concrete on May 6, 2011, after the formwork had been repaired had an average compressive strength of 6,761 psi. The reinforced

concrete block consisted of two layers of concrete, and so to remain cautious of the two different concrete strengths, only the lower average of 6,761 psi from the two concrete tests was used in the final calculations of the strength of the reinforced concrete block.

Table 4-1. Measured concrete compressive strengths

Cylinder	Block batch 1 compressive strength (psi)	Block batch 2 compressive strength (psi)	Pedestal compressive strength (psi)
1	8,184	6,862	6,970
2	7,960	6,698	7,051
3	7,674	6,722	6,954
Average	7,939	6,761	6,992

The reinforced concrete pedestal that encases that lower portion of the steel pole was made from a third batch of concrete. This pour was not made until June 17, 2011, since it required placement of the lower steel pole before casting the concrete. After removal of the formwork, an area surrounding the base of the pedestal was discovered in which honeycombing existed around the reinforcement cage. As a precaution to prevent an unwanted failure of the pedestal during testing, a ring of high-strength grout was placed along the bottom portion of the pedestal to fully encase the exposed area (Figure 4-1). Any additional strength from the high strength grout used to repair the pedestal was ignored for the purpose of strength calculations. The average concrete strength determined from the cylinder tests was 6,992 psi for the concrete pedestal.



Figure 4-1. Honeycomb around pedestal and repair of pedestal. Photo courtesy of FDOT.

#### 4.1.2 Tapered Steel Poles

The design of the tapered steel poles was done initially assuming a minimum yield strength of 55 ksi, but a more exact approximation of the yield strength is required to better estimate the predicted failure load. In order to determine the actual strength of the material used in the making of the steel poles, coupon tests were conducted by the pole manufacture. Three samples were tested and the results are shown in Table 4-2. The average yield strength of 65.2 ksi was used to determine more realistic values for the flexural and torsional capacities of the steel poles in the slip joint connection.

Table 4-2. Measured strengths of steel coupons

Steel coupon	Yield strength (ksi)	Tensile strength (ksi)
1	66.0	79.4
2	68.0	81.3
3	61.5	77.6
Average	65.2	79.4

Using the AISC and AASHTO specifications, an HSS16x0.375 section can be evaluated for bending, torsion, shear, and axial forces. Using an average yield strength of 65.2 ksi, which is 18 percent higher than the minimum specified yield strength, and the equations discussed previously in Section 3.1.3, the capacity of a similar tapered pole can be estimated. Both the AISC and the AASHTO specifications first examine the diameter-to-thickness ratio of hollow sections to determine if particular failure modes must be included in the design process. The section chosen for testing is classified as compact, so local buckling should not be a concern. The nominal flexural capacity of an HSS section with the material properties in Table 4-2 is 465 kip-ft, while the torsional capacity is 469 kip-ft.

According to the installation guidelines for high mast and sports lighting structures supplied by Valmont Structures, an acceptable slip joint is one that meets or exceeds the minimum required splice length and is tightly seated with only small gaps between the two

sections. In order to accomplish this, the poles must be aligned and then jacked together, typically with a come-along on each side of the joint, to create a tight fit (Valmont Structures 2002). Since the installation guidelines do not provide a specific value of jacking force to use in assembling the slip joint, the decision was made not to use any special jacking forces beyond the self-weight of the upper pole to assemble the slip joint being tested. The reasoning for this decision is twofold. First, there is no set standard for applying the force and so there is no assurance that each slip joint is being consistently assembled within any minimum specifications in the field. Second, a slip joint that is only snugly-fitted and exactly meets the minimum required length of slip joint may represent a worst-case scenario. If the slip joint can successfully transfer loads in a worst-case scenario, then it should be possible when proper design procedures are followed. In addition, the design of the proposed slip joint connection takes advantage of the possibility that the upper pole rotates about the lower pole under extreme wind conditions. Using jacking forces to fit the poles together could potentially hinder this design option.

Once the reinforced concrete pedestal has cured for a full 28 days, the two pole sections are fitted together to assemble the slip joint connection. Initial placement of the poles fell short of the minimum required slip joint length of 24 inches. Using only self-weight of the upper pole, the splice length reached 22 inches. Observation of the two poles revealed the presence of several small burrs on the faying surfaces in the area of the slip joint. In order to meet the minimum specified splice length, the burrs were ground down to smooth the surfaces and allow the poles to better slide by one another. To finally reach 24 inches, the poles were tapped slightly with a hammer at the free end of the upper pole, leaving only small gaps between the pole sections (Figure 4-2).

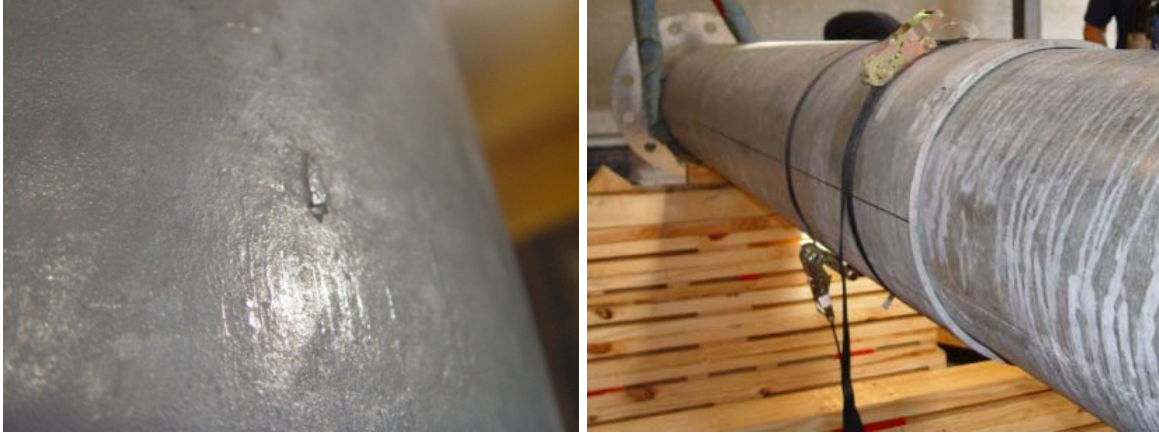


Figure 4-2. Small burrs on the surface of pole (left) and fitted slip joint (right). Photos courtesy of FDOT.

#### 4.1.3 Threaded Rods

After testing of the base connection was completed, the through-bolts in the connection were tested to determine the actual ultimate tensile strength. Ultimately, only A307 threaded rod was used during the experiment, and the through-bolts were tested in accordance with ASTM specifications for threaded rods, ASTM A307 (2003a) and ASTM F606 (2011). As is preferred in both specifications, full body specimens were tensile tested until rupture in the Tinius Olsen materials testing machine located in the structures lab at the University of Florida.

Four specimens were tested in total, but only three produced valid results. The invalid test result was caused by a failure of the threaded rod within the coupler nut used to hold the specimen in the test apparatus rather than the required rupture due to necking along the middle of the specimen (Figure 4-3). The tensile forces applied to each specimen were recorded until the bolts ruptured. Then the ultimate tensile stress was calculated for each valid test specimen using a tensile stress area of  $0.969 \text{ in}^2$  as defined by the above mentioned ASTM standards (Table 4-3).

Using the actual measured tensile strength of the bolts, the shear capacity of the through-bolted connection can be determined. Using the equations from Section 3.1.2.1, the nominal shear resistance of the through-bolts can be determined. The AASHTO shear resistance for a

single shear reaction of a bolt with an average ultimate tensile strength of 90.9 ksi is 42.5 kips. Therefore, the total shear resistance of three through-bolts, each of which contribute two shear reactions, is 255 kips. This shear capacity translates into 159 kip-ft of applied torsion in the test apparatus when using the actual average diameter of the shear plane in the slip joint region.

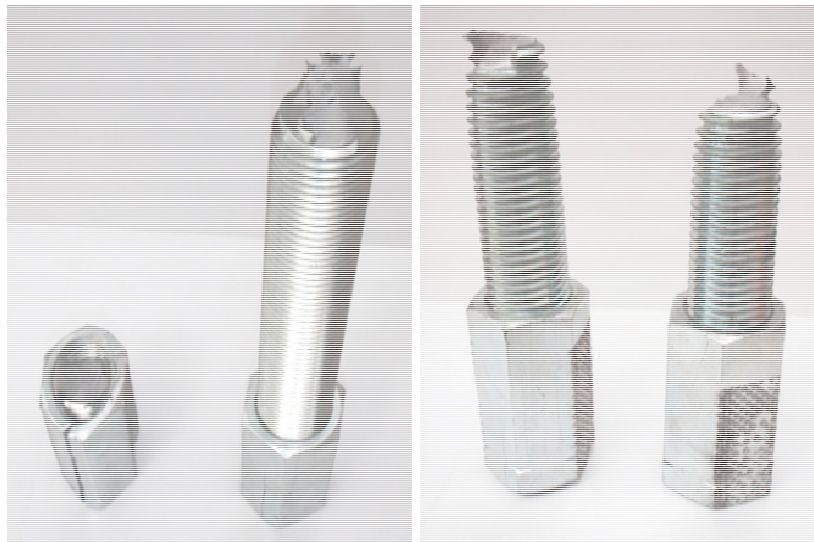


Figure 4-3. Examples of unacceptable and acceptable threaded rod test specimens. Photos courtesy of S. Dalton.

Table 4-3. Measured tensile force and strength of threaded rod specimens

Threaded rod specimen	Tensile force (kips)	Ultimate tensile strength (ksi)
1	88.4	91.2
2	88.2	91.0
3	87.8	90.6
Average	88.1	90.9

#### 4.1.4 Summary of Test Apparatus

Based on material tests for each of the main structural components, the actual measured material strengths were determined from an average of the results from each data set (Table 4-4). Also, the preliminary calculations to determine the applied failure loads of the various components of the test apparatus were recalculated to take into account the actual material strengths (Table 4-5). These values provided a more accurate account of the applied loads expected during testing.



Table 4-4. Specified materials for test apparatus with measured strengths

Item	Material grade	Average measured strength
Reinforced concrete block	Class IV	6,760 psi
Reinforced concrete pedestal	Class IV	6,992 psi
Tapered steel poles	ASTM A572, gr. 55	65.2 ksi (yield)
Threaded rods	ASTM A307, gr. 60	90.9 ksi (ultimate)
Washers	ASTM F436	
Nuts	ASTM A563, gr. A	

Table 4-5. Predicted test failure loads based on actual material strengths

Failure mode	Predicted failure moment (kip-ft)	Predicted failure load* (kip)
Concrete block test frame (6,761 psi concrete)		
Strut-and-tie torsion	451	50.1
Strut-and-tie moment	705	50.1
Channel tie-downs - floor	-	35.0
Tie-down bearing	-	33.0
Embedded pipe and stiffeners (6,992 psi concrete)		
Equivalent torsion from shear parallel to an edge	572	63.6
Equivalent torsion from side face blowout	804	89.3
Equivalent flexure from shear parallel to an edge	440	31.2
Equivalent flexure from side face blowout	571	40.5
Circular shaft - 36" (6,992 psi concrete)		
Threshold torsion**	64	-
Cracking torsion**	255	-
Torsion	444	49.3
Flexure (assume 17 bars yield)	456	32.4
Lever arm - HSS16x0.500 (42 ksi steel)		
Torsion	359	39.9
Flexure	392	43.6
Steel poles - 16" x 0.375" (65.2 ksi yield)		
Torsion only	469	52.1
Flexure only	465	33.0
Interaction torsion	228	25.4
Interaction flexure	355	25.4
Through-bolts - AASHTO shear resistance		
3 - 1.25"-diameter ASTM A307 (90.9 ksi tensile)	159	17.7
5 - 1.25"-diameter ASTM A193	n/a	n/a

\*Predicted failure loads are determined using a torsion arm of 9 feet and moment arm of 14 feet where appropriate.

\*\*Not a failure mode.

## **4.2 Instrumentation**

Proper instrumentation of the tapered bolted slip base connection is essential in understanding its behavior when transferring load from the upper pole section to the lower pole section. As revealed in the literature review, only limited information on the slip joint connection is available despite the popularity of its use in various fields. Rather than focus strictly on the specific point of failure of slip joint connections, there was great interest in determining how the slip joint transfers loads along its length. Consequently, the data obtained from the test program should reveal more specifically what is occurring within the region of the slip joint with respect to both flexure and torsion. In order to accomplish this, a comprehensive instrumentation schematic was required to obtain adequate data to determine how load is transferred through the tapered bolted slip base connection. A combination of strain gauges, linear variable differential transformers (LVDTs), a string potentiometer, a load cell, and actuator were required to collect relevant data for this study. The complete drawings detailing the exact location of each instrument are available in Appendix C.

### **4.2.1 Strain Gauges for Torsion**

Torsion in the pole was measured in line with the through-bolts in the slip joint connection. Theoretically, there should have been little to no impact due to bending on these gauges since they were situated on the theoretical flexural neutral axis, which was parallel with the floor when the poles were in the testing position. The goal of measuring strain along each face of the slip joint impacted primarily by torsion was to determine a relative distribution of the transfer of torsion by the through-bolts. Each component of the rosette gauges was wired separately to obtain independent readings that can be used to determine the shear strains along the joint (Figure 4-4).

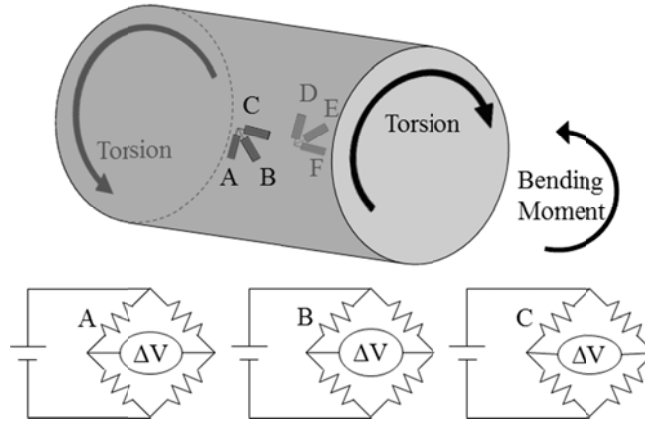


Figure 4-4. Wiring schematic for torsional rosette strain gauge arrangement

The placement of these gauges was strategically chosen to analyze whether or not the through-bolts were successfully transferring torsion from the outer pole section to the inner pole section (Figure 4-5). On the outer pole to the left of the first through-bolt, the effects of torsion in the pole were assumed to be at a maximum. Along the remaining length of the slip joint, one rosette strain gauge was placed midway between each through-bolt hole on opposite faces of the slip joint. This allowed the measurement of relative reductions in strain due to torsion in the outer pole as it was being transferred by the through-bolts to the inner pole. A rosette strain gauge placed halfway between the final through-bolt and the end of the slip joint was expected to measure nearly zero strain from torsion; and if not, then this may be an indication that friction may have a substantial role in the transfer of torsion between pole sections.

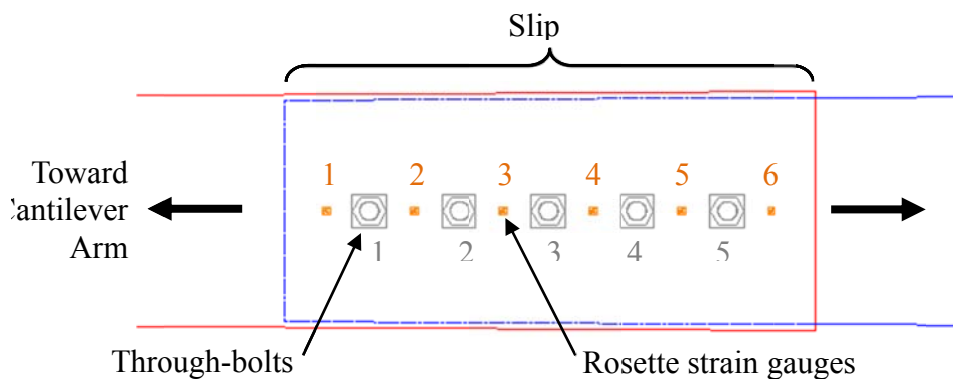


Figure 4-5. Arrangement of rosette strain gauges along the length of the slip joint

The total number of strain gauges required to examine the torsional characteristics of this connection was twelve rosette gauges, six gauges on opposite faces of the slip joint. Since each rosette gauge consists of three individually wired gauges, there were thirty-six total strain gauges and data sets committed to gathering data on the torsional happenings within the slip joint.

#### 4.2.2 Strain Gauges for Bending

In order to obtain data to depict the behavior of the slip joint in transferring flexure, strain measurements were collected and compared. Since principal interest lies in the transfer of bending along the slip joint, linear strain gauges were used for data collection. Each linear gauge was wired individually in a quarter-bridge configuration. Using linear gauges in this configuration allows the strain at each point of interest along the slip joint to be measured while keeping each location independent of the gauges on the opposite face of the slip joint (Figure 4-6).

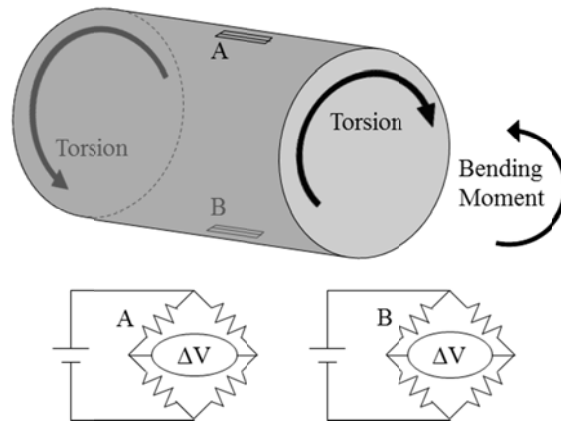


Figure 4-6. Wiring for flexural strain gauge arrangement

While the through-bolts are responsible for transferring torsion between the pole sections, the primary structural responsibility of the slip joint is to transfer the bending moment. As such, the arrangement of strain gauges intended to capture the behavior of the slip joint as it transfers bending moments must be capable of obtaining data for different scenarios. As one possible

extreme slip joint behavior, the pipe sections fit loosely together and remain rigid as the bending moment generates large concentrated loads at each end of the slip joint. The other extreme is that the poles fit tightly together, are allowed to deform under flexure, and behave as a uniform section without any discontinuities, so the slip joint bends as if it were a single pole (Figure 4-7).

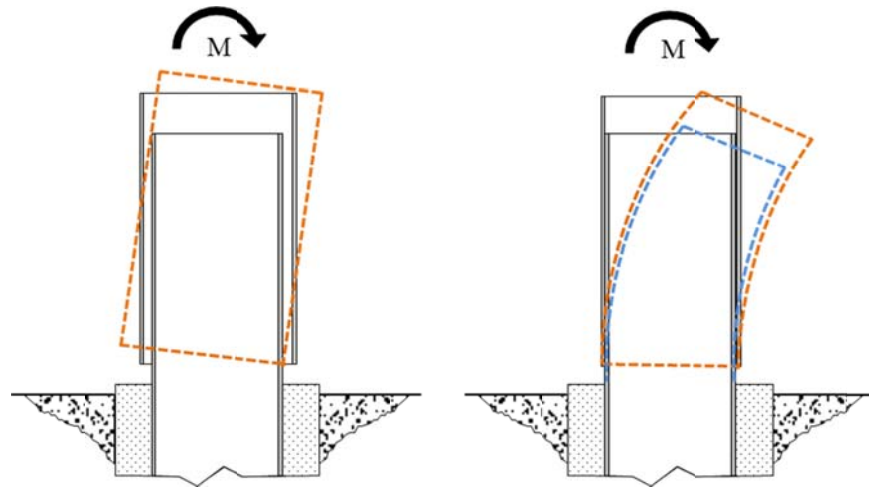


Figure 4-7. Extreme bending behavior of loosely-fitted and tight slip joints

In terms of strain activity along the slip joint, it was expected that there would be significantly more activity along the ends of the slip joint where the poles first come into contact and that the strains would likely decrease towards the center of the splice. It is important to note that while the poles in the slip joint may be in direct contact at one end of the splice, the poles of the slip joint on the same face but at the opposite end of the connection may be pulling away from each other.

There were also concentrated areas of interest at the ends of the slip joint where it was beneficial to collect more data. As a result, the strain gauges were concentrated at each end of the slip joint and reduced toward the middle of the splice length (Figure 4-8). The gauges at the ends of the slip joint were located at third points between the end of the slip joint and the through-bolt. Moving toward the middle, gauges were spaced at half points between adjacent through-bolts and so on.

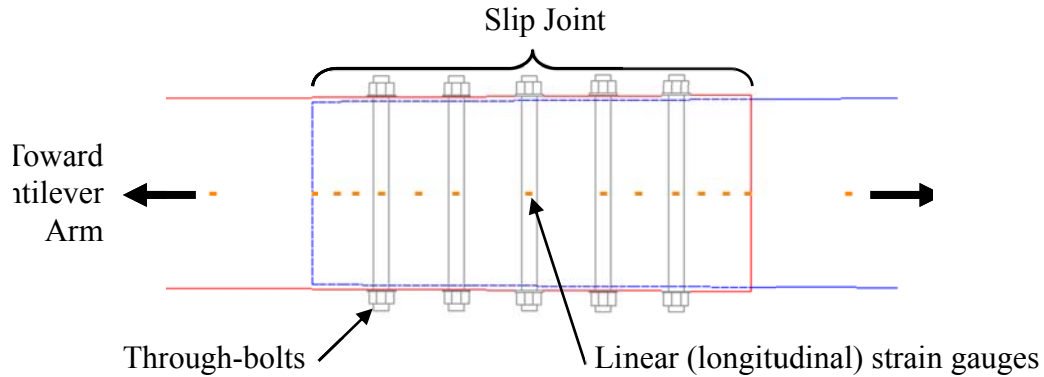


Figure 4-8. Arrangement of linear strain gauges for bending

The total number of strain gauges required to examine the flexural characteristics of this tapered bolted slip base connection was thirty linear gauges, fifteen gauges on opposite faces of the slip joint. It is important to note that the flexural strain gauges and torsional strain gauges did not lie on the same faces of the slip joint. The torsional gauges were placed on the faces of the slip joint that correspond to the theoretical flexural neutral axis, while the flexural gauges were placed on the faces that experience the most impact from bending. Since each linear gauge was a single gauge wired independently of any other gauge, there were a total of thirty gauges and hence thirty data sets to gather information on the flexural behavior along the length of the slip joint.

#### 4.2.3 Displacement Gauges

Displacements along the length of the slip joint were measured using a series of linear variable differential transformers (LVDTs). The configuration was similar to that used in the previous two FDOT projects related to this topic. An arrangement of four LVDTs was placed at four locations along the length of the test poles to measure horizontal and vertical displacements (Figure 4-9). These displacements were then used to calculate the rotations of the test poles and slip joint as well as the deflection along the length of the test apparatus.

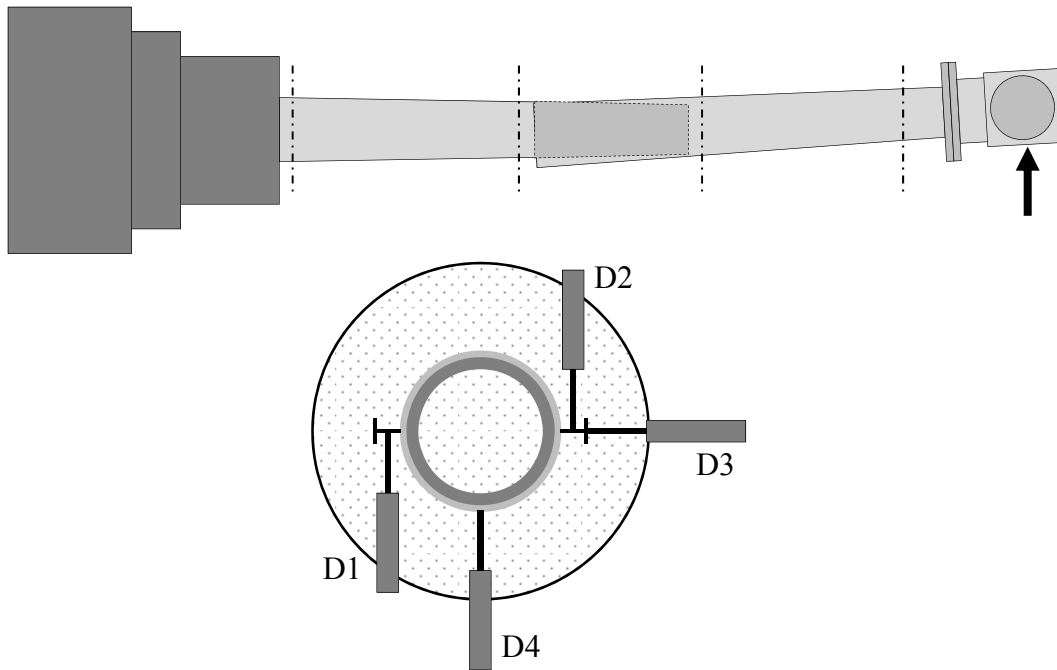


Figure 4-9. LVDT arrangement at each of the four indicated locations along test apparatus

In addition to the LVDTs measuring displacements along the test poles, a string potentiometer was required to measure the displacement of the cantilever arm at the point of load application. The purpose of the string potentiometer was to measure the total stroke of the load actuator piston. In order to fail the through-bolts, it was expected that the total stroke could be at least 18 inches. The available LVDTs did not measure displacements in this range, and so a string potentiometer was the preferred instrument in this case.

#### 4.2.4 Load Cell and Actuator

The applied load at the end of the cantilever arm was applied using an Enerpac hydraulic cylinder to lift the lever arm. The lifting system was controlled manually based on the displacement rate of the plunger. In order to measure the load being applied to the end of the cantilever arm, a compression load cell capable of measuring up to 100 kips is placed on top of the plunger of the hydraulic cylinder (Figure 4-10).



Figure 4-10. Load cell and actuator used for applying load to test apparatus. Photo courtesy of S. Dalton.

### **4.3 Testing Procedure**

Two tests were originally planned for this project. The first was related to the prediction of through-bolt failure and the second related to overall observation of slip joint behavior. As discussed in Chapter 5, the first test failed at higher loads than expected and eliminated the need to perform the second test. The concept behind each of the originally planned tests is discussed below.

#### **4.3.1 Prediction of Through-bolt Failure**

The first planned test was of the through-bolted part of the connection to determine if the through-bolt failure can be reasonably predicted using standard design procedures set forth by AASHTO. Of the two planned experiments, this first one was most like the design of this slip joint as used in field applications. The goal was that under extreme wind loads, the through-bolts are the first and only structural component to fail, relieving the structure of excessive torsional loads that may cause pole or foundation failures. Doing so allows the sign to pivot about the embedded pole, but more importantly, remain upright so as not to create a safety hazard for



drivers. This experiment was designed so that the bolt failure occurs well before any other component of the test apparatus was predicted to fail; therefore, the same test apparatus could be fitted with new through-bolts and used for the second test.

This first test only used three A307, grade A through-bolts in the slip joint connection to minimize the torsional resistance of the connection relative to the remainder of the test apparatus. This was expected to force a failure of the through-bolts before any other component of the test apparatus experiences any significant reaction to the applied load. If the through-bolts failed as predicted in Section 4.1.3, then it could be assumed that the equations set forth by AASHTO and AISC are sufficient for the design of this type of connection. If they did not fail as expected, then it is possible that other design considerations in addition to the design equations in the AASHTO and AISC specifications must be accounted for when designing the tapered bolted slip joint connection.

#### **4.3.2 Observation of Slip Joint Behavior**

The second test was intended to examine the behavior of the slip joint connection, particularly with respect to bending. To accomplish this, additional through-bolts would have been added to the slip joint to meet or exceed the predicted torsional capacity of the pole sections. This would have allowed an opportunity to compare the strength of the slip joint as well as its effectiveness in transferring torsion and flexure relative to the predicted strengths and failure modes of the pipe sections and the through-bolts. This information is essential in understanding how to best design the slip joint as it is being applied to cantilever structures.

For the second test, the number of through-bolts placed in the slip joint was to be increased to five and the material changed to A193, grade B7. These five through-bolts would have provided a torsional capacity of 389 kip-ft, which is higher than the 360 kip-ft torsional capacity of the tapered steel poles. By exceeding the torsional capacity of the steel poles with that of the

through-bolts, the flexural capacity of the slip joint could be compared to that of the flexural capacity of the tapered steel poles. If the slip joint failed in flexure before the steel poles, then this would indicate a flaw in the structural application of slip joints in cantilevered signal and sign structures. If, on the other hand, the steel poles or concrete pedestal experienced failure before the slip joint, then it would be likely that the slip joint is adequate in transferring flexural loads from one pole section to the other for use in cantilevered signal and sign structures. Again, it is important to remember that the number of through-bolts planned to be used in this second test exceeded the number of through-bolts that are recommended in field applications. Therefore, if failure of the slip joint did not occur during the second test that provides excessive torsional capacity and allows for a larger applied bending load, then it would support the notion that the slip joint may not fail under normal conditions.

## CHAPTER 5 FINDINGS

The findings of the test program are summarized in the following sections. The details and results of the test program are explained with reference to the failure mode of the test apparatus and how the predicted results compare to the actual results of testing. Any discrepancies between the predicted and actual results are identified and addressed. Finally, the data collected from the instrumentation are presented in graphical form followed by detailed discussion of what each data plot indicates.

### **5.1 Test Outcome**

#### **5.1.1 Predicted vs. Actual Failure**

The test conducted at the FDOT Marcus H. Ansley Structures Research Center in Tallahassee, Florida on August 18, 2011, implemented the use of three A307 through-bolts in the test apparatus. As mentioned previously, the initial predicted failure load for these three through-bolts with an ultimate tensile strength of 60 ksi was 12.5 kips. The predicted strength was later revised based on the actual cross-section of the slip joint and the results of the tensile tests on the through-bolts. The more accurate tensile strength provides a predicted applied failure load of 17.7 kips using the AASHTO specifications for bolted connections.

The actual applied load on the test apparatus reached 27.7 kips at its failure capacity. This load well exceeds the predicted failure load even when taking into consideration the actual tensile strength of the through-bolts. In order to explain the substantial increase in the predicted and actual failure loads, the effects of friction within the slip joint must be included in the analysis of the connection.

### 5.1.2 Failure Mode

The intent of the test program was to conduct two separate tests that would evaluate the capability of the through-bolts to transfer torsion and the slip joint to transfer flexure. The design of the first test was intended to allow for failure of the through-bolts in the slip joint while precluding all other failure modes. However, the actual ultimate tensile strength of the threaded rods was much greater than the upper bound values that had been anticipated and the test apparatus experienced pipe buckling along the region of the embedded pole near the access panel before the through-bolts completely sheared (Figure 5-1). Although the pole buckled prior the expected through-bolt failure, the pole did not buckle prematurely. The applied load reached and exceeded the predicted load for the pole capacity based on the interaction of flexure and torsion.



Figure 5-1. Pipe buckling near the access panel on the embedded pole. Photo courtesy of S. Dalton.

Upon removal of the through-bolts from the slip joint connection, it was discovered that all of the through-bolts had begun to kink under the applied load and that one had started to experience shear failure (Figure 5-2). Although the exact applied load to cause a complete shear failure of the through-bolts was not obtained, it is probably reasonable to say that it was close to the actual applied failure load of 27.7 kips.

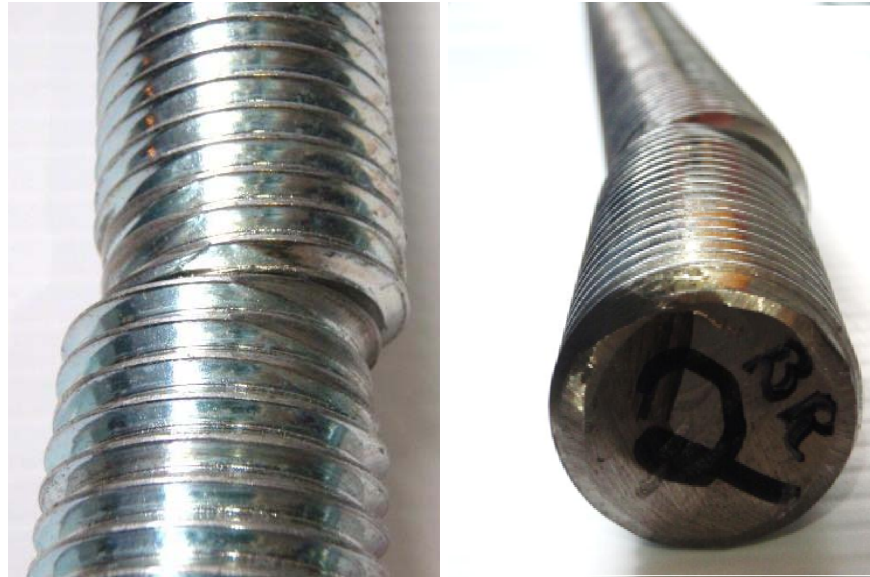


Figure 5-2. Bolt shear and kink in through-bolt. Photos courtesy of S. Dalton.

Since the embedded pole experienced failure due to pipe buckling, it was not possible to conduct the second test as planned. Fortunately, the presence of shearing in one of the through-bolts achieves the goal of the first test, which is to determine if the through-bolts can adequately transfer the torsional loads and if the AASHTO design equations are adequate. Since the capacity of the through-bolts well exceeded the predicted failure load, the bolts are capable of transferring torsion as needed. In addition, the purpose of the second test was to determine if the slip joint could adequately transfer flexure between the two poles. Since the pole buckled in a region away from the slip joint and after its predicted failure load, it is reasonable to say that the slip joint is at least capable of transferring flexure between sections and in some cases it may not be the weakest structural component.

### **5.1.3 Effects of Friction**

The test of the slip joint connection revealed that the actual applied load at the end of the lever arm was higher than anticipated to cause failure of the through-bolts. Observations of the slip joint during testing showed that the upper pole in the slip joint rotated about the lower pole

causing contact on the compression face of the poles at the end nearest the foundation and also on the tension face of the poles at the end away from the foundation (Figure 5-3). It was also observed that the compression side of the outer pole shifted longitudinally toward the foundation under loading. This indicates that frictional resistance for both torsion and flexure must be examined. The coefficient of friction for the tested slip joint can be bracketed using the following values: 0.8 for plain steel-to-steel connections (Ramsdale 2006) and 0.45 for galvanized steel-to-galvanized steel connections (Bui 2010). For design purposes, the AASHTO specifications (2010) use a slip coefficient of 0.33 for hot-dip galvanized surfaces and a value of 0.50 for unpainted blast-cleaned surfaces in slip-critical bolted connections.

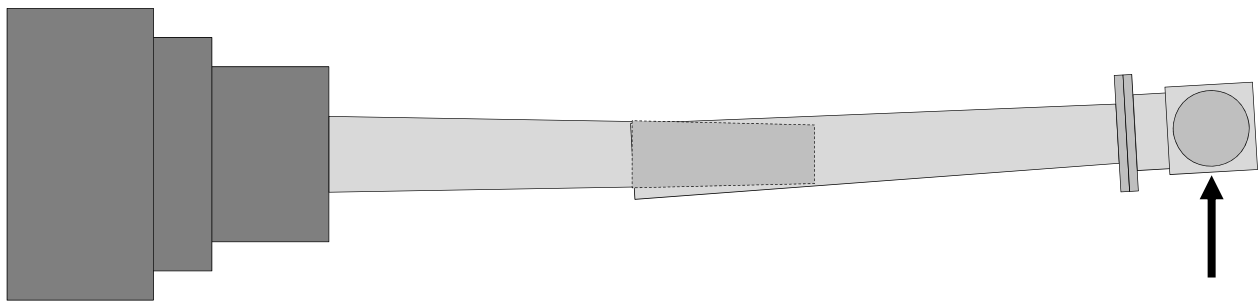


Figure 5-3. Contact of poles within slip joint region

The analysis that follows includes an evaluation of friction as the likely reason for the higher actual applied load that caused failure during the test. When examining how flexural loads are being transferred through the slip joint, it is necessary to evaluate two cases. The first case assumes that the poles are perfectly rigid and that flexure was transferred through concentrated forces at either end of the slip joint (Figure 5-4). The second case assumes that the flexural load is distributed across some length of the slip joint creating resultant forces away from its ends (Figure 5-5). The impact of having contact surfaces that extend along the length of the slip joint reduces the distance between the resultant normal forces on the poles.

Consequently, the magnitudes of the normal force and the applied load increase.

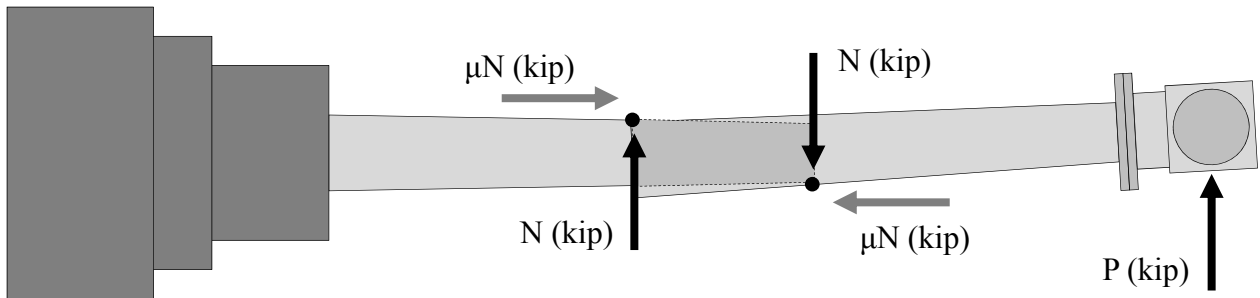


Figure 5-4. Concentrated internal couple transferring applied load through slip joint

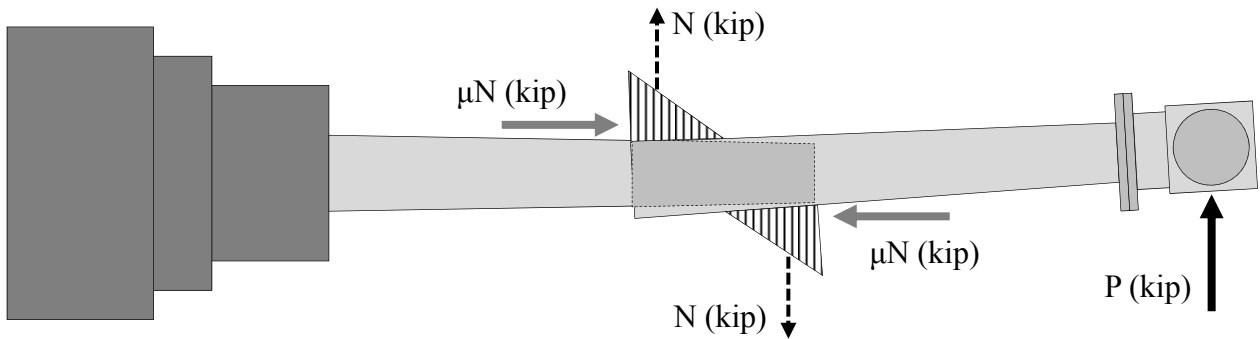


Figure 5-5. Distributed internal couple transferring applied load through slip joint

The through-bolts in the slip joint connection were fastened with snug-tight nuts, so that no normal forces would be applied to the walls of the poles. Therefore, the first step in analyzing the effects of friction on the applied load required to shear the through-bolts is to examine the normal forces generated by the flexural component of the applied load. In the case with concentrated loads as depicted in Figure 5-4, the normal force ( $N$ ) can be expressed as a function of the applied load ( $P$ ) and the coefficient of friction ( $\mu$ ). The same is true for the case in which the normal load is distributed along the length of the slip joint as in Figure 5-5. Once the expression for the normal force is determined, it is possible to use the expression to evaluate the impact of friction in the case of torsional loading.

In order to evaluate the effects of friction on the predicted applied load to cause bolt shear, the shear resistance of the through-bolts must be determined. Based on the AASHTO specification discussed in Section 3.1.2.1 above, the shear resistance can be determined. For a

bolt diameter of 1.25” and an ultimate tensile strength of 90.9 ksi, the predicted shear resistance per bolt shear reaction (i.e. there are two reactions per through-bolt) is approximately 42.5 kips. Taking this value and the expression of the normal force determined from the flexural analysis into consideration, the applied load can be determined (Figure 5-6).

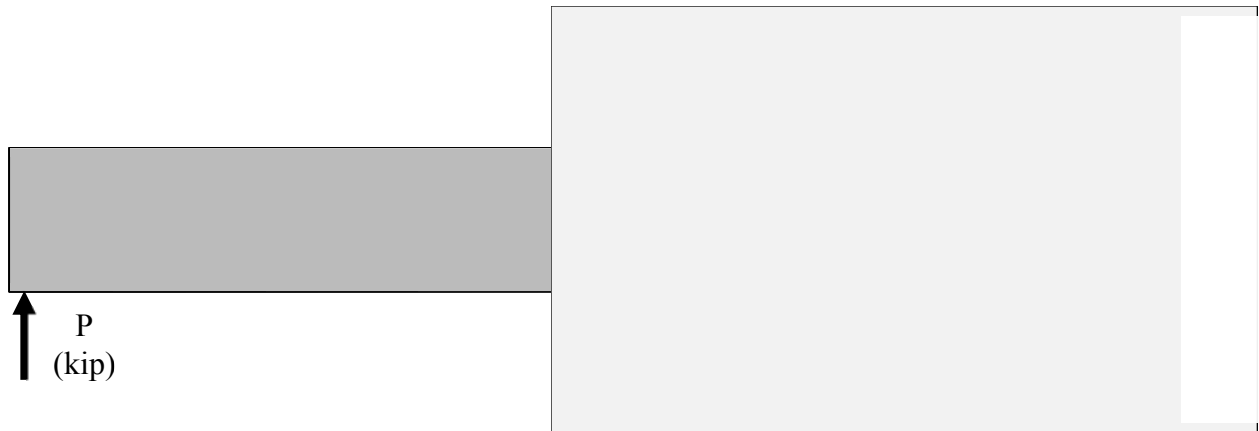


Figure 5-6. Frictional and bolt shear resistance to torsion

The details of the complete analysis are included in Appendix D and the results are presented in Figure 5-7. The data presented in the graph represent the predicted applied load for the test apparatus with three through-bolts having an ultimate tensile strength of 90.9 ksi and shear strength computed in accordance with the AASHTO specifications. The triangular normal load distribution on each face of the slip joint is assumed to extend half the length of the slip joint splice as shown in Figure 5-5.

These results of the frictional analysis indicate that the presence of friction within the slip joint region increases the ability of the tapered bolted slip joint connection to carry more applied load. The applied load increases gradually due to friction and also due to the distribution of load along a bearing length within the slip joint. The range of coefficients of friction that are indicated by the two curves and the actual failure load falls within the range of 0.45 to 0.80 that are typical for steel connections. The exclusion of the lower bound value of 0.45 as the actual



coefficient of friction for this connection may be a result of the removal and collection of galvanization material in the area of bearing between the pole sections, exposing more plain steel than galvanized and increasing the coefficient of friction. It also suggests that the actual load to cause a shear failure of the through-bolts could have been as high as 33 kips, much higher than the predicted 17.7 kips.

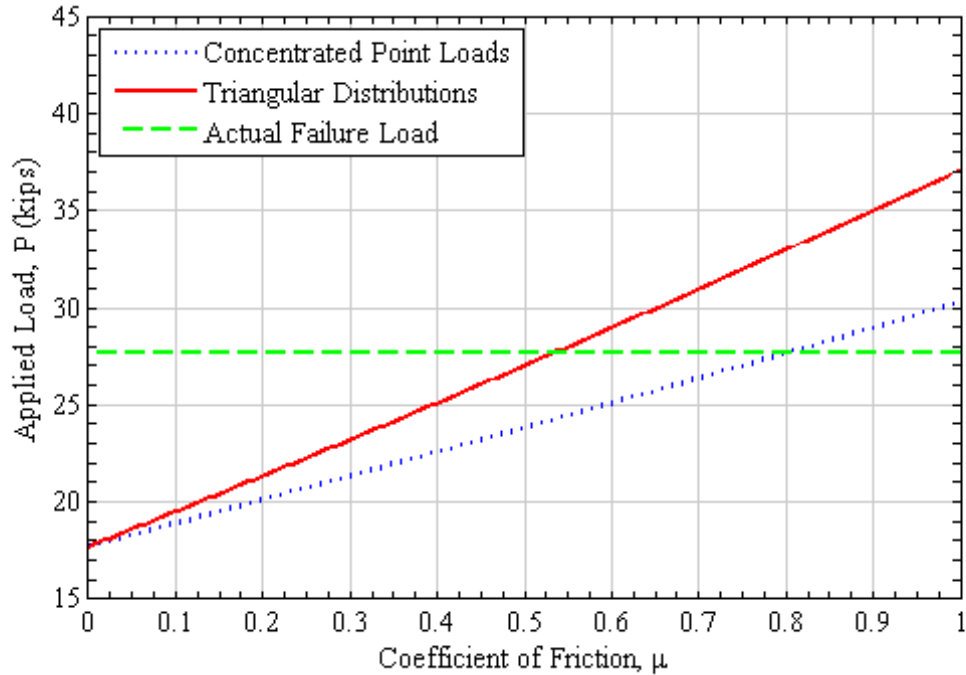


Figure 5-7. Plot of the impact of friction on predicted applied load

The predicted failure load taking into consideration the AASHTO slip coefficient of 0.33 for hot-dip galvanized surfaces in slip-critical bolted connections of steel elements is less than the actual failure load of the test apparatus. Although the AASHTO slip coefficient conservatively underestimates the strength of the connection, this value may prove useful when trying to include the effects of friction in a tapered bolted slip base connection. It can provide a more realistic value of the failure load for a given through-bolted connection without overestimating the strength of the connection.

## 5.2 Summary of Data

All of the data collected during testing were analyzed in order to determine the behavior of the tapered bolted slip base connection and its ability to transfer both flexural and torsional loads. In order to preserve the integrity of the data collected, careful consideration was given to the method of data collection and analysis. Data were collected at a frequency of 10 hertz and load was applied initially using a displacement controlled rate of 0.25 inches per minute until the connection was fully engaged, and then the load rate was readjusted to approximately 1 inch per minute. The data as shown have been modified to eliminate periods of unloading of the test apparatus in order to reset the actuator piston at the end of the lever arm (Figure 5-8). Also, data from a few of the instruments were deemed invalid and could not be used for analysis. Once the data columns from these instruments were removed from the overall data set, the remaining data were evaluated for the behavior of the connection in transferring load.

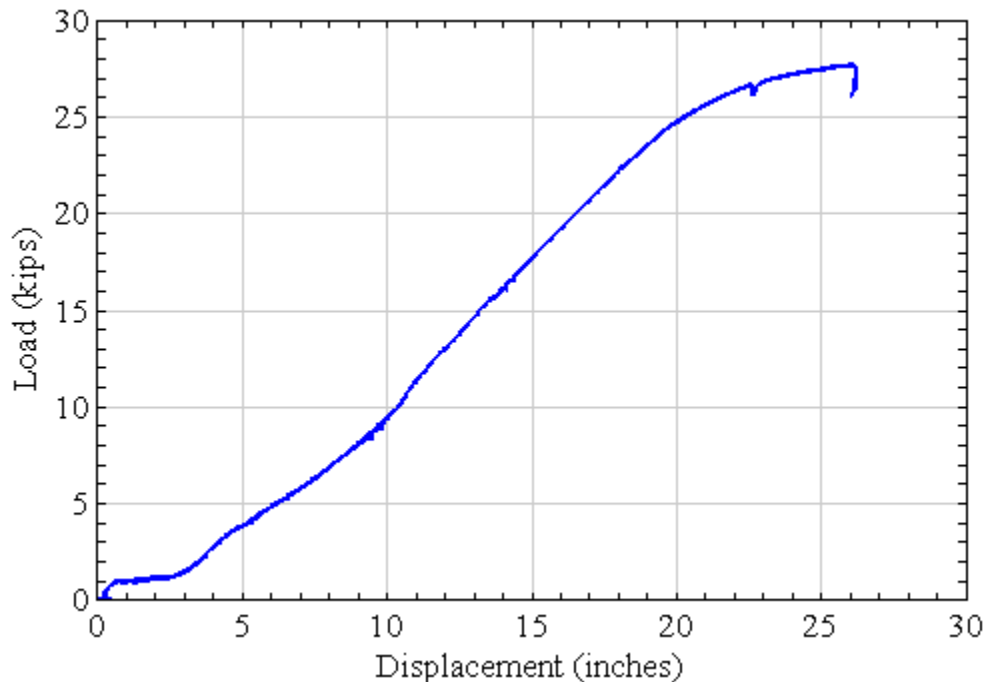


Figure 5-8. Plot of the applied load versus stroke after unloading times removed

### 5.2.1 Flexural Strain Data

The flexural behavior of the slip joint as it transfers load from one pole to the other was captured using a series of linear strain gauges placed at strategic locations along the length of the slip joint on the tension and compression faces of the outer pole (Figure 5-9). Only one of the flexural strain gauges was found to be faulty, and so a detailed picture of the strain along the slip joint was obtained. The variation in strain on the outer pole was examined for various magnitudes of applied load to determine how the load is transferred as it increases. The plot of this data for three loads – 5 kips, 10 kips, and the maximum load of 27.7 kips – can be seen in Figure 5-10. The dashed lines represent the gauges on the tension face of the outer pole while the solid lines represent the gauges on the compression face. The location of the slip joint is measured from its center outward toward the edges of the splice length. The negative distances are closest to the lever arm of the test apparatus and the positive distances increase toward the concrete pedestal.



Figure 5-9. Flexural strain gauges on compression face of outer pole along the slip joint. Photo courtesy of S. Dalton.

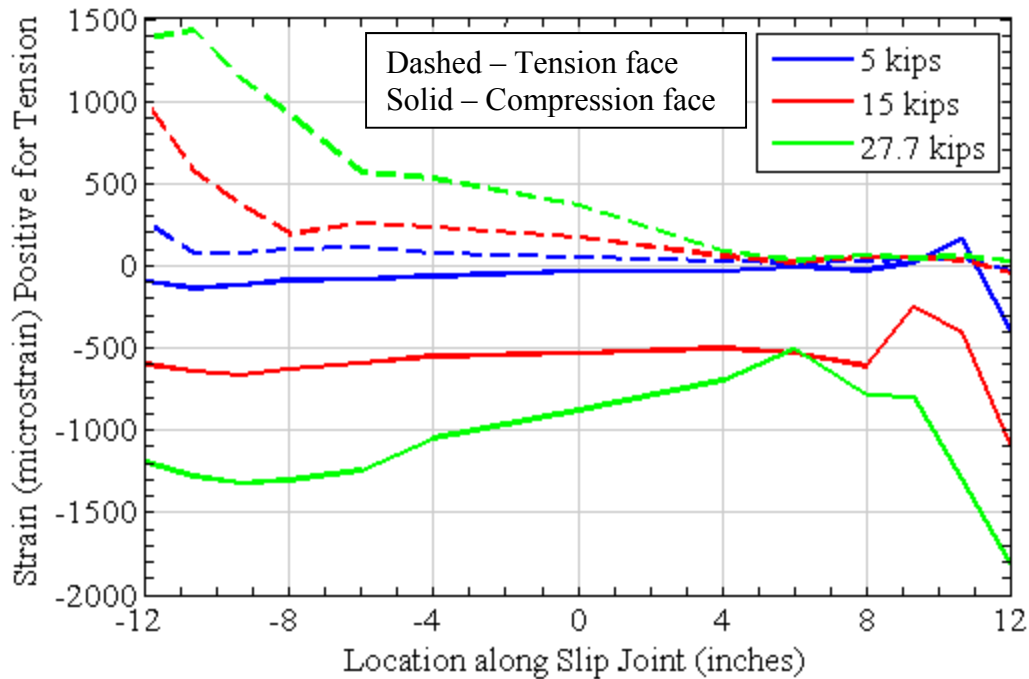


Figure 5-10. Flexural strain measured along the length of the slip joint

The flexural strain plot indicates the strain on the surface of the outer pole. The tension face, which is shown in Figure 5-10 with dashed lines, indicates that the tension load is transferred mostly at the edge of the slip joint and tapers off toward the center of the splice length. After the taper, the strain is relatively small and ultimately approaches zero. However, at the end of the slip joint nearest the concrete pedestal, the strain appears to become slightly negative. This confirms observations made during testing that the base of the outer pole began to deform slightly as it pulled away from the inner pole as the applied load increased (Figure 5-11). The oblong deformation at the base of the outer pole would cause the steel to stretch transversely, which in turn causes compression in the strain gauges and explains the negative strain readings.

The strain gauges on the compression face shown as solid lines in Figure 5-10 also reveal information about the transfer of load between the two poles. At the end of the slip joint nearest to the lever arm, it is expected that the outer and inner poles are not in direct contact. The strain

gauge data support this, because the measured flexural strain remains mostly constant over the length of the slip joint at lower applied loads and gradually decreases with higher loads. Approximately 6 inches from the end of the slip joint nearest the concrete pedestal, the compressive strain is at a minimum magnitude and then increases quickly toward the edge of the slip joint. The compression face of the outer pole is being pressed against the wall of the inner pole, and so the outer pole appears to experience some additional compression deformation in the area that is in direct contact with the inner pole. This explains why the strain readings increase in magnitude toward the edge of the splice nearest the concrete pedestal.



Figure 5-11. Oblong deformation at the base of the outer pole during loading. Photo courtesy of S. Dalton.

The flexural strain plot indicates that at smaller applied loads the normal forces in the slip joint are transferred right along the edges of the splice length as shown in Figure 5-4. However, as the load increases it appears that the normal forces are transferred over a length of the slip joint on either face. Looking at the maximum load case, the normal forces appear to be mostly transferred over a length of about 6 inches from either end of the slip joint; this is similar to what is depicted in Figure 5-5. Observation of the poles after the connection had been disassembled confirms the theory that the normal forces are being transferred over a length of the slip joint. Scratches observed on both the inner and outer poles indicate direct contact between the two

members and measurements of the length of the scratched area correspond to the length indicated in the flexural strain plot (Figure 5-12). In addition, a slight indentation in the same area of the inner pole indicates some plastic deformation along the end of the slip joint, which also confirms an area of direct contact between the two pole sections (Figure 5-13).



Figure 5-12. Scratches on the tension face of the inner pole. Photo courtesy of S. Dalton.



Figure 5-13. Plastic deformation on the tension face of the inner pole in slip joint region. Photo courtesy of S. Dalton.

Overall, the strain readings on the compression and tension faces in addition to the observations of scratches on the surfaces of the poles support the theory that flexural loads are transferred in a linearly distributed fashion as indicated in Figure 5-5. In conjunction with the analysis of friction in the slip joint, this type of load transfer through the connection generates

larger resultant normal forces than if the load is transferred at concentrated points at the far ends of the splice length due to the short moment arm between forces. Therefore, the walls of the poles should be designed taking this into consideration to prevent undesirable slip joint failures due to localized buckling (Kai and Okuto 1974).

The results of the flexural strain data collected during testing for this project support the overall findings of the Sumitomo study with respect to the flexural behavior of the slip joint connection. As expected, larger strains were measured at the ends of the slip joint where the poles were in direct contact. Although as previously discussed, the Sumitomo recommendation of a splice length of at least 1.7 times the diameter of the pole sections may be high for the diameter-to-thickness ratios more commonly associated with poles used in FDOT structural applications, the flexural behavior of the slip joint as tested agrees with those behaviors described in the Sumitomo report (K. Okuto, letter to ASCE, May 31, 1977).

### **5.2.2 Torsional Strain Data**

The torsional behavior of the slip joint as it transfers load from one pole to the other was captured using a series of rosette strain gauges placed between each of the through-bolt holes along both faces of the theoretical flexural neutral axis on the outer pole (Figure 5-14). Strain gauges at two locations, one on each face of the slip joint, were found to be faulty and had to be removed from the data set. Due to the limited number of locations for monitoring torsion, the loss of these two gauges hindered the ability to interpret results regarding the transfer of torsion along the length of the slip joint.

The data from each component of the rosette gauges were used to calculate shear strain on the outer pole using the equation:  $\gamma_{xy} = 2\varepsilon_{45} - (\varepsilon_0 + \varepsilon_{90})$ . This shear strain was examined for various magnitudes of applied load to determine how the load is transferred. The plot of this

data for three loads – 5 kips, 10 kips, and the maximum load of 27.7 kips – can be seen in Figure 5-15. The dashed lines represent the gauges on the left face of the outer pole, which is closest to the point of load application, while the solid lines represent the gauges on the right side facing away from the point of load application. The determination of the left and right faces of the slip joint are based on the front view of the test apparatus. The locations of the through-bolts have been indicated on the plots by highlighting the vertical grid line that coincides with the location of each bolt. The location of the slip joint is measured from its center outward toward the edges of the splice length. The distances are most negative towards the lever arm and become more positive along the slip joint moving towards the concrete pedestal.

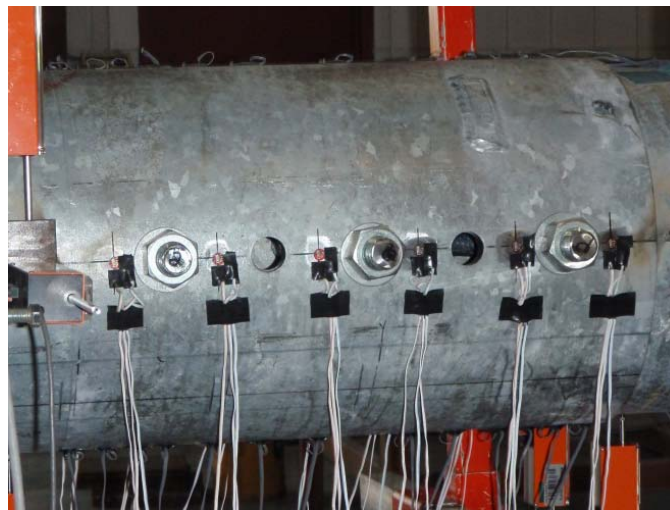


Figure 5-14. Rosette strain gauges located between bolt holes. Photo courtesy of S. Dalton.

The orientation of the rosette strain gauges are such that the torsional loading impacts all of the gauges on both faces of the slip joint in the same manner (Figure 4-4). In other words, the torsional loading as it is applied at the lever arm causes all of the diagonal gauges in the rosettes to experience compression. Given that the gauges are situated on the theoretical flexural neutral axis, there is little to no impact from flexure and the majority of the strain is measured by the diagonal gauges. As a result, the shear strain calculations largely mirror the measured diagonal



strains and explains why the results on both faces produce negative strains. The more negative strains indicate larger torsional effects on the surface of the outer pole.

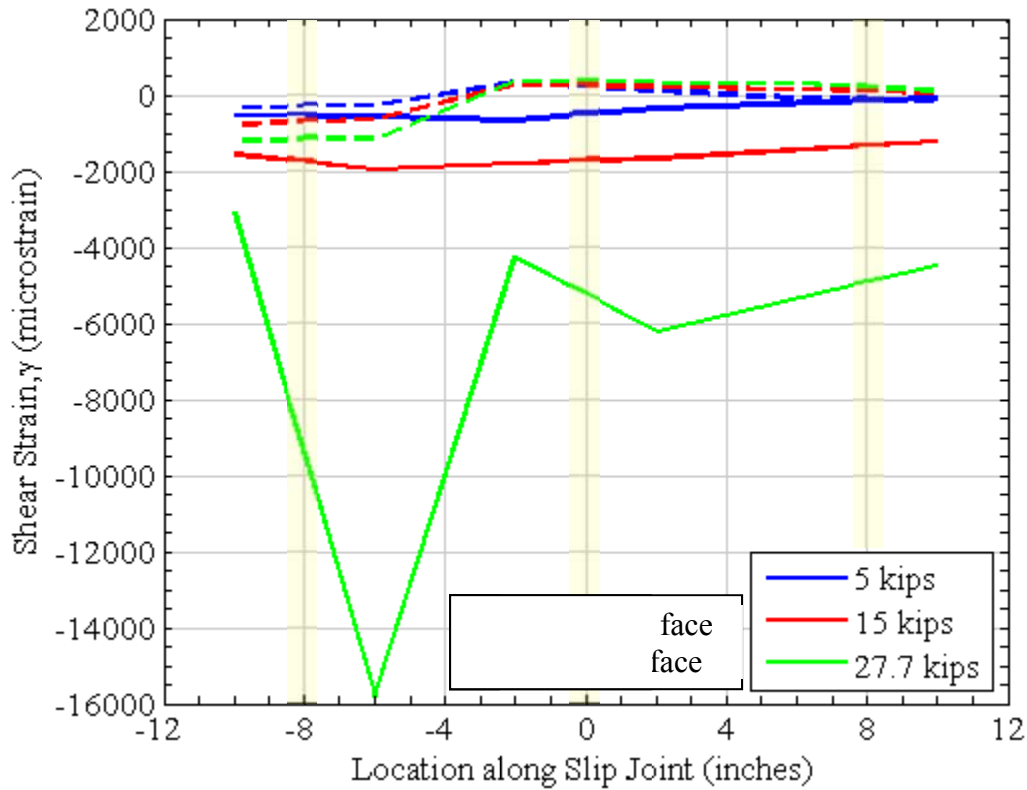


Figure 5-15. Plot of shear strain measured along slip joint for select load cases

The plot of the shear strain along the length of the slip joint shown in Figure 5-15 appears to show very little change in activity for all but the maximum load case on the right face of the slip joint. The green lines indicate what is happening at failure of the test apparatus, and it is important to note that the strain gauges may have been stretched beyond their acceptable range at this point during testing. In order to get a better view of the activity for the other load magnitudes and locations, the vertical axis of the plot is adjusted to display values from -2500 microstrain to 1000 microstrain (Figure 5-16). The locations of each of the three through-bolts are highlighted in yellow on the plots to help decipher how they contribute to the transfer of load.

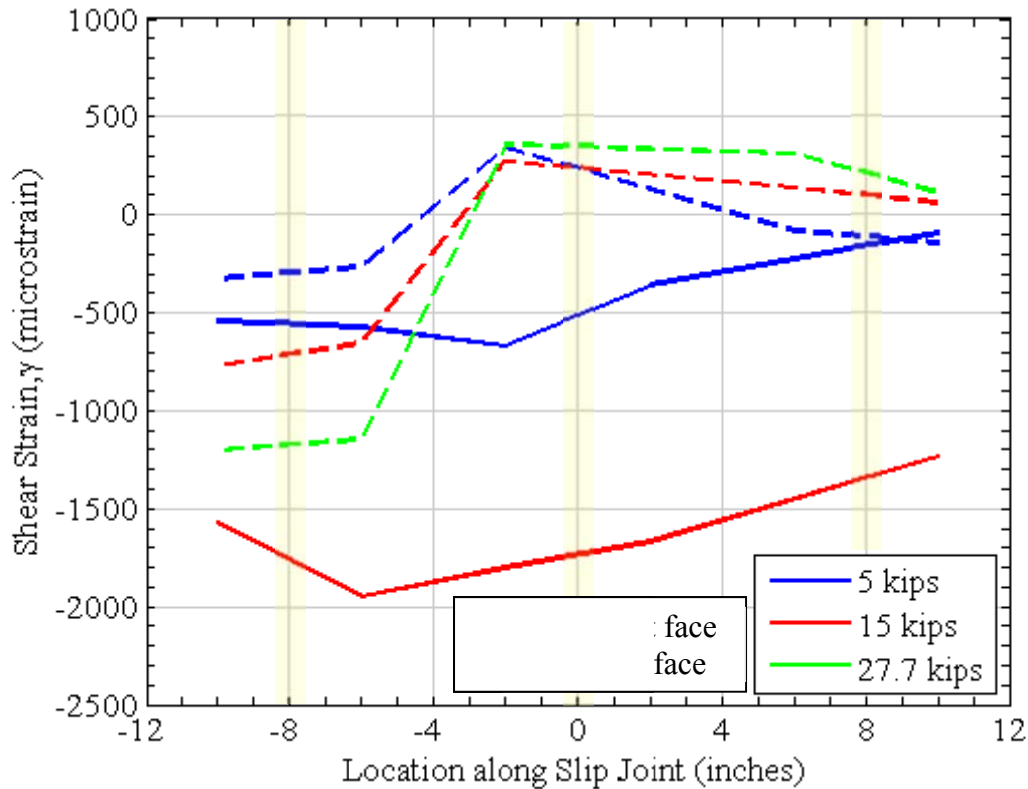


Figure 5-16. Plot of shear strain measured along slip joint for select load cases (limited view)

The plot in Figure 5-16 seems to indicate that the faces of the slip joint along the bolt holes are experiencing different reactions to the torsional loading. On the left face of the slip joint, there appears to be a dramatic drop in the shear strain between the first and second through-bolts and very little change in shear strain between the second and third through-bolts to the end of the slip joint. On the other face, the shear strains appear to stay more evenly distributed along the length of the slip joint with the most significant drop in shear strain happening between the second and third through-bolts and the end of the slip joint.

In order to understand this behavior, more careful examination of the test apparatus and through-bolts must be conducted. During testing, separation of the two pole sections was observed near the base of the outer pole (Figure 5-17). Assuming that the separation of the pole surfaces occurs symmetrically around the cross-section, then the side facing away from the

applied load is still in contact at the through-bolt while the side facing the applied load is not. This may indicate that friction is playing a role for one set of rosette gauges and not the other.

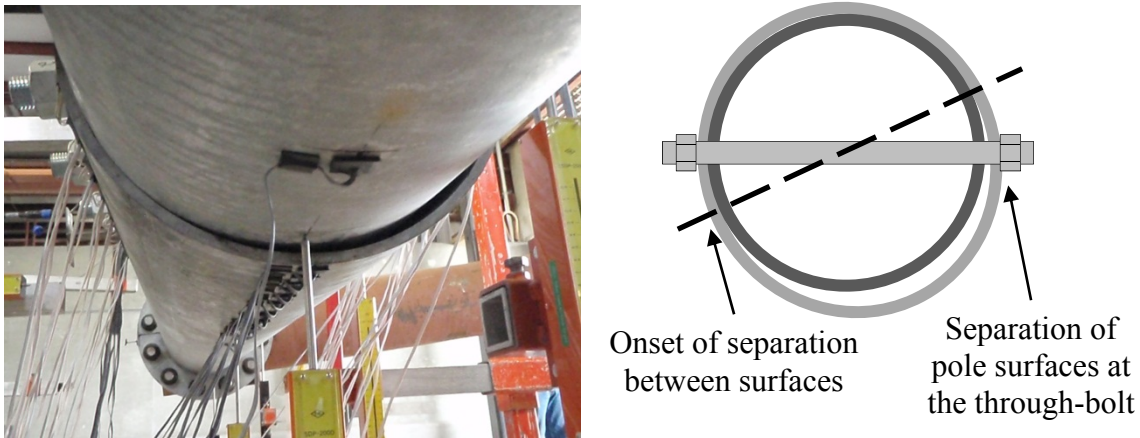


Figure 5-17. Rear view of the separation of pole surfaces during testing. Photo courtesy of S. Dalton.

After testing was complete and the slip joint disassembled, the through-bolt holes were observed on both faces of the slip joint on both of the pole sections. Measurements of the bolt hole deformations indicated that all of the through-bolts were engaged at each end. Each of the bolt holes deformed approximately 1/16” and bearing on the through-bolts flattened all the threads in contact with the bolt holes. However, the through-bolts themselves indicated that perhaps one end of each through-bolt was carrying more load than its respective other end. The through-bolt nearest to the lever arm bent mostly on the end closest to the applied load, while the other two bolts bent mostly on the opposite end (Figure 5-18). The through-bolt nearest to the concrete pedestal was closest to shearing off when the test apparatus failed. The measurements of the approximate angles of bend at each end of the through-bolts are summarized in Table 5-1.

Table 5-1. Measure of the approximate angle (degrees) of the bend in each through-bolt

Bolt	End facing load (left side)	End facing away from load (right side)
Near lever arm (top)	4	2
Center of splice (middle)	1	4
Near concrete pedestal (bottom)	0	7

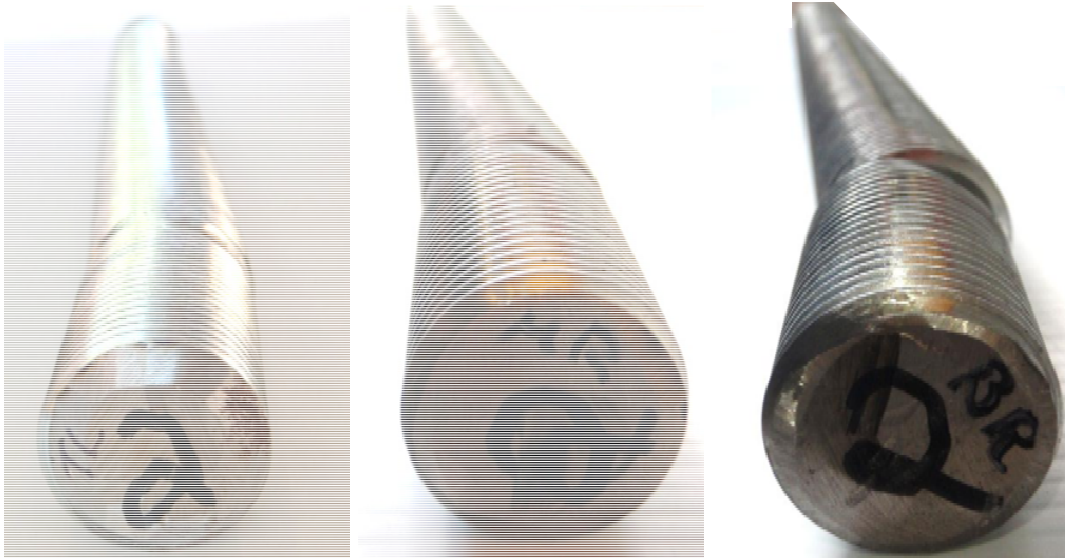


Figure 5-18. Principal bend in each through-bolt. Photos courtesy of S. Dalton.

Combining what is known about the separation of the pole sections, how the through-bolts bent under loading, and the plots of shear strain data shown in Figure 5-15 and Figure 5-16, the transfer of load through the slip joint can be interpreted. Looking at the plot of the shear strains along the right face of the slip joint, the solid lines appear to indicate only a slight change in the overall shear strain as a result of the through-bolts. In fact, the shear strain does not drop off to or near zero after the last through-bolt in the connection indicating that perhaps friction is transferring much of the load on this face of the pole in the area with the greatest normal forces. Considering the plot of shear strains along the left face of the slip joint and the bend in the top through-bolt, the dashed lines appear to indicate a significant drop in the magnitude of shear strain between the first and second through-bolt, which may suggest that the first through-bolt is transferring most of the load on that face. However, the strain does not drop significantly until after the first through-bolt suggesting another scenario.

Looking more closely at the plot, the magnitudes on the left face are initially much lower than on the right face. Considering how the flexural load is transferred by contact of the poles at

opposite ends of the slip joint on opposite faces, it is reasonable to suggest that friction plays a substantial role for the left face nearest the lever arm in the same manner as it does for the right face near the pedestal. In other words, contact of the poles on the left face near the lever arm allows friction to transfer a significant amount of torsion to the lower pole before the first rosette gauge can measure the strain on the surface of the outer pole; whereas no contact on the right face near the lever arm allows the rosette gauge to measure more torsion initially. It seems somewhat counterintuitive that two gauges on the the same cross-section can measure two separate strain values for an applied torsion, but given the distortion observed in the pole, it makes this explanation more plausible (Figure 5-19).

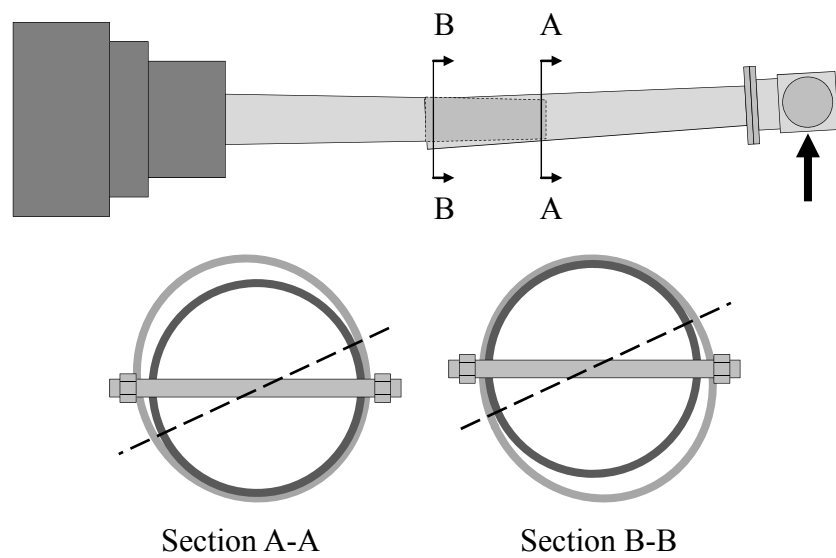


Figure 5-19. Cross-sections of slip joint during loading from a rear view of test apparatus

The shear strain data, evidence of contact surfaces, and bends in the through-bolts seem to provide a detailed picture of the behavior of the tapered bolted slip base connection in regards to the transfer of torsional load between the two pole sections. What is certain is that all of the through-bolts were bearing on the bolt holes by the end of the test and that they all experienced varying degrees of bend along the shear plane. The bends appear to be more substantial in areas

where the faying surfaces are directly in contact, hence concentrating the shearing forces on the bolts. It is also reasonable to suggest that friction plays a substantial role in transferring torsional load based on the magnitude of the applied failure load compared to the predicted failure load of the through-bolts, even after accounting for the actual tensile strength of the bolt material.

### **5.2.3 Deflection Data**

The deflection data collected during testing were obtained using the same LVDTs that were used to calculate the rotations of the test poles. As previously mentioned, there were some issues with the gauges getting stuck and as a result some of the data plots do not provide a complete picture of the displacement data. The data from the vertical displacement plots were then used to make a plot of the deflection along the length of the test poles, which can then be compared to the expected deflection of a similar cantilever beam structure. The data collected from the horizontally oriented LVDTs appear to be invalid because of some strange occurrences within the data plots and were disregarded for purposes of analysis.

The vertical displacement data gathered from the LVDTs are first organized by which side of the test apparatus the LVDT is measuring. The assignment of the left, right, and bottom LVDTs is based on a frontal view of the test apparatus (Figure 5-20). The left face of the slip joint is closest to the applied load, while the right face is directed away from the applied load. The bottom face of the test poles is then identified as the surface facing the floor. Once the LVDTs are grouped by which face they are measuring, they are then plotted based on their location along the length of the test pole. The load path is followed from the lever arm down through the connection to the concrete pedestal; consequently, the phrase “before the slip joint” indicates the end of the slip joint near the lever arm while the phrase “after the slip joint” indicates the end near the concrete pedestal.

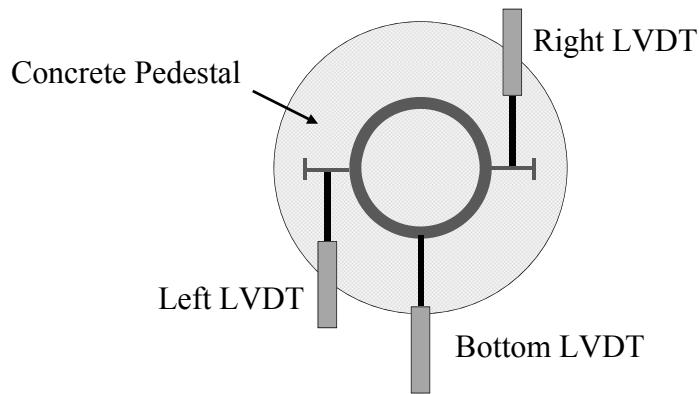


Figure 5-20. Section view of LVDT placement

The LVDTs measuring the vertical displacements along the left edge of the test apparatus present the most incomplete data sets (Figure 5-21). The gauges after the slip joint and near the lever arm both experienced instances of being stuck and prevented data collection. One of the gauges was able to be freed and the missing data were interpolated in order to provide a more complete, although perhaps not totally accurate, representation of the behavior. Regardless, any interpolated data points were not used for further analysis.

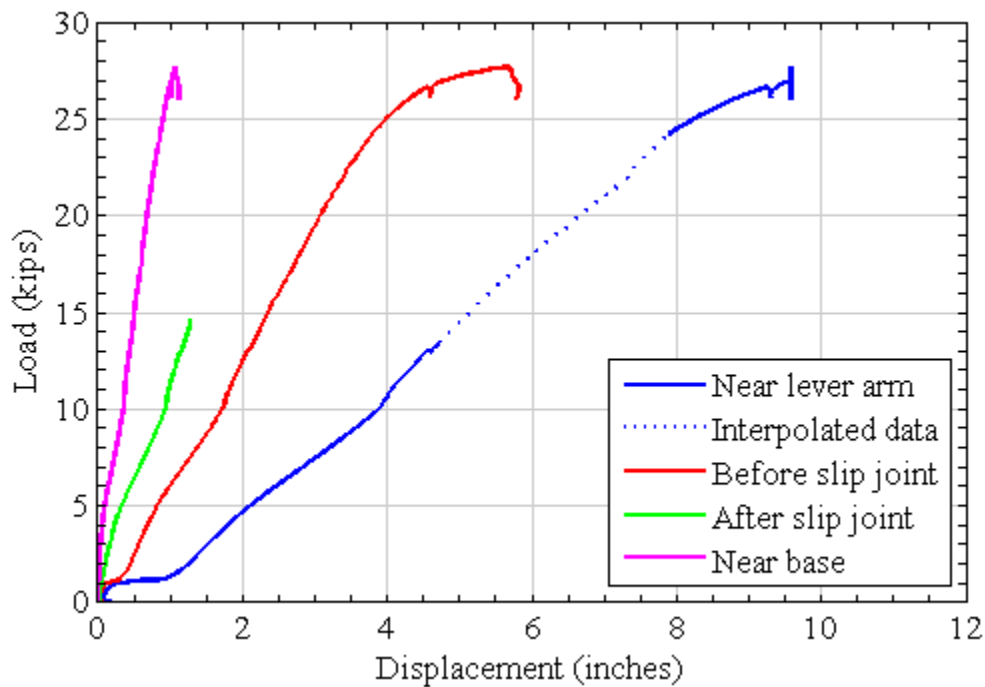


Figure 5-21. Vertical displacements along the left edge of the test poles

The LVDTs measuring the vertical displacements along the right and bottom edges of the test poles provide more accurate data sets than the LVDTs along the left edge. The LVDT data along the right edge were complete in all but the gauge near the lever arm (Figure 5-22). The same is true of the displacement data gathered along the bottom edge of the test poles (Figure 5-23). As a result, the data from these two faces are used to determine the rotations of the test poles at each of the four locations indicated in Figure 4-9.

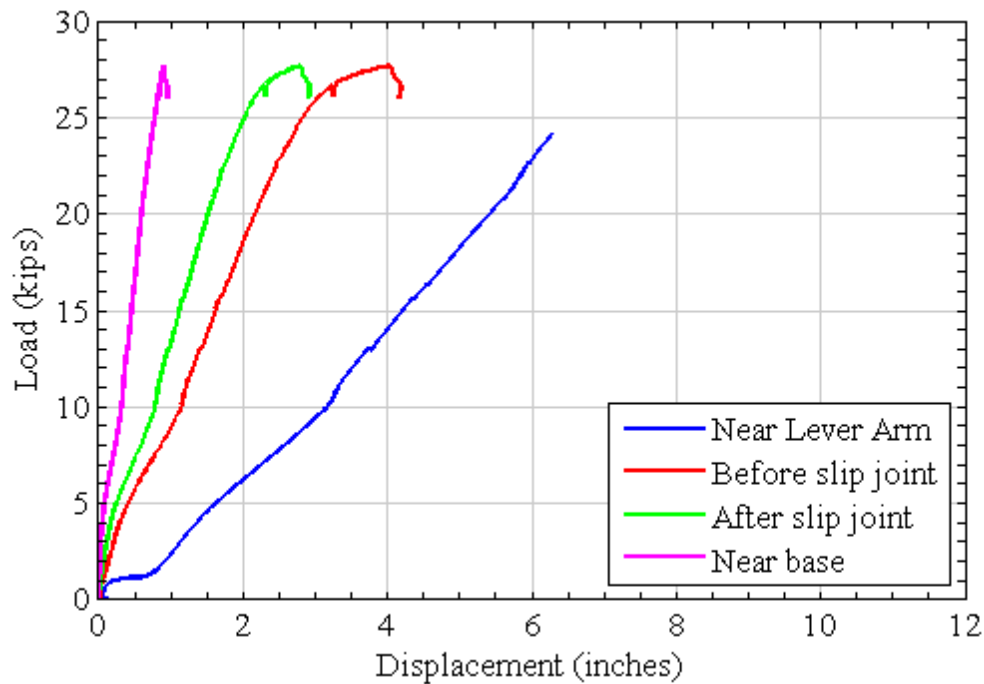


Figure 5-22. Vertical displacements along the right edge of the test poles

To compare how the test poles deflected along the length of the structure, the measured vertical displacements from the LVDT data are compared to the theoretical deflection of a cantilever beam with a concentrated point load at the free end. First the raw data collected from the LVDTs are plotted for select load cases (Figure 5-24). According to theory, the poles should not have deflected so much near a fixed support; however, the reinforced concrete block and pedestal did not remain perfectly rigid during testing. The concrete pedestal is especially subject to experiencing vertical displacement due to the applied flexural load. In order to correct for



this, the deflection data must be shifted and rotated down slightly to account for the deflection in the pedestal, so that the data can be compared with theoretical values.

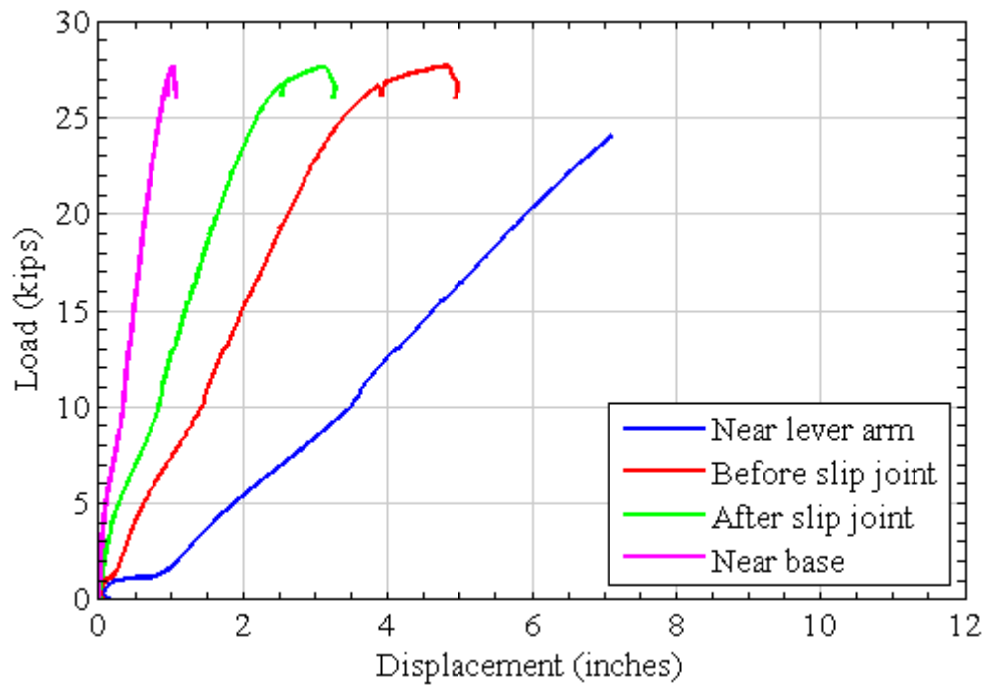


Figure 5-23. Vertical displacements along the bottom edge of the test poles

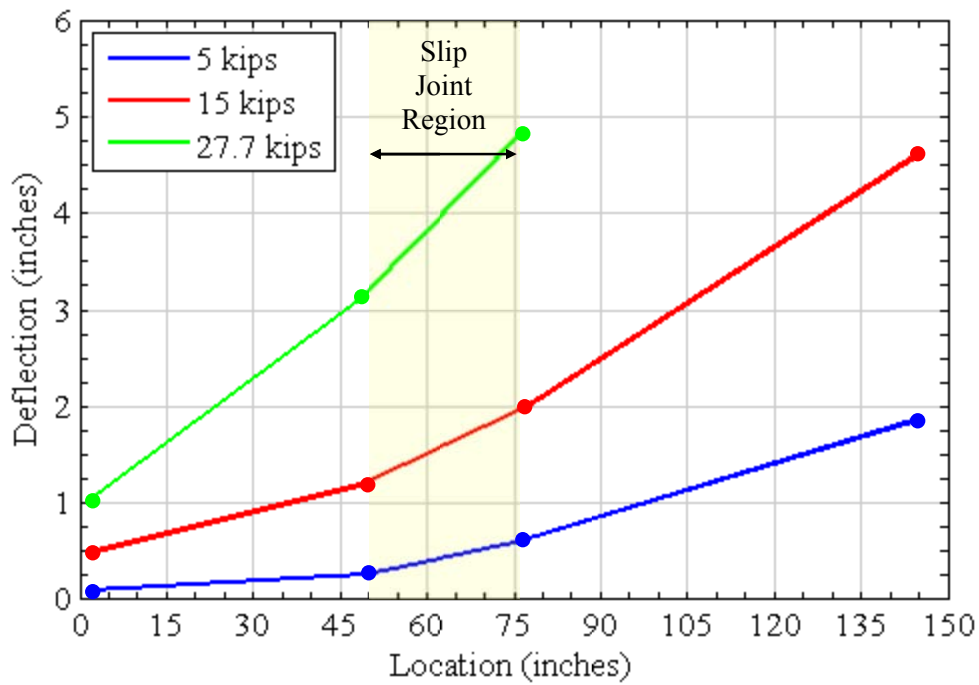


Figure 5-24. Unaltered deflection data along the length of the test poles

Once the deflection data have been modified to account for the deflection and rotation of the support, it can be compared to the theoretical beam deflection for a cantilever with a point load at its free end. The beam deflection plot compares deflections at two load magnitudes that are both within the elastic range of the test apparatus (Figure 5-25). The comparison with the theoretical values shows that the embedded pole experiences deflections very close to the predicted theoretical values. The slip joint region experiences greater deflections than theoretical values indicate, but this is expected due to the loosely-fitted connection. This additional deflection also creates additional curvature along the slip joint that carries through to the end of the test poles, increasing the deflections near the lever arm even more. If a more snugly-fit connection had been made by applying jacking forces during assembly, then the deflections of the upper pole would fall more in line with the theoretical values.

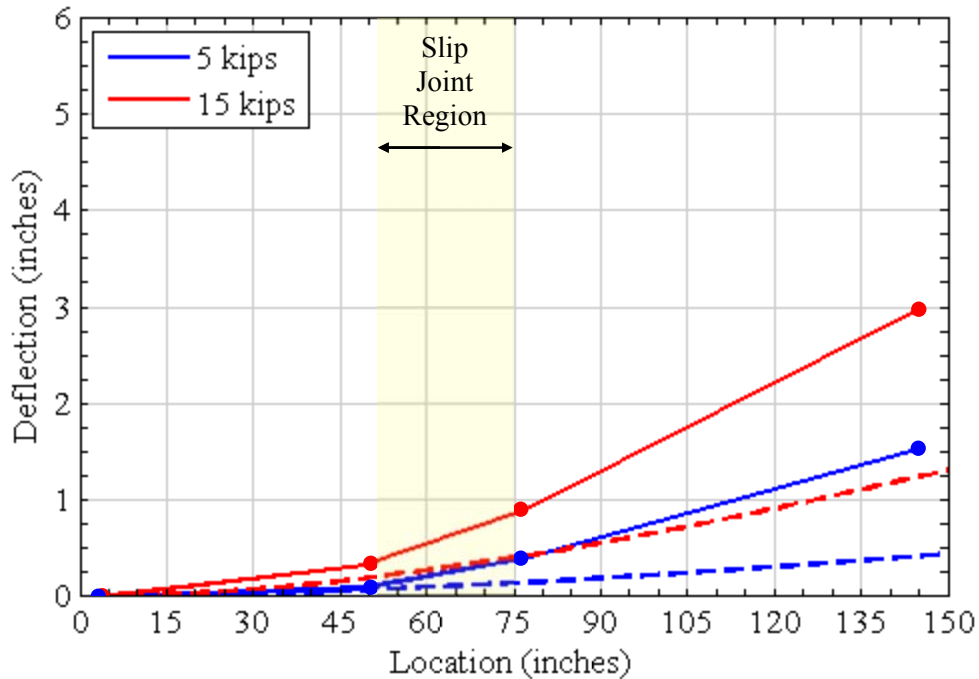


Figure 5-25. Deflection along the length of test poles adjusted for pedestal displacements

#### 5.2.4 Rotational Data

The plots of the rotational data are derived from the series of LVDTs arranged around the cross-section of the poles at four locations along the length of the test apparatus (Figure 4-9). Originally, rotations were intended to be calculated using the vertical LVDTs on both the left and right faces of the slip joint; however, some of the LVDTs were lost during testing. Others became stuck and did not register displacements for short periods during testing until they were freed; fortunately, this mostly occurred during the unloading and reloading phases and was easily corrected. For those LVDTs that quit reading displacements all together, the data plots end abruptly prior to reaching the failure load.

As a result of the problems with the LVDT data, the rotations were calculated for two cases: (1) using the vertical displacements from the left and right LVDTs and (2) using the vertical displacements from the right and bottom LVDTs (Figure 5-26). The results of each analysis are displayed in Figure 5-27. The dotted lines represent the first method and end abruptly when the data from the left side gauges are no longer valid. The solid lines represent the results from the second method and are more complete than the first. For the most part the lines match up well, and the differences between the dotted and solid lines may be explained by slight horizontal movements of the test poles that impact the readings of the bottom LVDTs.

The plot of applied torsion versus rotation shows how the poles rotate as a system and more specifically the degree of slack within the connection. The curves for the rotation of the embedded pole begin increasing immediately and maintain a relatively constant rate of rotation. On the other hand, the curves for the rotation of the outer pole increase initially and then flatten out near 10 kip-ft of applied torsion. This flattening of the curve persists for roughly 0.75 degrees before the upper poles are capable of carrying any additional load. This flattened region of the curve is attributable to slop in the joint associated with the loose-fitted connection and the

oversize of the bolt holes. Once all the slack is taken up in the joint and all the components are fully engaged, the upper pole is able to carry more torsion. The change in rotation along the length of the slip joint is calculated by taking the difference between the values before and after the slip joint (Figure 5-28). Here again, the curve has a flattened region due to slop in the connection, but the slope of the curve once the connection is able to carry load is a more accurate representation of the change in rotation occurring across the overall length of the joint.

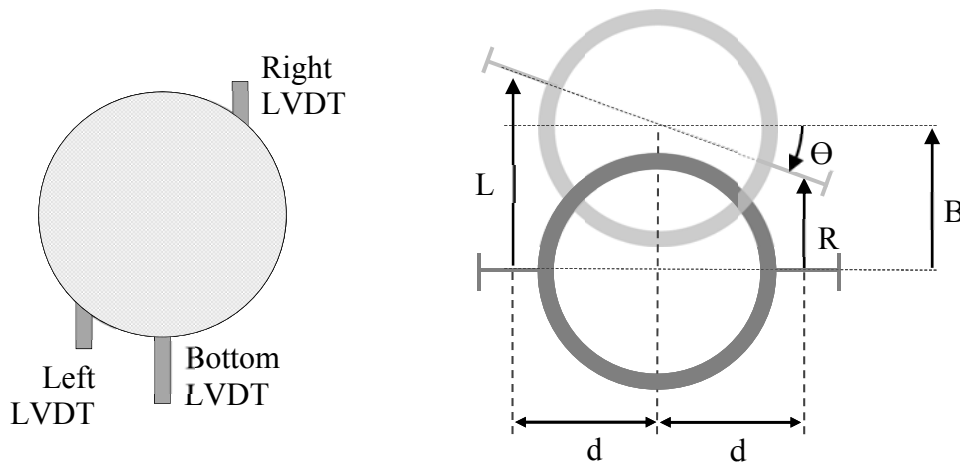


Figure 5-26. Geometry of vertical displacements used to calculate section rotation

The measured rotations can be compared to theoretical values for the expected angle of twist of a singular pole. The valid range for the comparison is in the elastic region of the curves for given values of torsion. The angle of twist for a circular section can be determined by:  $\phi = TL/JG$ . The theoretical angle of twist is calculated using an average diameter for the poles and corresponding polar moment of inertia (J). The modulus of rigidity (G) is estimated to be 11,200 ksi. Since there is some unmeasured amount of rotation occurring along the length of the concrete pedestal, the length of the theoretical pole is equal to the distance between the top of the torsional plates within the foundation to the set of LVDT's nearest to the lever arm (Figure 5-29). This allows the theoretical angle of twist to begin along the plane of the embedded pipe and plate assembly when torsion is initially transferred to the foundation. The lines plotting the theoretical

angles of twist on the upper pole sections have been shifted over to account for slack in the connection (Figure 5-30).

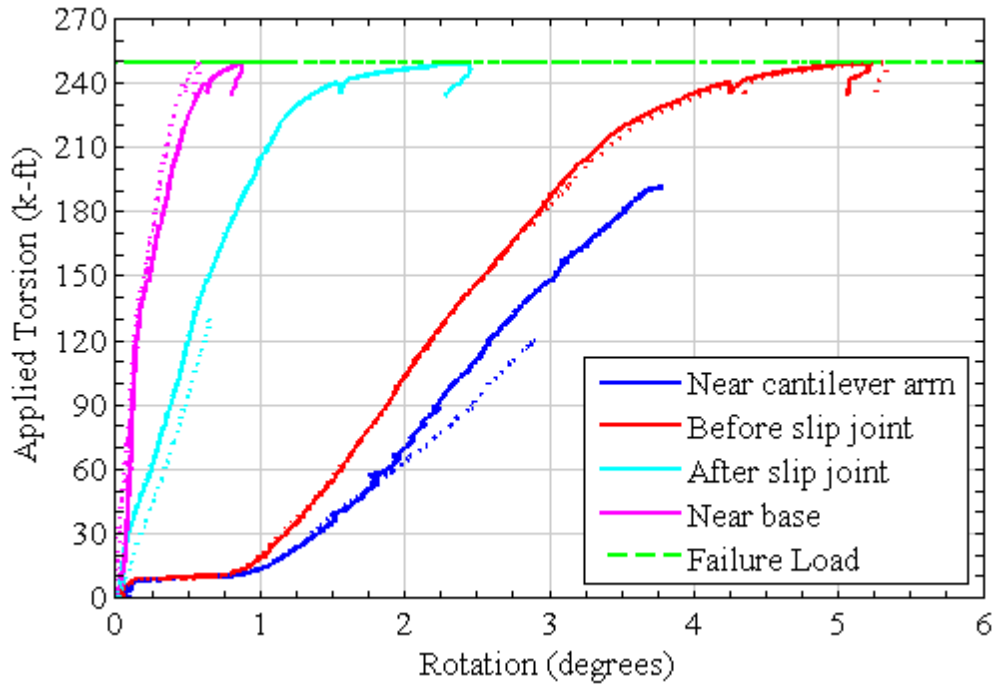


Figure 5-27. Plot of applied torsion versus the calculated rotation of the poles

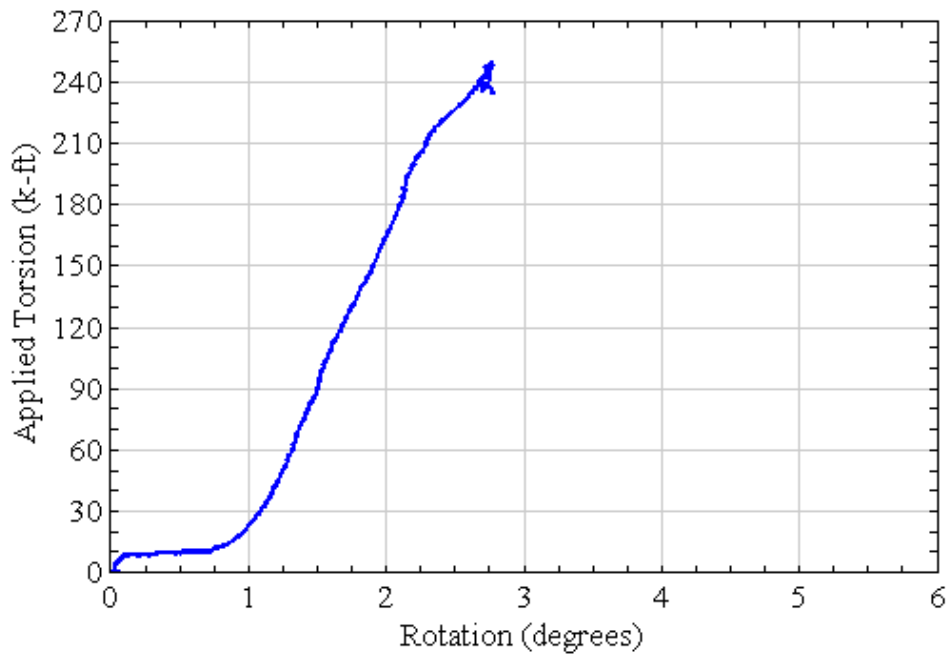


Figure 5-28. Change in rotation between outer and inner poles across slip joint

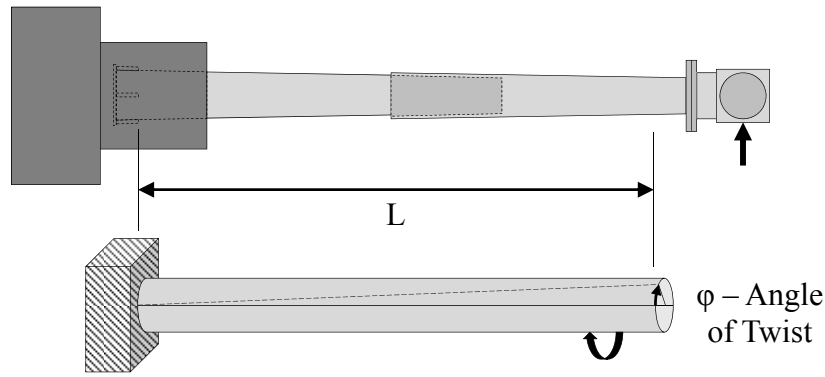


Figure 5-29. Comparison of rotation in test poles with theoretical pole

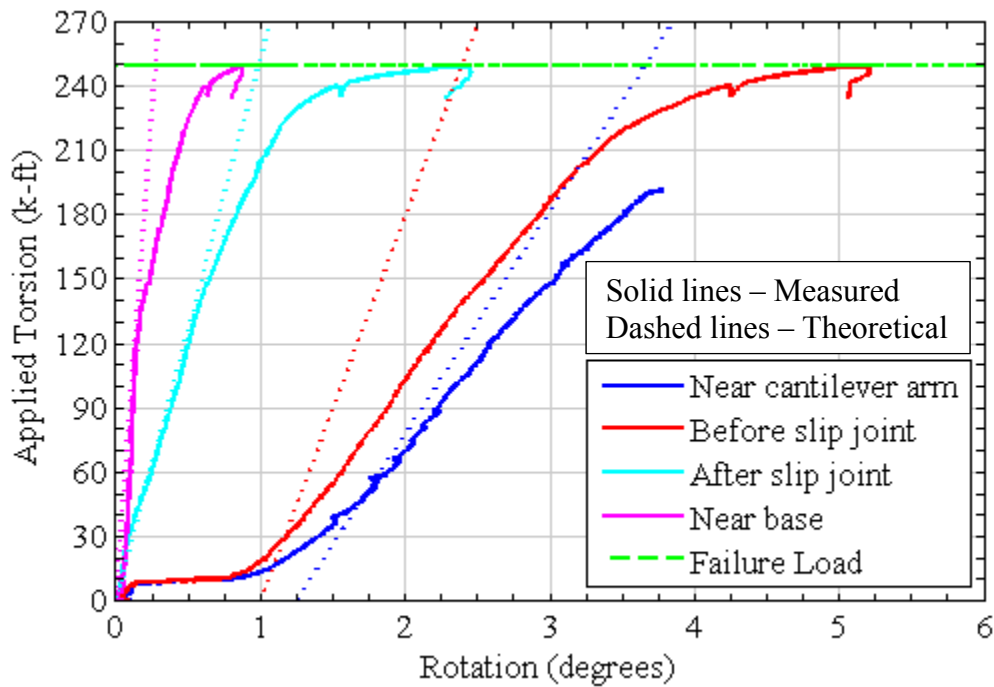


Figure 5-30. Measured rotation along length of poles with the predicted angle of twist

The comparison between the measured and theoretical rotations can be made primarily by the slopes of the lines in the elastic region of loading. The slopes of the measured and theoretical lines appear to match up well along the embedded pole, especially below an applied torsion of 140 kip-ft. The slopes of the measured and theoretical lines on the outer pole do not seem to match up nearly as well. Since slack in the joint is taken out at the beginning of loading, the differences between the two lines cannot be attributed to that. However, it is possible that the

differences in slope are a result of the threaded rods bearing on the bolt holes. This bearing causes gradual deformations at the bolt holes as well as crushing of the threads on the bolts. This explains the larger measured rotations along the length of the upper pole, hence increasing the slopes of the measured lines.

## CHAPTER 6 DISCUSSION

The implementation and results of the test program suggest a number of items to address with respect to the use of the tapered bolted slip base connection in field applications. It is important to look beyond the engineering design of the strength and stability of the structure and also examine factors that impact the structure from the beginning to the end of its service life. Select issues regarding the construction, maintenance, and design of the structure must be considered in order to make an informed decision regarding the plausibility of this base connection as an alternative to the current anchor bolt and annular plate system.

### **6.1 Constructability Concerns**

As with any new design that goes beyond the typically implemented designs and field applications, there are issues to be addressed. A design that seems advantageous in theory may present a number of challenges when making it a reality. The tapered bolted slip base connection is no exception. In order to construct the design, a number of constructability concerns must be considered, some of which have been discussed with contractors of cantilever sign structures for feedback and suggestions.

#### **6.1.1 Placement and Alignment of the Embedded Pole**

One of the first issues to address during construction is the placement of the embedded pole within the reinforcement cage of the concrete pedestal and maintaining proper alignment while the concrete cures. In a typical anchor bolt design, the anchor bolts are placed within the reinforcement cage and cast into the concrete. Then, the monopole with an annular plate are hoisted into position and aligned with leveling nuts. The embedded pipe, on the other hand, must be suspended at the proper height and properly aligned.



There are a number of options to consider for suspending the pipe at the required height. One option is to use some additional reinforcement placed horizontally across the reinforcement cage to support the weight of the embedded pole. The additional rebar will simply be cast-in-place with the rest of the reinforcement and the pole. This along with alignment rebar and external bracing provides both vertical support and proper vertical alignment. This approach was used in the construction of the test apparatus (Figure 6-1). However, it may be important to note that this approach may not be feasible with larger sections if the weight of the pole resting on the rebar causes it to deflect greatly. As long as the proper height is maintained and the reinforcement cage is not distorted by the additional weight, then this can be an acceptable, low cost option for placing the embedded pole.



Figure 6-1. Alignment rebar within pedestal and external bracing of embedded pole. Photos courtesy of FDOT.

Another option involves slightly modifying the original design of the embedded pole and plate assembly. Rather than try to suspend the pole at the appropriate height within the foundation, the pole can extend the full pedestal depth and rest on the bottom of the excavated hole or formwork. In order to take advantage of the full height of the pedestal for the concrete

breakout cone, the welded plates should not be positioned at the base of the pole. Instead they can be welded at the desired height above the base of the pole (Figure 6-2). This way the pole can rest on the ground without having to be suspended in air until the concrete is poured while still taking full advantage of the breakout cone. This option would also require external bracing for proper vertical alignment.

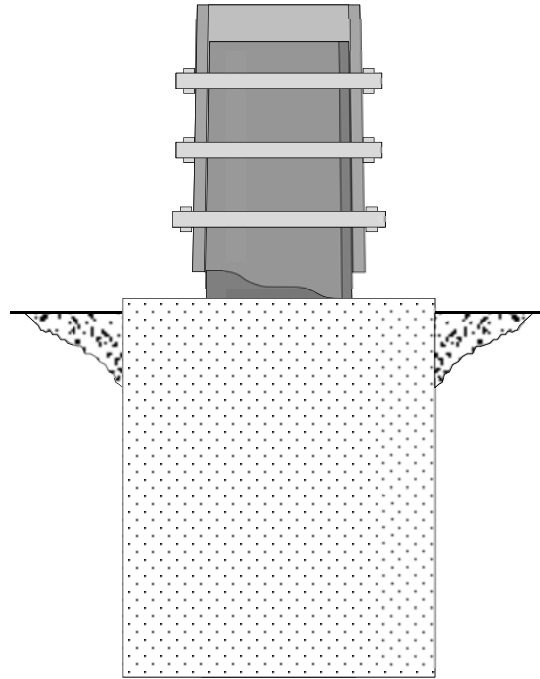


Figure 6-2. Alternate embedment design

### **6.1.2 Placement of the Upper Pole Section**

Once the embedded pole has been placed in the foundation and the concrete reaches adequate strength to continue construction of the superstructure, it is time to place the upper pole section to create the slip joint. The embedded pole will likely have to extend several feet above ground to allow room for any access panels and provide sufficient space for any unexpected slip of the two mating pole sections. This means the upper pole may have to be hoisted higher than in the typical case involving a base connection with anchor bolts. This probably will not cause

any additional problems, but should be noted in case it impacts the height of the crane required for hoisting the monopole of the superstructure into position (Figure 6-3).



Figure 6-3. Placement of the upper pole for the test apparatus using an overhead lift. Photo courtesy of FDOT.

Manufacturer's guidelines for slip joints in high-mast lighting applications require that the pole sections making up the slip joint make a tight-fit with only small gaps between sections. In order to do this, a pair of jacking devices, such as come-alongs, positioned on opposite sides of the joint can be used to force the poles together in order to obtain the minimum required slip joint length and adequate tightness of the connection. According to the installation guidelines, the exact force applied to the joint will vary based on what is required to obtain the minimum splice length, but at the very least should meet or exceed the self-weight of the superstructure to prevent unwanted slip during placement of those structural components (Valmont Structures 2002).

It may be possible to apply the necessary jacking forces to the poles while they are in their upright position, but the installation guidelines also allow for the jacking forces to be applied

before they are hoisted into position. In this case, that means the embedded and upright poles will have to be jacked together on the ground and then hoisted into place as a single unit, which also means that the support used to position the embedded pole within the foundation must support the self-weight of both the embedded and upper poles. It also means that care must be given to ensure the poles do not slide apart or place undue stress on the through-bolts while being hoisted into position.

### **6.1.3 Placement of Through-bolts in the Slip Joint**

The most difficult part of placing the through-bolts in the slip joint is proper placement and alignment of the bolt holes. Since the self-weight of the superstructure may cause settlement of the upper pole and the bolt holes must be drilled through both poles, it is imperative that the final position of the poles be known before drilling holes through both pole sections. This is one reason the current manufacturer's installation guidelines for high mast light poles require that a jacking force equal to or greater than the self-weight of the poles be applied to the joint. Depending on whether the poles are jacked together on the ground or in the upright position, may depend on the best approach for placing the bolt holes.

If the poles are fitted together on the ground, then it may be possible to also drill the bolts holes while the poles are horizontal. This will only work if the poles are properly fitted so that they will not slip under self-weight of the superstructure. Any slippage would add unplanned stress to the through-bolts. Drilling of the bolt holes with the poles on the ground would certainly simplify access to the work space. As can be seen in Figure 6-4, a steel I-beam was secured to the outer pole for use as a support for the equipment required to drill the bolt holes through the slip joint connection. The use of heavy metal supports and equipment makes this procedure appealing if it can be done at or near ground level.

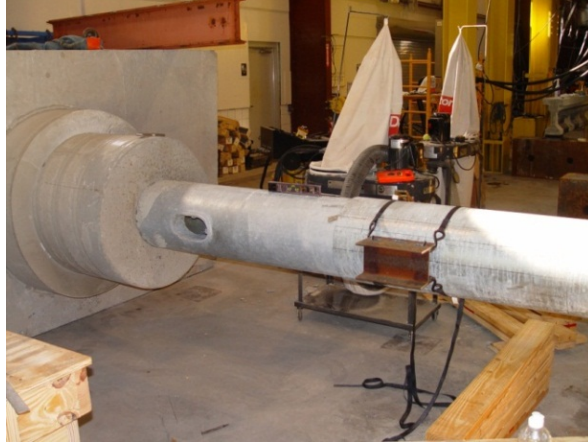


Figure 6-4. A short I-beam for supporting the drilling equipment for placement of bolt holes. Photo courtesy of FDOT.

If instead the poles are fitted together in the upright position, then the self-weight of the upper pole will make it easier to ensure that the poles do not experience additional slippage. However, accessing the work space and getting the necessary equipment in place becomes much more difficult. Since the slip joint could be positioned as much as eight feet above ground, the use of ladders, scaffolding equipment, or bucket trucks may be necessary to drill the bolt holes and place the through-bolts. Perhaps the same framing or scaffolding system used to maintain alignment of the poles while the concrete cures can also be used for placement of the through-bolts.

## **6.2 Maintenance Concerns**

Once the tapered bolted slip base connection is constructed and placed in service, maintenance of the structure becomes the next major concern. Regular inspections are recommended to ensure the integrity of the connection and that the rest of the structure remains intact. Of particular concern with regards to maintenance are the fatigue, corrosion, and repair of various structural components. More specifically, corrosion within the concrete and along the interface of the steel poles in the slip joint region must be monitored to ensure that moisture is not accumulating in these vulnerable spaces.

### 6.2.1 Fatigue Inspections

The importance of fatigue inspections and the structural components that are susceptible to fatigue are discussed in Section 2.4 above. Although the AASHTO fatigue rating for this type of base connection is much higher than the anchor bolt and annular plate system currently in use, it still requires regular inspections. These inspections are particularly important considering that this type of base connection has not previously been used with cantilever signal and sign structures, nor is a slip joint connection commonly associated with the transfer of both flexure and torsion. When inspecting the tapered bolted slip base connection, it is important to examine the through-bolts and longitudinal seam welds of the poles.

The through-bolts are intended to resist the torsional loads in extreme wind conditions without the influence of the bending moment from the extreme wind conditions; consequently, the through-bolts should be aligned parallel to the mast arm. However, this places them directly in line with the cyclic bending moments associated with galloping loads, which when they occur cause the mast arm to vibrate vertically as opposed to the horizontal motion associated with wind loading. Even though the slip joint is responsible for transferring bending moments, it is still possible that the swaying motion of the upper pole section could impact the through-bolts as it transfers moment from the galloping loads to the inner pole. Since galloping loads are considerably small relative to extreme wind loading conditions, the impact on the through-bolts should be minimal. However, it is important to make certain that these fatigue loads are not causing any substantial damage to the through-bolts.

In addition to the through-bolts, the longitudinal seam weld of the poles should also be examined. This may be more relevant for the upper pole section given the deformations observed during testing (Figure 5-11). Although longitudinal weld fatigue is more commonly associated with multi-sided sections, the round sections also have a seam weld that requires

inspection (Figure 6-5). The location of the seam weld may also impact its ability to resist wearing due to fatigue. Seam welds are most likely impacted by repetitive flexural loading that pulls the seam apart, much as the upper steel pole during testing was being stretched transversely at its base because of oblong deformation of the round cross-section (Figure 5-11). Therefore it seems reasonable to place the seam weld along the flexural neutral axis to minimize any deformations. However, the bolt holes in the connection should not coincide with the seam weld. One approach might be to maintain minimum edge distance requirements for bolts holes near a free edge when trying to determine how far from the bolt holes the weld should be placed. Regardless, there is no way to ensure the seam weld will not experience any fatigue.



Figure 6-5. Longitudinal seam weld placed to the right of through-bolt holes. Photo courtesy of S. Dalton.

### **6.2.2 Corrosion Inspections**

Corrosion of the tapered bolted slip base connection is another area for concern and should be monitored regularly throughout the service life of the structure. Some of the methods employed during assembly of the test apparatus create a number of corrosive vulnerabilities and should be considered carefully in the fabrication and construction processes. There are also

some concerns regarding corrosion based simply on the characteristics of how the slip joint is fitted together. For this same reason, proper inspection of the connection may be difficult.

Some of the methods employed during assembly of the slip joint remove the galvanization from the surface of the poles and may eventually lead to problems with corrosion. For example, metal burrs on the surface of the poles in the region of the slip joint splice prevented the slip joint from reaching the minimum required splice length and had to be ground down, which removes galvanization from the faying surfaces within the slip joint region (Figure 4-2). Also, through-bolt holes had to be drilled once the actual slip joint length was determined. Both of these necessary steps in the assembly process exposed bare steel to the elements.

After testing was completed, the test apparatus was disassembled and relocated outside the FDOT Marcus H. Ansley Structures Research Center. One month later, the steel poles were revisited for additional observation. After only one month, rust was visible in the areas that had been ground down and along the inner walls of the bolt holes (Figure 6-6). Fortunately, the amount of rust present after only one month is minimal relative to the wall thickness of the pole sections, although prolonged exposure may ultimately impact the service life of the structure. Unfortunately, these are necessary steps in the assembly process. The burrs are likely caused by the galvanization process and therefore cannot be ground down prior to galvanization. Also, the location of the bolt holes is dependent on the final fit of the slip joint and may be impacted by the outcome of the galvanization process. One option is to treat the bolt hole areas with corrosion-resistant coating or paint before placing the through-bolts. Another option may be to drill the bolt holes prior to galvanization and then use jacking forces to ensure proper positioning, if necessary.





Figure 6-6. Rust on the surface of a pole and within the bolt holes. Photo courtesy of S. Dalton.

In addition to the vulnerabilities presented by the fabrication and assembly processes, the physical connection of the slip joint may make it susceptible to corrosion. Unlike the current anchor bolt and annular plate base connection, the slip joint connection consists of two overlapping surfaces that have the potential to trap water and debris. If any small gaps exist between the mating surfaces of the two poles, then it may allow space for water and air to generate pack rust within the slip joint. Pack rust can cause separation of plate elements as it builds in the crevice between them, and may cause additional stress in the pole walls (Ward 2009). Although the open end of the slip joint is pointing toward the ground, capillary action may pull water on the surface of the poles up into the slip joint. In addition, the presence of bolt holes along the length of the slip joint may allow water access to the interior of the connection. The overlap of steel members along the splice length makes inspection for corrosion difficult.

One more area of concern regarding corrosion is not in the connection itself, but in the interface between the embedded pole and concrete. The interface between the pole and concrete is not likely to make a perfect bond, leaving a small crack around the perimeter of the pole. This may leave room for water and debris to collect along the base of the pole. Similarly, the embedded pole acts as a barrier within the concrete foundation, preventing water from draining

properly through the concrete. Both possibilities make the base of the pole structure susceptible to corrosion over time.

A solution to this problem may come from masonry construction. The addition of weep holes to the design of the foundation may provide a path for any trapped water to drain to the exterior. A few small holes can be drilled through the pole wall and wicks drawn through to the edge of the foundation. Another option may involve placing small plastic tubes through the holes to provide a conduit for water to drain from the interior of the embedded pole as needed. The idea is to place only a few very small pathways to allow water drainage without impacting the overall strength of the concrete or bond between the concrete and steel.

### **6.2.3 Repair of Base Connection**

A typical maintenance concern to consider is the repair of structural components in the event of damage or a complete failure. Repairs of the connection may be necessary due to structural component failures in the event of extreme loading conditions or could be the result of numerous years of exposure to fatigue and corrosion. In either case, it is necessary to examine the repair process in order to compare it to the current base connection system.

In the event of structural failures due to extreme loading conditions, there are three basic failure modes to consider with respect to the tapered bolted slip base connection. If the base connection fails due to flexural loading, there could be two forms of pipe buckling. One form of pipe buckling might occur within the slip joint splice length as a result of large normal forces being transferred through the slip joint. These normal forces bearing on the walls of the poles could be too great and ultimately cause pipe buckling. This type of failure could be due to a slip joint splice length that is designed too short for the structural loads and is seen in the study conducted by the Sumitomo Metal Industries, Ltd. (Kai and Okuto 1974). The second form of pipe buckling might occur along the length of the poles, particularly near access panels that

create stress concentrations. This was the case observed during testing of the slip joint (Figure 5-1). Although, technically this is not a failure of the base connection itself, the poles are an essential component of the base connection.

In either case, the base connection will need to be disassembled in order to replace the buckled pole section. If the outer pole buckles, the mast arm assembly and base connection will have to be removed from the damaged section of pole so that a new pole can be installed. If the embedded pole section buckles, then the entire superstructure will have to be removed while a new embedded pole assembly is cast into a new foundation. This is probably more likely to occur than buckling in the upper pole due to the location of the access panel in a region of large flexural moment and also because there is a large normal force pushing against the free end of the inner pole within the slip joint.

In order to prevent having to remove the entire superstructure in cases of buckling in either of the poles, an alternative option may be feasible. Looking back to the design of the welded sleeve connection, a similar type of repair might be possible for this type of structure. Since the welded sleeve connection was derived from the use of a couple of half-shell plates to repair damaged poles, then it may be possible to reinforce the buckled area if it does not occur near the access panel or other obstruction. This may only work if the structural deflections due to buckling are small and the remainder of the structure is still acceptably sound.

Although a flexural failure of the base connection would require significant repairs, they do not vary greatly from the repairs that would be required for a flexural failure of the current anchor bolt and annular plate base connection. A flexural failure in the current base connection system could mean that the superstructure pole has buckled near the annular plate, the annular plate has experienced significant bending and is no longer flat, the weld connecting the annular

plate and pole has failed, or even that the anchor bolts have been pulled out of the concrete foundation. The first three cases all require the superstructure be taken down to either repair the annular plate connection or replace the monopole altogether. If the failure occurs with the anchor bolts, then new anchor bolts may have to be cast in a new foundation.

If instead, a torsional failure of the tapered bolted slip base connection occurs, then hopefully the through-bolts have sheared off and the sign has only rotated around the embedded pole. If this occurs, then repair of the base connection would involve rotating the mast arm assembly back into its proper position, which could require the use of some heavy equipment to pull the sign or signal structure around, and then replacing the through-bolts. This varies greatly from the torsional failures of the anchor bolt and annular plate base connection failures that were observed in Florida in 2004, in which the entire superstructure fell to the ground and the concrete foundation was destroyed by the anchor bolts (Cook and Halcovage 2007).

In addition to structural failures, the effects of fatigue and corrosion may also require repairs to the proposed base connection design. Fatigue of the pole section should not be any more problematic than is currently seen with existing high-mast lighting towers or the weld fatigue associated with annular plates. Fatigue in the through-bolts also should not present any greater of a challenge than is seen with anchor bolts. Rather the problems with corrosion of the slip joint may require the most attention.

If corrosion is persistent within the slip joint and allowed to continue over several years without proper maintenance, then the repair of the tapered bolted slip base connection could mean that both the embedded pole and the upper pole need replacement. In order to prevent the development of pack rust between the two pole sections in the slip joint, it may be necessary to apply a sealant around the base of the slip joint so that water cannot be absorbed into the space

between pole sections through capillary action. This is not considerably unlike the corrosion of the anchor bolts and annular plate system, which could require replacement of both parts if too much corrosion is allowed to take place.

### **6.3 Design Guidelines**

The design of the tapered bolted slip base connection consists of designing two main components: the slip joint and the through-bolts. The slip joint, which consists of the two adjoining poles, must be designed to have an adequate slip joint length to transfer flexure, while the pole sections must be capable of withstanding the flexural and torsional loads. The through-bolts must be designed for the proper torsional load depending on the desired behavior of the connection. The appropriate design procedure for the embedded pipe and plate assembly has already been discussed in detail by Cook and Jenner (2007).

#### **6.3.1 Slip Joint Splice Length Design**

The AASHTO *Standard Specifications for Structural Supports for Highway Signs, Luminaires and Traffic Signals* (2009) identifies a minimum required splice length of 1.5 times the inner diameter of the outer pole section. The FDOT specifies a minimum splice length of 1.5 times the diameter of the poles plus an additional 6 inches to allow for slip. This can be found indirectly in the FDOT *Design Standards* (2010) and more explicitly in the notes of the High Mast Lighting program (FDOT, 2007a). There is no additional check for the required pipe thickness in the region of the slip joint.

The pole sections used to construct the slip joint should first be designed to resist both the flexural and torsional loads that must be carried from the mast arm to the foundation. The design must also take into account any axial or shear load resulting from the applied loads on the structure. The appropriate guidelines for the design of round pole sections can be found in both the AASHTO *Standard Specifications for Structural Supports for Highway Signs, Luminaires*

*and Traffic Signals* as well as the *AASHTO LRFD Bridge Design Specifications*. The major concern regarding tapered poles is that the strength is verified along the length of the pole, particular at the top and base of each pole member, since the taper changes the cross-sectional properties from one end to the other. Granted, a change in diameter of 0.14 inches per foot of length is relatively small, it could have a more serious impact on longer lengths of pole and should be taken into consideration. Once the poles have been designed for adequate flexural and torsional strength, the length of the slip joint can be determined.

### **6.3.2 Through-bolt Design**

The purpose of the through-bolts in the tapered bolted slip base connection is to transfer the entire torsional load from the upper pole to the embedded pole through the slip joint. The design of the through-bolts in the connection must adhere to AASHTO guidelines for bolted connections, which are discussed in Section 3.1.2. During testing of the base connection, the test apparatus was able to take on load well beyond the predicted value to cause a shear failure of the through-bolts, which leads to the debate of whether or not to include the effects of friction in the design of the through-bolts.

The design of the through-bolts for use in the tapered bolted slip base connection can simply be done using the same design procedures associated with typical bolted connections. The test of the base connection indicates that the AASHTO predicted strength of the through-bolts can be quite conservative when shear controls the design. Using only the AASHTO guidelines to determine the strength will provide a base connection that is more than adequate to transfer torsional load across the through-bolts.

The cause behind the larger magnitude failure load compared to the predicted AASHTO failure load is due to the presence of friction in the connection. Friction helps transfer some of the torsional load from the upper pole to the embedded pole and reduces the percentage of the

applied load that must be carried solely by the through-bolts. Although the slip joint was loosely-fitted, the flexural loads created normal forces on the surfaces of the poles that then impacted the transfer of torsional load. This is discussed in greater detail in section 5.1.3. This explains why the through-bolts did not fail as had been originally expected and why the connection was able to carry more load than anticipated.

From a structural design standpoint, the bolted connection guidelines in AASHTO are capable of providing ample factors of safety for the through-bolted component of the tapered bolted slip base connection. The presence of friction in the joint increases the factors of safety to prevent unwanted failure. On the other hand, the presence of friction may make it more difficult to determine the actual failure load of the through-bolted connection without first having knowledge of the coefficients of friction and the tensile strength of the bolts. This could prevent the through-bolts from failing prior to any other structural component and prohibit the desired failure mode where the mast arm and superstructure are able to pivot about the embedded pole in extreme wind conditions. Also, if the manufacturer's guidelines for jacking the two poles together are followed, this will only add friction and make this failure mode more difficult to achieve.

Therefore, the worst-case design scenario for the through-bolts is to assume that friction does not contribute to the strength of the connection. This requires that the through-bolts carry the entire torsional load from the mast arm down to the foundation and reduces the expected torsional capacity of the connection. Since friction will always be present in the slip joint splice, it will add to the torsional capacity of the connection. If friction is to be included in the design of the tapered bolted slip base connection, then a coefficient of friction of 0.33 is recommended in accordance with AASHTO's specifications for hot-dip galvanized faying surfaces (2010).

## CHAPTER 7 CONCLUSIONS

The literature review and test program indicate a number of advantages and disadvantages of the tapered bolted slip base connection as an alternative to the anchor bolt and annular plate system found in most of the cantilever signal and sign structures in use today. Ultimately, there are a number of questions to answer with regard to the ability of the alternative base connection to transfer load from the superstructure to the foundation, the necessary design procedures, and the constructability and maintenance challenges.

The first and most essential element in any structural design is ensuring that adequate strength can be provided to resist applied loads. The base connection for a cantilever signal or sign structure must be able to successfully transfer both flexural and torsional loads from wind in addition to any shear and axial load. In this type of connection, the flexural load is intended to be carried through the slip joint while the torsional load is transferred by the through-bolts.

The results of the test program indicate that the tapered bolted slip joint connection can be designed to adequately transfer flexural and torsional loads using typical section sizes associated with these types of cantilever signal and sign structures. The pole sections should be designed for all torsional, flexural, axial, and shear loads as required using the AASHTO specifications.

The test program also suggests that the torsional capacity of the tapered bolted slip base connection can be determined using the design procedures for bolts provided by the AASHTO specification. The bolt design strengths obtained by AASHTO are conservative for this type of connection, providing more than enough shear resistance to withstand the applied torsion. The flexural interaction of the pole sections as well as any jacking forces applied during assembly of the joint increases the contribution of friction to resisting the torsional load, as was seen by the increase from the predicted to the actual test failure load.



At this stage of developing the appropriate design procedures for the through-bolted component of the base connection, it is most reasonable to discard the notion of being able to have a planned failure mode in which the through-bolts are sheared off under high wind loads and the upper portion of the structure is allowed to pivot around the embedded pole. This does not imply that it is impossible to design for such a failure mode, as is proven possible by the frictional analysis discussed previously. It does infer that given the material information currently available to engineers during the design process and quantifying frictional resistance, will make it difficult to predict actual through-bolt failures under specific loads. Most of the ASTM standards specify minimum required material strengths, but do not restrict the maximum strength. As was seen in the case of the test specimen, the ASTM A307 threaded rods were specified to have a minimum tensile strength of 60 ksi and were tested to an ultimate tensile strength of nearly 91 ksi.

All things considered, the tapered bolted slip base connection is capable of transferring loads adequately and so can be considered a viable option to the anchor bolt and annular plate system currently in use. The fatigue rating of the load transfer system has been improved by eliminating welds and anchor bolts, both of which have poor AASHTO fatigue ratings, and replacing them with a slip joint and through-bolts. The improved fatigue rating is beneficial in terms of design and maintenance of the new base connection system.

All of the concerns regarding construction and maintenance of the base connection are either on par with the current system or an improvement. As with any new design, there are a number of plausibility issues to work through during implementation, but some suggestions for the major areas of concern have been provided. These concerns regarding the construction of

cantilever signal and sign structures may be further addressed by conducting another research project that focuses on the implementation of this base connection in field applications.

Further areas of study related to this topic may involve a field study and possibly considering other alternatives for the base connection. A field study may involve constructing a number of full-scale cantilever structures fitted with signs or signals as appropriate to troubleshoot any issues that may arise during that process. Once the structures are in place, their performance in the field will be monitored under normal conditions to determine if there are any problems with settlement in the slip joint that might place unwanted stress on the through-bolts. It may also be possible to simulate extreme wind loading conditions using the hurricane wind simulator at the University of Florida. This will provide more insight into the ability of the base connection to transfer larger than normal loads and possibly even the plausibility of planning for the through-bolts to shear off as the first structural mode of failure.

Additional research into alternative base connections that do not involve the use of the embedded pipe and plate assembly developed by Cook and Jenner (2010) may also be considered. For instance, further investigation into the directly embedded spun cast prestressed pole designs with a steel superstructure may be considered as an alternate base connection that moves away from exposed steel components protruding from the foundation near grade. This could be potentially promising with respect to corrosion of steel elements near the ground by eliminating the galvanic cell between two metals.

Another possibility is eliminating the base connection from the system entirely. Since the embedded pipe and plate assembly was developed and proven adequate for transferring load to the foundation and the pipe protrudes out of the concrete, it may be reasonable to simply extend the pipe the full desired height of the monopole and connect it directly to the mast arm. Of

course, this alternative still presents some of the same challenges as the tapered bolted slip base connection, but it does eliminate some of the concerns of fatigue and corrosion that are associated with having a base connection in the structural design.

In conclusion, the investigation showed the tapered bolted slip base connection is capable of transferring the torsional and flexural loads from cantilever signal and sign structures to the foundation. It is the final recommendation of this research program to follow up this project with the implementation of a field testing program as previously mentioned.

## REFERENCES

- American Association of State Highway and Transportation Officials (AASHTO). (2009). *Standard specifications for structural supports for highway signs, luminaires and traffic signals*, 5th Ed., AASHTO, Washington, DC.
- American Association of State Highway and Transportation Officials (AASHTO). (2010). *LRFD bridge design specifications*, 5th Ed., AASHTO, Washington, DC.
- American Concrete Institute (ACI). (2008). *Building code requirements for structural concrete and commentary*, ACI 318-08, ACI, Farmington Hills, MI.
- American Institute of Steel Construction (AISC). (2005). *Steel construction manual*, 13th Ed., AISC, Chicago, IL.
- American Institute of Steel Construction (AISC). (1997). *Hollow structural sections connections manual*, 1st Ed., AISC, Chicago, IL.
- American Society of Civil Engineers (ASCE). (2006). *Design of steel transmission pole structures*, ASCE/SEI 48-05, ASCE, Reston, VA.
- ASTM. (1993a). "Standard specification for alloy-steel and stainless steel bolting materials for high-temperature service." *A193-93*, ASTM, West Conshohocken, PA.
- ASTM. (1993b). "Standard specification for carbon and alloy steel nuts for bolts for high-pressure and high-temperature service." *A194-93*, ASTM, West Conshohocken, PA.
- ASTM. (2000). "Standard specification for carbon and alloy steel nuts." *A563-00*, ASTM, West Conshohocken, PA.
- ASTM. (2002a). "Standard specification for structural bolts, steel, heat treated, 120/105 ksi minimum tensile strength." *A325-02*, ASTM, West Conshohocken, PA.
- ASTM. (2002b). "Standard specification for structural bolts, alloy steel, heat treated, 150 ksi minimum tensile strength." *A490-02*, ASTM, West Conshohocken, PA.
- ASTM. (2003a). "Standard specification for carbon steel bolts and studs, 60000 psi tensile strength." *A307-03*, ASTM, West Conshohocken, PA.
- ASTM. (2003b). "Standard specification for hardened steel washers." *F436-03*, ASTM, West Conshohocken, PA.
- ASTM. (2006). "Standard specification for spun cast prestressed concrete poles." *C1089-06*, ASTM, West Conshohocken, PA.
- ASTM. (2007). "Standard specification for high-strength low-alloy columbium-vanadium structural steel." *A572-07*, ASTM, West Conshohocken, PA.

- ASTM. (2011). "Standard specification for determining the mechanical properties of externally and internally threaded fasteners, washers, and rivets." *F606-11*, ASTM, West Conshohocken, PA.
- Beese, W. (1995). "Analysis of annular base plates subjected to moment." M.E. report, University of Florida, Gainesville, FL.
- Bui, L. H. (2010). "Development of an impact-breakaway, wind-resistant base connection for multi-post ground signs." Ph.D. dissertation, University of Florida, Gainesville, FL.
- Chan, J. (2003). *Managing transmission line steel structures*, Version 1, Electric Power Research Institute, Palo Alto, CA.
- Cook, R. A. and Bobo, B. J. (2001). "Design guidelines for annular base plates." *FDOT Report BC354-04*, FDOT, Tallahassee, FL.
- Cook, R. A., Ellifritt, D. S., Schmid, S. E., Adediran, A., and Beese, W. (1995). "Design procedure for annular base plates." *FDOT Report 0510697*, FDOT, Tallahassee, FL.
- Cook, R. A., and Halcavage, K. M. (2007). "Anchorage embedment requirements for signal/sign structures." *FDOT Report BD545-54*, FDOT, Tallahassee, FL.
- Cook, R. A., Hoit, M. I., and Nieporent, S. B. (1998). "Deflection calculation model for structures with annular base plates." *FDOT Report 0151697*, FDOT, Tallahassee, FL.
- Cook, R. A., and Jenner, K. L. (2010). "Alternative support systems for cantilever signal/sign structures." *FDOT Report BDK75 977-04*, FDOT, Tallahassee, FL.
- Cook, R. A., McVay, M. C., and Britt, K. C. (2003). "Alternatives for pile splices." *FDOT Report BC354-80, Part 1*, FDOT, Tallahassee, FL.
- Dexter, R. J., and Ricker, M. J. (2002). "Fatigue-resistant design of cantilevered signal, sign, and light supports." *NCHRP Report 469*, National Cooperative Highway Research Program, Transportation Research Board of the National Academies, Washington, DC.
- Federal Highway Administration (FHWA). (2005). *Guidelines for the installation, inspection, maintenance and repair of structural supports for highway signs, luminaries, and traffic signals*, U. S. Department of Transportation, Washington, DC.
- Florida Department of Transportation (FDOT). (2007a). High Mast Lighting: Mathcad 13 Program (Version 2.0) [Software]. Available from <http://www.dot.state.fl.us/structures/Programs/setupHighmastLightingV2.0.exe>
- Florida Department of Transportation (FDOT). (2007b). Cantilever Overhead Sign Program (Version 5.1) [Software]. Available from <http://www.dot.state.fl.us/structures/Programs/setupCantileverV5.1.exe>

- Florida Department of Transportation (FDOT). (2010). *Design standards for design, construction, maintenance, and utility operations on the state highway system*, FDOT, Tallahassee, FL.
- Fouad, F. H., Davidson, J. S., Delatte, N., Calvert, E. A., Chen, S. E., Nunez, E., and Abdalla, R. (2003). "Structural supports for highway signs, luminaires, and traffic signals." *NCHRP Report 494*, National Cooperative Highway Research Program, Transportation Research Board of the National Academies, Washington, DC.
- Kaczinski, M. R., Dexter, R. J., and Van Dien, J. P. (1998). "Fatigue-resistant design of cantilevered signal, sign and light supports." *NCHRP Report 412*, National Cooperative Highway Research Program, Transportation Research Board of the National Academies, Washington, DC.
- Kai, T. and Okuto, K. (1974). "Discussion: How safe are your poles?" *Journal of the Structural Division*, 100(9), 1954-1955.
- Kulak, G. L., Fisher, J. W., and Struik, J. H. A. (2001). *Guide to design criteria for bolted and riveted joints*, 2nd Ed., American Institute on Steel Construction, Chicago, IL.
- Lee, H. K., Kim, K. S., and Kim, C. M. (2000). "Fracture resistance of a steel weld joint under fatigue loading." *Engineering Fracture Mechanics*, 66(4), 403-419.
- McVay, M., Bloomquist, D., Forbes, H., and Johnson, J. (2009). "Prestressed concrete pile installation: Utilizing jetting and pressure grouting." *FDOT Report BD545-31*, FDOT, Tallahassee, FL.
- Ramsdale, R. (2006). "Reference tables: Coefficient of friction." Retrieved from <http://www.engineershandbook.com/Tables/frictioncoefficients.htm>
- Reid, K. (2003). "Annular base plate design guidelines." M.E. report, University of Florida, Gainesville, FL.
- Tempel, J. van der, and Shipholt, B. L. (2003). "The slip joint connection: Alternative connection between pile and tower." *Dutch Offshore Wind Energy Converter project DOWEC-F1W2-JvdT-03-093/01-P*, Energy Research Centre of the Netherlands, Petten, Netherlands.
- United States Department of Agriculture. (2008). "Guide specifications for steel single pole and h-frame structures." *Rural Development Utilities Programs Bulletin 1724E-204*. Retrieved from <http://www.usda.gov/rus/electric/pubs/1724e-204.pdf>
- Valmont Structures, Inc. (2002). *Installation guidelines: High mast and sports lighting structures*, Valmont, Valley, NE.
- Ward, B. R. (2009, January). "The falling sky: Aging high-mast light towers a growing concern in U.S." *Roads and Bridges*, 52-55.

APPENDIX A  
DESIGN OF TAPERED BOLTED SLIP BASE CONNECTION

The appropriate AASHTO specifications for designing the tapered bolted slip base connection are discussed in Chapter 3. The design of the slip joint consists primarily of the design of the poles to ensure adequate strength for both torsion and flexure, the design of the through-bolts for adequate shear and bearing strength, and the design of the appropriate slip joint length to transfer the flexural loads through the connection. Since the poles are tapered, they require checks at each cross-section along the length of the poles for design purposes.

As an example, a single cross-section is shown in the calculations that follow. The cross-section chosen for the design of the tapered steel poles is the base of each of the pole members where the outer diameter is 16 inches. This section is chosen as a point of comparison for the behavior of the tapered member versus a similar sized HSS member with the hope that the tests reveal the tapered section perform at least as well as an HSS section.

**A.1 Capacity of Steel Pole Section**

**Properties of Tapered Steel Poles at Base**

Outer diameter	$D := 16\text{in}$	
Wall thickness	$t := 0.375\text{in}$	
Length of member	$L := 8\text{ft} + 4\text{in}$	
Elastic modulus	$E := 29000\text{ksi}$	
Yield strength	$F_y := 65.2\text{ksi}$	
Inner diameter	$D_i := D - 2t$	$D_i = 15.25\text{in}$
Area moment of inertia	$I := \frac{\pi}{64} \cdot (D^4 - D_i^4)$	$I = 562.1\text{in}^4$
Distance to extreme stress face	$c := D \div 2$	$c = 8\text{in}$
Elastic section modulus	$S := I \div c$	$S = 70.3\text{in}^3$
Plastic section modulus	$Z := \frac{D^3 - D_i^3}{6}$	$Z = 91.6\text{in}^3$
Torsional constant (AISC conservative equation)	$C := \frac{\pi \cdot (D - t)^2 \cdot t}{2}$	$C = 143.8\text{in}^3$

### A.1.1 Analysis of the Flexural Capacity of the Pole Section

The first reference for the determination of the flexural capacity of the pole section is the *Standard Specifications for Structural Supports for Highway Signs, Luminaires, and Traffic Signals* (AASHTO 2009). The location and heading of the following calculations correspond to the location and heading of each calculation in the respective code.

#### 5.5.2 Local Buckling Width-to-Thickness Ratios

$$\lambda := \begin{cases} \lambda \leftarrow \frac{D}{t} \\ \text{return "compact" if } \lambda \leq 0.13 \cdot \frac{E}{F_y} \\ \text{return "non-compact" if } \lambda \leq 0.26 \cdot \frac{E}{F_y} \\ \text{return "slender" if } \lambda \leq 0.45 \cdot \frac{E}{F_y} \\ \text{return "Exceeds local buckling limit" if } \lambda > 0.45 \cdot \frac{E}{F_y} \end{cases} \quad \lambda = \text{"compact"}$$

#### 5.6 Allowable Bending Stress for Round Members

$$F_b := \begin{cases} F \leftarrow 0.66F_y \text{ if } \lambda = \text{"compact"} \\ F \leftarrow 0.39 \cdot F_y \cdot \left[ 1 + \frac{0.09 \left( \frac{E}{F_y} \right)}{\left( \frac{D}{t} \right)} \right] \text{ if } \lambda = \text{"non-compact"} \\ F \leftarrow 0.39 \cdot F_y \cdot \left[ 1 + \frac{0.09 \left( \frac{E}{F_y} \right)}{\left( \frac{D}{t} \right)} \right] \text{ if } \lambda = \text{"slender"} \\ F \leftarrow \text{"Not Applicable"} \text{ otherwise} \\ \text{return } F \end{cases} \quad \begin{array}{l} \text{Includes a factor} \\ \text{of safety of } \underline{1.5} \\ \text{per commentary.} \\ \\ F_b = 43 \text{ ksi} \end{array}$$

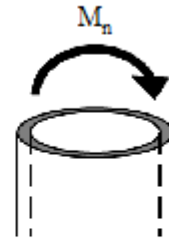
$$M_b := 1.5 \cdot F_b \cdot S \quad M_b = 377.9 \text{ ft} \cdot \text{kip}$$



As a point of comparison, the flexural capacity of the pole section determined by the above allowable stress design (ASD) specification is compared with a similar specification in the *LRFD Bridge Design Specifications* (AASHTO 2010).

6.12.2.2.3 Circular Tubes - Nominal flexural resistance of non-composite circular tube (HSS)

$$\begin{aligned}
 M_n := & \left\{ \begin{array}{l} \lambda \leftarrow \frac{D}{t} \\ \text{return "Exceeds local buckling limit" if } \lambda > 0.45 \cdot \frac{E}{F_y} \\ F_{cr} \leftarrow \frac{0.33 \cdot E}{\lambda} \\ M_y \leftarrow F_y \cdot Z \\ M_{lb} \leftarrow \text{if } \left[ \lambda \leq \frac{0.31 \cdot E}{F_y}, \left( \frac{0.021 \cdot E}{\lambda} + F_y \right) \cdot S, F_{cr} \cdot S \right] \\ M \leftarrow \min(M_y, M_{lb}) \\ \text{return } M \end{array} \right.
 \end{aligned}$$



$M_n = 465.3 \text{ ft} \cdot \text{kip}$

Since the objective of these calculations is to determine the actual failure load of the pole section and the two calculations for the flexural capacity vary from one another, the *Steel Construction Manual* (AISC 2005) is referred as an alternate means of confirmation of the flexural capacity.

Chapter F, Section F8 - Nominal Flexural Strength

$$\begin{aligned}
 M_n := & \left\{ \begin{array}{l} F_{cr} \leftarrow \frac{0.33 \cdot E}{\frac{D}{t}} \\ M \leftarrow \min \left[ F_y \cdot Z, \left( \frac{0.021 \cdot E}{\frac{D}{t}} + F_y \right) \cdot S, F_{cr} \cdot S \right] \\ M_n \leftarrow \text{if } \left( \frac{D}{t} < \frac{0.45 \cdot E}{F_y}, M, \text{"Not Applicable"} \right) \\ \text{return } M_n \end{array} \right.
 \end{aligned}$$

$M_n = 465.3 \text{ ft} \cdot \text{kip}$

Since the more recent AASHTO specification and the AISC manual agree with one another and both are load and resistance factor design (LRFD) methods, the value of the nominal moment capacity was estimated as 465 kip-ft for the purpose of designing the test apparatus.

### A.1.2 Analysis of the Torsional Capacity of the Pole Section

As in the case of the flexural analysis, the first reference for the determination of the torsional capacity of the pole section is the *Standard Specifications for Structural Supports for Highway Signs, Luminaires, and Traffic Signals* (AASHTO 2009). The AASHTO code is somewhat vague with respect to the torsional capacity of steel poles and refers to the following shear stress formulation that is derived from a torsional shear equation.

#### 5.11.1 Allowable Shear Stress (derived from Torsional Shear equation)

$$F_v := \text{if} \left[ \frac{D}{t} \leq 1.16 \cdot \left( \frac{E}{F_y} \right)^{\frac{2}{3}}, 0.33F_y, \frac{0.41E}{\left( \frac{D}{t} \right)^{1.5}} \right]$$

Includes a factor of safety of **1.75** per commentary.  
 $F_v = 21.5 \text{ ksi}$

$$V_n := \begin{cases} A_g \leftarrow \frac{\pi}{4} \cdot (D^2 - D_i^2) \\ V \leftarrow \frac{F_v \cdot A_g}{2} \\ \text{return } 1.75V \end{cases}$$

$V_n = 346.6 \text{ kip}$

Given the lack of differentiation between the shear and torsional capacities in the AASHTO specifications, the AISC steel manual is referred to again for clarification. The AISC specification has clear and separate considerations for shear and torsion, which are as follows:

Chapter G, Section G6 - Nominal Shear Strength

$$\begin{aligned}
 V_n &:= A_g \leftarrow \frac{\pi}{4} \cdot (D^2 - D_i^2) \\
 L_v &\leftarrow \frac{1.5D + 6\text{in}}{2} \\
 F_c &\leftarrow \max \left[ \frac{1.60E}{\sqrt{\frac{L_v}{D} \cdot \left(\frac{D}{t}\right)^{1.25}}}, \frac{0.78E}{\left(\frac{D}{t}\right)^{1.5}} \right] \\
 F_{cr} &\leftarrow \text{if}(F_c \leq 0.6F_y, F_c, 0.6F_y) \\
 V &\leftarrow \frac{F_{cr} \cdot A_g}{2} \\
 \text{return } &\frac{V}{1.30}
 \end{aligned}$$

*Note:*  $L_v$  here is defined as the distance from maximum to zero shear force (assume zero shear occurs at midpoint of splice) and is calculated using the FDOT standard of  $1.5D + 6$  inches to account for galvanization as per the Highmast Lighting software program. For these  $D/t$  ratios, the  $0.6F_y$  condition will control for  $F_{cr}$  and length to zero shear does not impact shear strength.

$$V_n = 277 \text{ kip}$$

Chapter H, Section H3.1 - Nominal Torsional Capacity

$$\begin{aligned}
 T_n &:= F_c \leftarrow \max \left[ \frac{1.23E}{\sqrt{\frac{L}{D} \cdot \left(\frac{D}{t}\right)^{1.25}}}, \frac{0.60E}{\left(\frac{D}{t}\right)^{1.5}} \right] \\
 F_{cr} &\leftarrow \text{if}(F_c \leq 0.6F_y, F_c, 0.6F_y) \\
 T &\leftarrow F_{cr} \cdot C \\
 \text{return } &T
 \end{aligned}$$

*Note:* For these  $D/t$  ratios, the  $0.6F_y$  condition will control for  $F_{cr}$  and thus length of the member does not impact torsional strength.

$$T_n = 468.8 \text{ ft-kip}$$

Normally, in design practice for these types of structures for the FDOT, the AASHTO specifications would control the design despite the conservative results for torsional capacity. However, the objective here is to try to accurately determine the torsional capacity of the pole section, so the results of the AISC method are used for this purpose. Although less conservative, the differentiation between shear and torsion that has been accepted by this code may result in a more realistic failure prediction for the pole section.

### A.1.3 Analysis of the Interaction of Torsion and Flexure for the Pole Section

The results above indicate flexural and moment capacities for the pole section assuming that the loads are applied independently of each other. In practice, the interaction of applied flexure and torsion generates a combination of stresses that influence and reduce the overall

section capacity. The first equality comes from the AASHTO specifications while the second comes from the AISC specification. Here again, the AASHTO code does not differentiate between shear and torsion, but a comparison with the AISC interaction relationship shows that the proportions of the loads are relatively the same.

### 5.12.1 Vertical Cantilever Pole Type Supports

The interaction of simultaneously applied axial, bending, and shear/torsional forces must not exceed the value of 1.0 based on the following interaction equation:

$$\frac{f_a}{0.6F_y} + \frac{f_b}{C_A \cdot F_b} + \left( \frac{f_v}{F_v} \right)^2 \leq 1.0$$

### Chapter H, Section H3.2 - Combined Torsion, Shear, Flexure, and Axial Force

$r$  = required strength under given load conditions

$c$  = AISC design capacity of the member

$$\left( \frac{P_r}{P_c} + \frac{M_r}{M_c} \right) + \left( \frac{V_r}{V_c} + \frac{T_r}{T_c} \right)^2 \leq 1.0$$

**Note:** When  $T_r < 0.20T_c$  then cumulative effects should be determined by Section H1 (ignoring torsion). When  $T_r > 0.20T_c$  then use this interaction equation.

Eliminate axial and shear forces from the interaction curve.

Torsion moment arm for applied load:

$$T_{arm} := 9\text{ft}$$

Flexural moment arm for applied load:

$$M_{arm} := 14\text{ft}$$

Capacity for the pole section considering torsion only:

$$T_n = 468.8\text{ft}\cdot\text{kip}$$

Capacity for the pole section considering flexure only:

$$M_n = 465.3\text{ft}\cdot\text{kip}$$

Write equations for the moment-to-torsion ratio and the interaction curve over the range of nominal torsion values.

Range of torsional values:

$$T_r := 0, 1\text{kip}\cdot\text{ft} .. T_n$$

Moment-to-flexure ratio:

$$MT_r(T_r) := \frac{M_{arm}}{T_{arm}} \cdot T_r$$

Rearrangement of the interaction equation:

$$M_r(T_r) := \left[ 1 - \left( \frac{T_r}{T_n} \right)^2 \right] \cdot M_n$$

Solve for the root of the moment-to-flexure ratio and interaction equation to determine the predicted failure moments for both flexure and torsion. Dividing these moments by their respective moment arms, solve for the applied failure load that can be expected for the pole section.

Root Equation:

$$\text{Failure}(T_r) := M_r(T_r) - MT_r(T_r)$$

Expected failure torsion:

$$\text{Failure}_T := \text{root}(\text{Failure}(T_r), T_r, 0, T_n)$$

$$\text{Failure}_T = 228.2 \text{ ft} \cdot \text{kip}$$

$$\text{Applied\_TLoad} := \frac{\text{Failure}_T}{T_{arm}}$$

$$\text{Applied\_TLoad} = 25.4 \text{ kip}$$

Expected failure flexural moment:

$$\text{Failure}_M := M_r(\text{Failure}_T)$$

$$\text{Failure}_M = 355 \text{ ft} \cdot \text{kip}$$

$$\text{Applied\_MLoad} := \frac{\text{Failure}_M}{M_{arm}}$$

$$\text{Applied\_MLoad} = 25.4 \text{ kip}$$

Based on this analysis, it was expected that the actual applied failure load for the test poles would occur at 25.4 kips based on the interaction of flexure and torsion using the actual material strengths of the steel. The results of the interaction curve are plotted as follows:

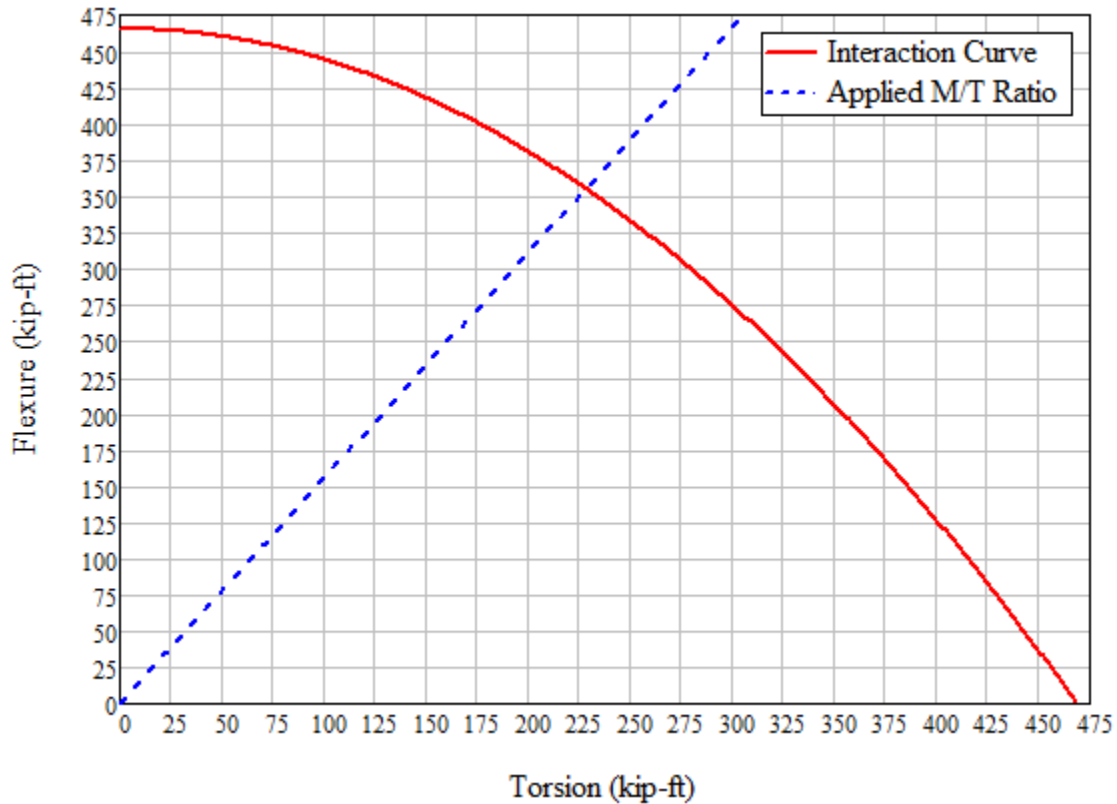


Figure A-1. Steel pole interaction curves for torsion and flexure

## A.2 Capacity of Through-bolted Connection

The controlling design code for cantilever signal and sign structures, Standard Specifications for Structural Supports for Highway Signs, Luminaires, and Traffic Signals (AASHTO 2009), refers to the LRFD Bridge Design Specifications (AASHTO 2010) for the design of bolted connections. The location of each calculation in the design code is included in the heading of the respective calculations that follow.

### Tapered Steel Pole Properties

Taper of pole sections	Taper := 0.14in ÷ ft	
Average outer diameter of lower pole within slip joint	$d_{se} := 16\text{in} - \text{Taper} \cdot 88\text{in}$	$d_{se} = 14.97\text{in}$
Wall thickness of embedded pole	$t_{se} := 0.375\text{in}$	
Average outer diameter of upper pole within slip joint	$d_{su} := 16\text{in} - \text{Taper} \cdot 12\text{in}$	$d_{su} = 15.86\text{in}$
Wall thickness of upper pole	$t_{su} := 0.375\text{in}$	
Yield strength	$F_{sy} := 65.2\text{ksi}$	
Tensile strength	$F_{su} := 79.4\text{ksi}$	

### Through-Bolt Properties

Bolt type	A307 Grade A	
Ultimate bolt tensile stress	$F_{ub} := 90.9\text{ksi}$	
Nominal bolt tensile stress	$F_{nt} := 0.75 \cdot F_{ub}$	AISC Table J3.2
Nominal bolt shear stress (bearing connections)	$F_{nv} := 0.40F_{ub}$	AISC Table J3.2
Diameter of through-bolt	$d_b := 1.25\text{in}$	
Nominal area of through-bolt	$A_b = 1.23\text{in}^2$	
Number of through-bolts in connection	$n := 3$	
Number of shear planes per bolt interaction	$N_s := 1$	

#### A.2.1 Analysis of Shear Strength

The first step in determining the strength of any bolted connection is to determine the type of bolted connection and compare the shear strength and the bearing strength. The determination of the shear strength of the connection is calculated according to the following AASHTO specification:

### 6.13.2.7 - Shear Resistance (Assume threads in the shear plane)

Nominal shear resistance per bolt interaction	$R_{ns} := 0.38 \cdot A_b \cdot F_{ub} \cdot N_s$ $R_{ns} = 42.5 \text{ kip}$
Nominal shear resistance for the entire connection	$R_{nsc} := 2 \cdot n \cdot R_{ns}$ $R_{nsc} = 254.9 \text{ kip}$

As a point of comparison, the shear strength is also calculated using the specifications for bolted connections in the AISC steel manual.

### Chapter J, Section J3.6 - Shear Strength (Pretensioned bolts - assume threads in shear plane)

Nominal shear resistance per bolt interaction	$R_{ns} := A_b \cdot F_{nv} \cdot N_s$ $R_{ns} = 44.7 \text{ kip}$
Nominal shear resistance for the entire connection	$R_{nsc} := 2 \cdot n \cdot R_{ns}$ $R_{nsc} = 268.3 \text{ kip}$

Since the values of the two calculations differ by only about 5 percent and the AISC code specifically denotes this calculation for pretensioned bolts, the AASHTO value was used for the shear capacity of the connection.

## A.2.2 Analysis of Bearing Strength

An alternate failure mode for bolted connection is due to bearing on the connected material. The AASHTO specification determines the bearing strength of a bolted connection by:

### 6.13.2.9 - Bearing Resistance at Bolt Holes

#### Nominal Bearing Resistance Calculations

Nominal bearing resistance of bolt holes (clear and end distances $> 2.0 \times \Phi_{\text{bolt}}$ )	$R_{nb} := 2.4 \cdot d_b \cdot t_{se} \cdot F_{su}$ $R_{nb} = 89.3 \text{ kip}$
Nominal bearing resistance for the entire connection	$R_{nbc} := 2 \cdot n \cdot R_{nb}$ $R_{nbc} = 536 \text{ kip}$

This value is again compared with the bearing strength determined from the AISC steel manual.

*Chapter J, Section J3.10 - Bearing Resistance at Bolt Holes*

Clear distance in the direction of force

$$L_c := \pi \cdot \left( \frac{d_{se}}{2} \right) - \left( d_b + \frac{1}{16} \text{in} \right)$$
$$L_c = 22.2 \text{in}$$

*Nominal Bearing Resistance Calculations*

Nominal bearing resistance of bolt holes

$$R_1 := 1.2 \cdot L_c \cdot t_{se} \cdot F_{su} \quad R_1 = 793.5 \text{ kip}$$

$$R_2 := 2.4 \cdot d_b \cdot t_{su} \cdot F_{su} \quad R_2 = 89.3 \text{ kip}$$

$$R_{nb} := \text{if}(R_1 \leq R_2, R_1, R_2)$$

$$R_{nb} = 89.3 \text{ kip}$$

$$R_{ntbc} := 2 \cdot n \cdot R_{nb}$$

$$R_{ntbc} = 536 \text{ kip}$$

The values from both specifications are the same. In addition to this bearing resistance, the AISC code has an additional bearing consideration for bolt bearing on the thin walls of HSS sections, which are similar to the tapered poles used in this design.

*Part 7, AISC pg. 7-13 - Special Consideration for HSS Bolt Bearing*

*Nominal Bearing Resistance Calculations*

Nominal bolt bearing per through-bolt on HSS

$$R_{ntb} := 1.8 \cdot F_{sy} \cdot d_b \cdot t_{se}$$

$$R_{ntb} = 55 \text{ kip}$$

Nominal bolt bearing per through-bolt on HSS

$$R_{ntbc} := 2 \cdot n \cdot R_{ntb}$$

$$R_{ntbc} = 330.1 \text{ kip}$$

Taking all of these values into consideration, the controlling failure mode for the through-bolted component of the tapered bolted slip base design is shear strength of the bolts. Therefore, the AASHTO shear strength is used to determine the predicted failure load of the test apparatus under torsional loading. Since it is most desirable to have the through-bolts fail in shear prior to any other structural failure, the predicted applied failure load for the through-bolts should be less than the predicted failure obtained from the analysis of the tapered steel poles.



Solve for the expected failure load taking into account the location of the shear plane based on an average diameter of the slip joint region, the torsional moment arm, and the total shear resistance of the bolts in the connection.

Torsional moment arm

$$T_{\text{arm}} := 9\text{ft}$$

Total shear resistance contributed by through-bolts

$$R_{\text{nsc}} = 254.9\text{ kip}$$

Average diameter of shear plane in slip joint region

$$d_{\text{se}} = 14.97\text{ in}$$

Torsional resistance

$$T_{\text{b}} := \frac{R_{\text{nsc}} \cdot d_{\text{se}}}{2}$$

$$T_{\text{b}} = 159\text{ ft}\cdot\text{kip}$$

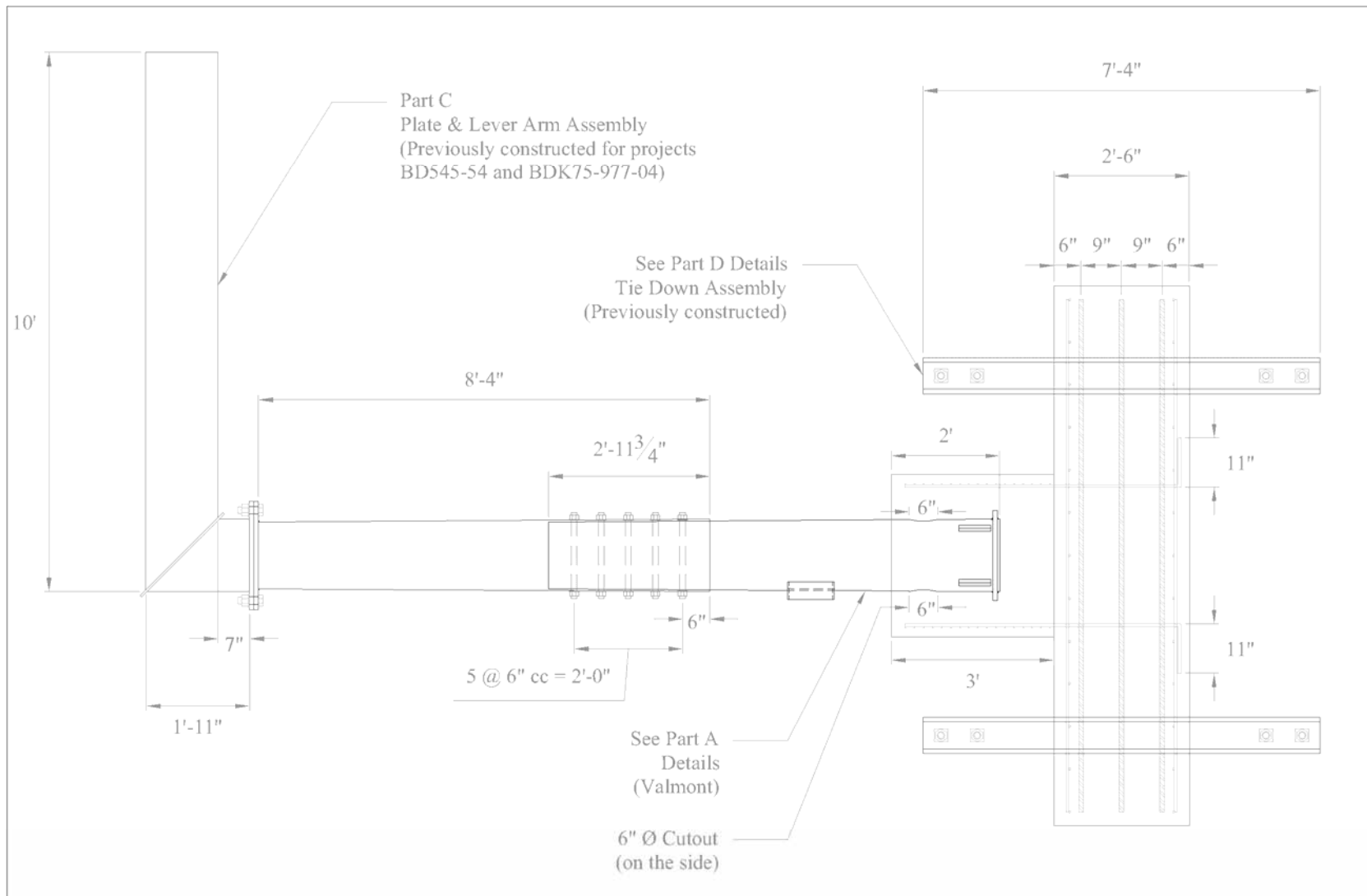
Predicted failure load at lever arm

$$P := \frac{T_{\text{b}}}{T_{\text{arm}}}$$

$$P = 17.7\text{ kip}$$

## APPENDIX B CONSTRUCTION DRAWINGS

The drawings that follow were submitted to the Florida Department of Transportation (FDOT) Marcus H. Ansley Structures Research Center in Tallahassee, Florida for construction of the test apparatus. The dimensions indicated on the drawings, particularly those related to the length of the slip joint and location and spacing of the through-bolts, may not reflect the dimensions of the assembled test apparatus. Due to the variable nature of the fit of the slip joint connection and the decision not to use jacking forces to obtain a specific slip joint splice length, the design was adjusted as required during the assembly process.





	Project Investigator: <b>R. A. Cook</b>	<b>Top View - Test Apparatus</b>	Date of Last Revision: <b>6-9-2011</b>	
	Project Manager: <b>A. Pavlov</b>		<b>BDK75 977-32: Base Connections for Signal/Sign Structures</b>	

Figure B-1. Top view of test apparatus

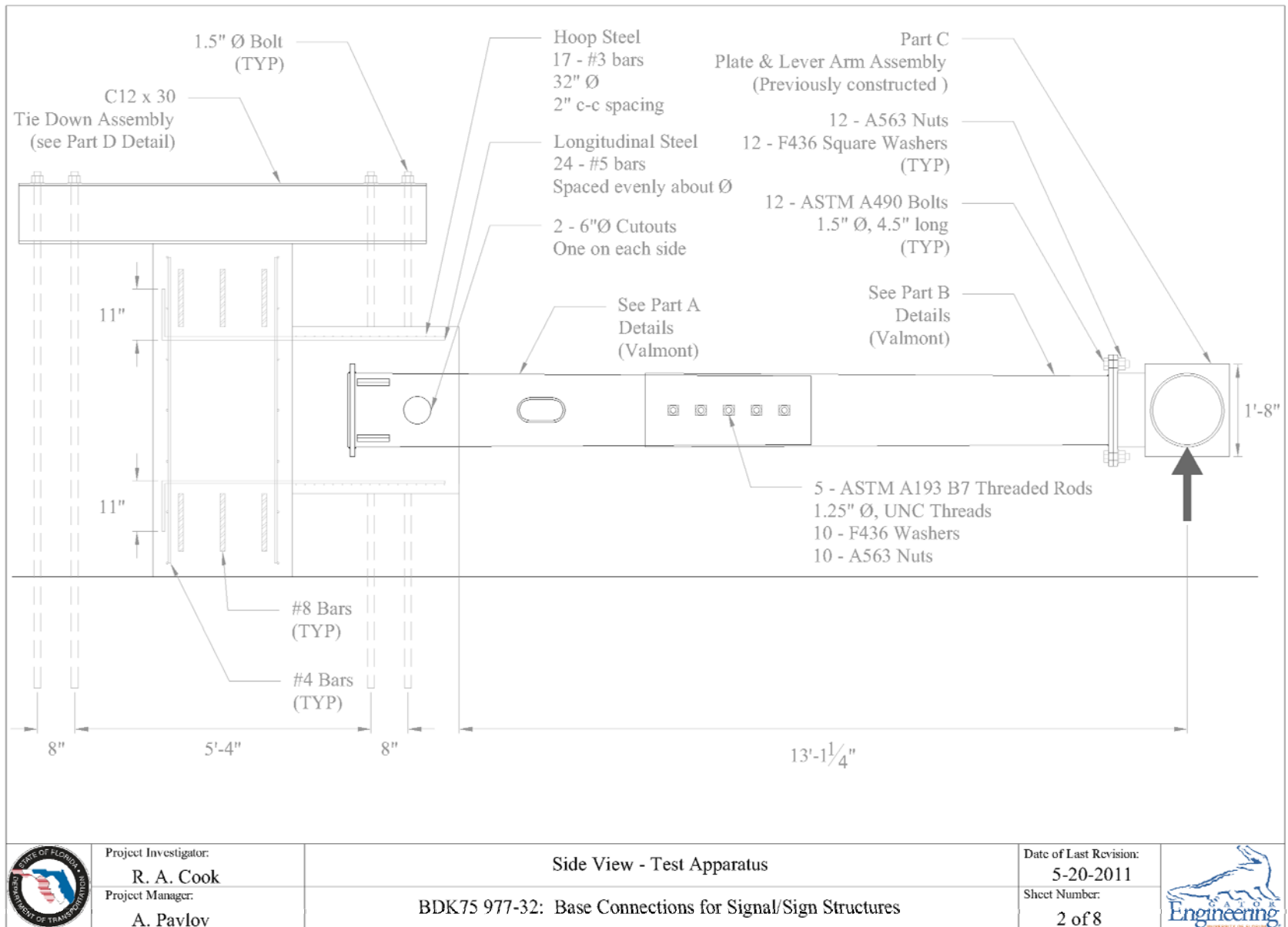


Figure B-2. Side view of test apparatus

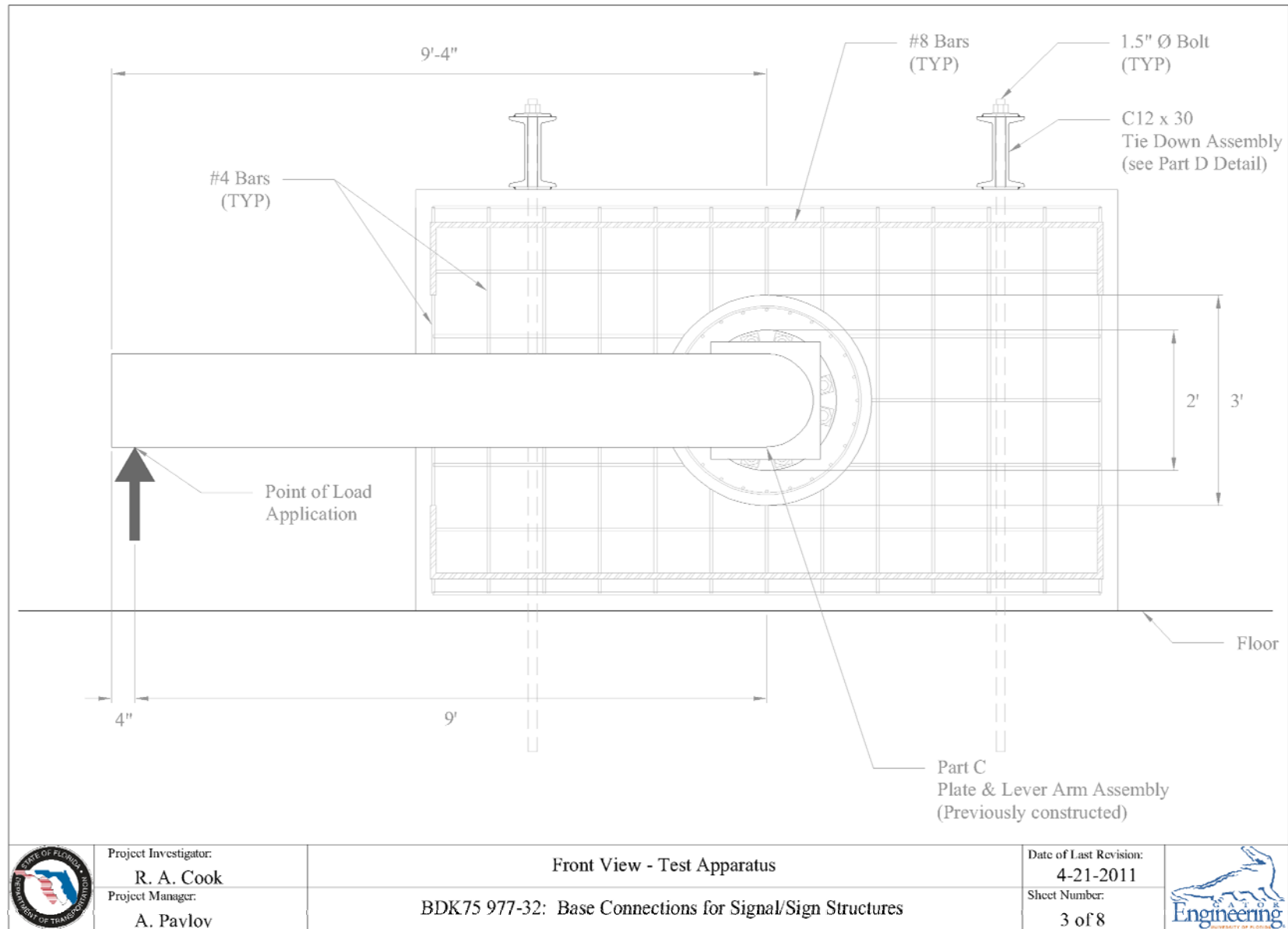


Figure B-3. Front view of test apparatus

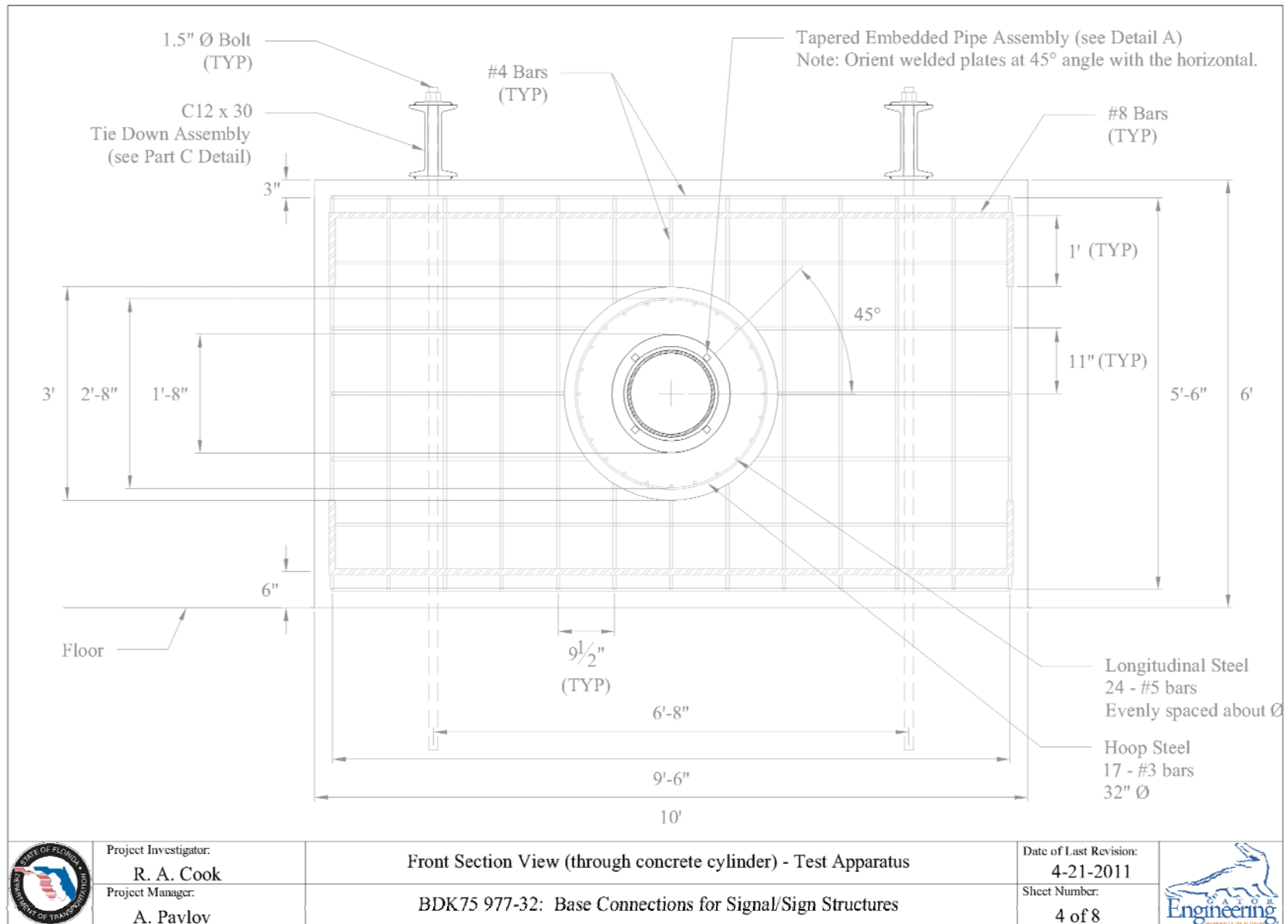


Figure B-4. Section view through the concrete pedestal

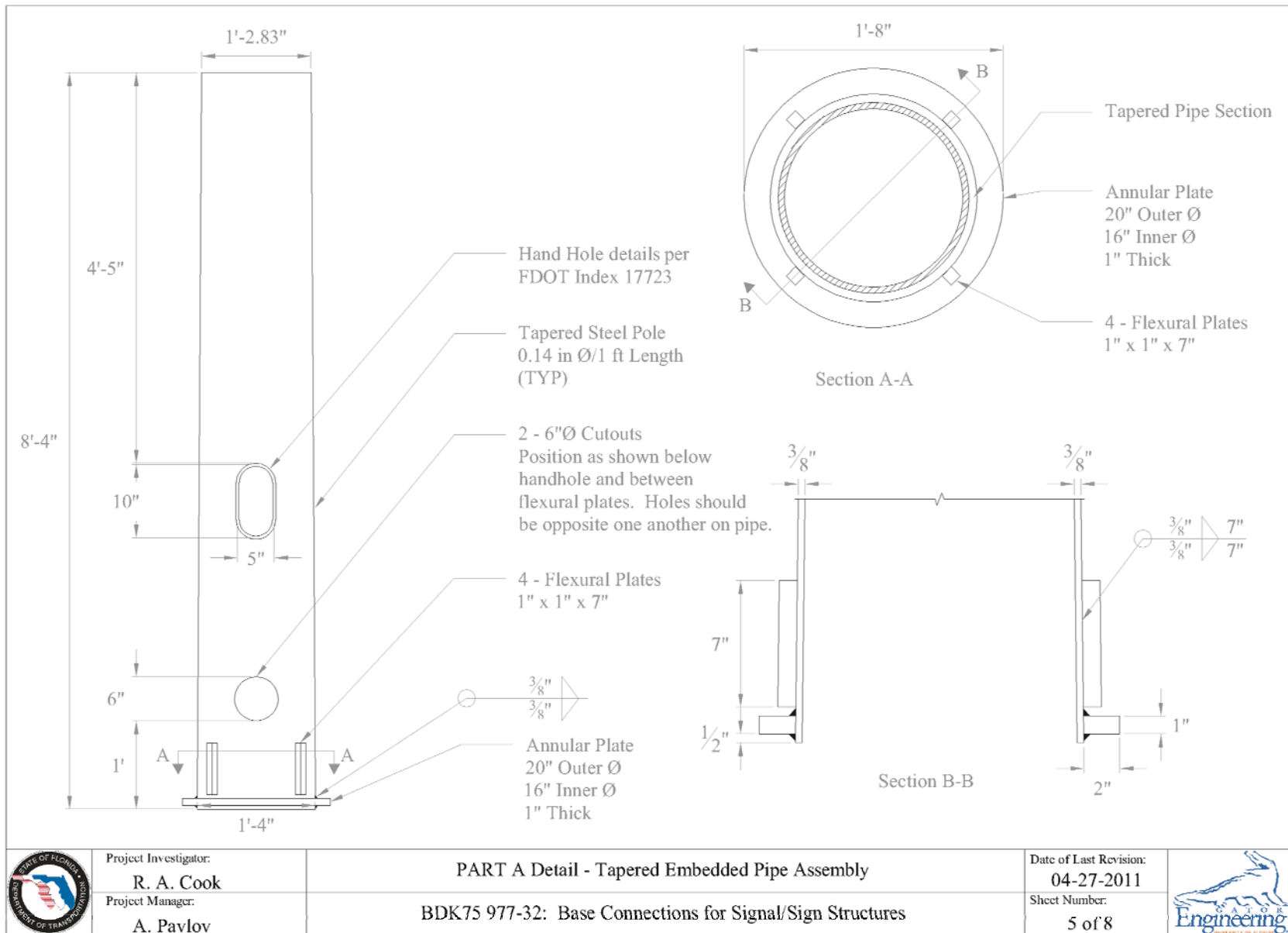


Figure B-5. Detail of the embedded pole with torsional and flexural plates

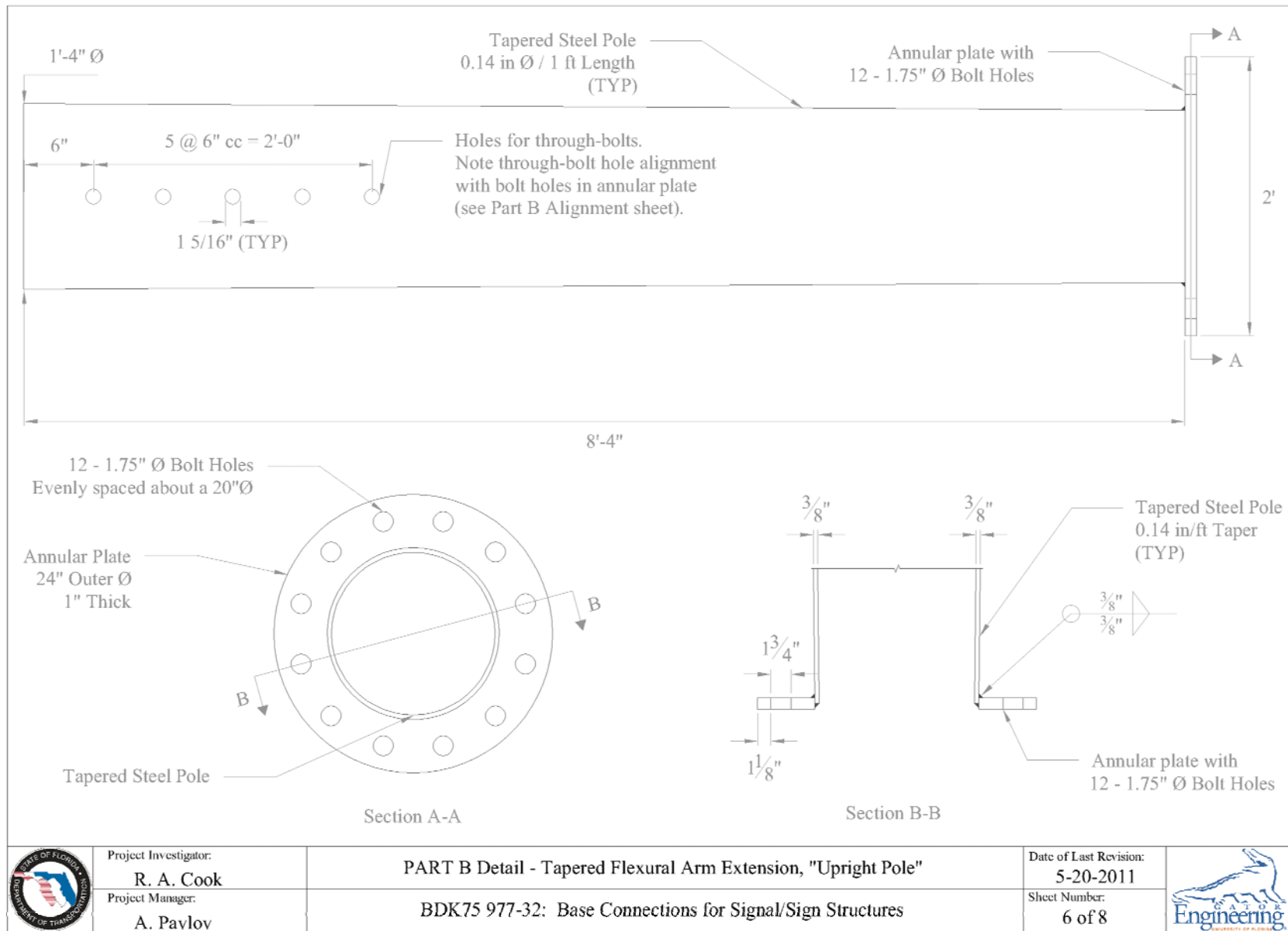


Figure B-6. Detail of the outer pole member



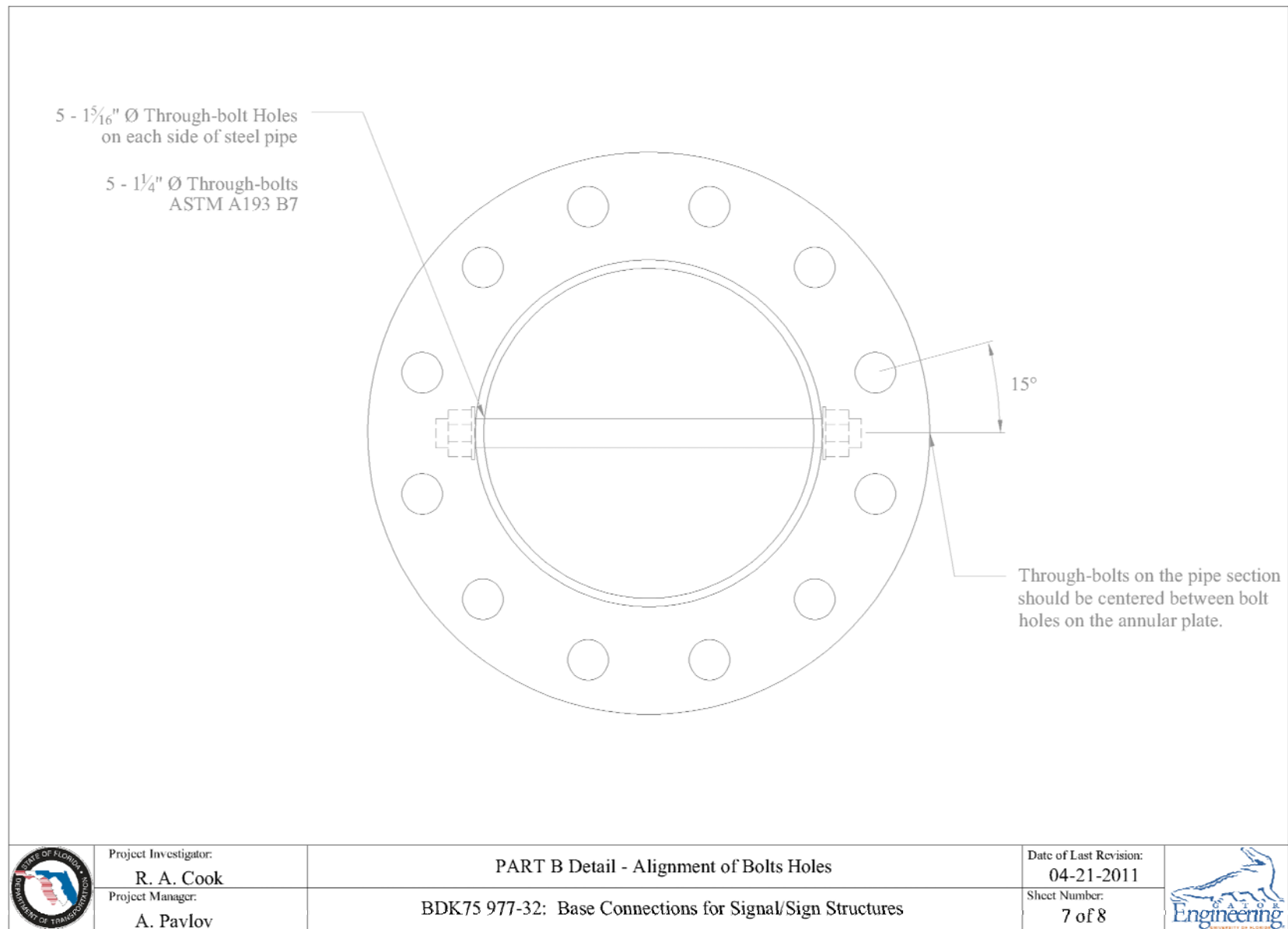
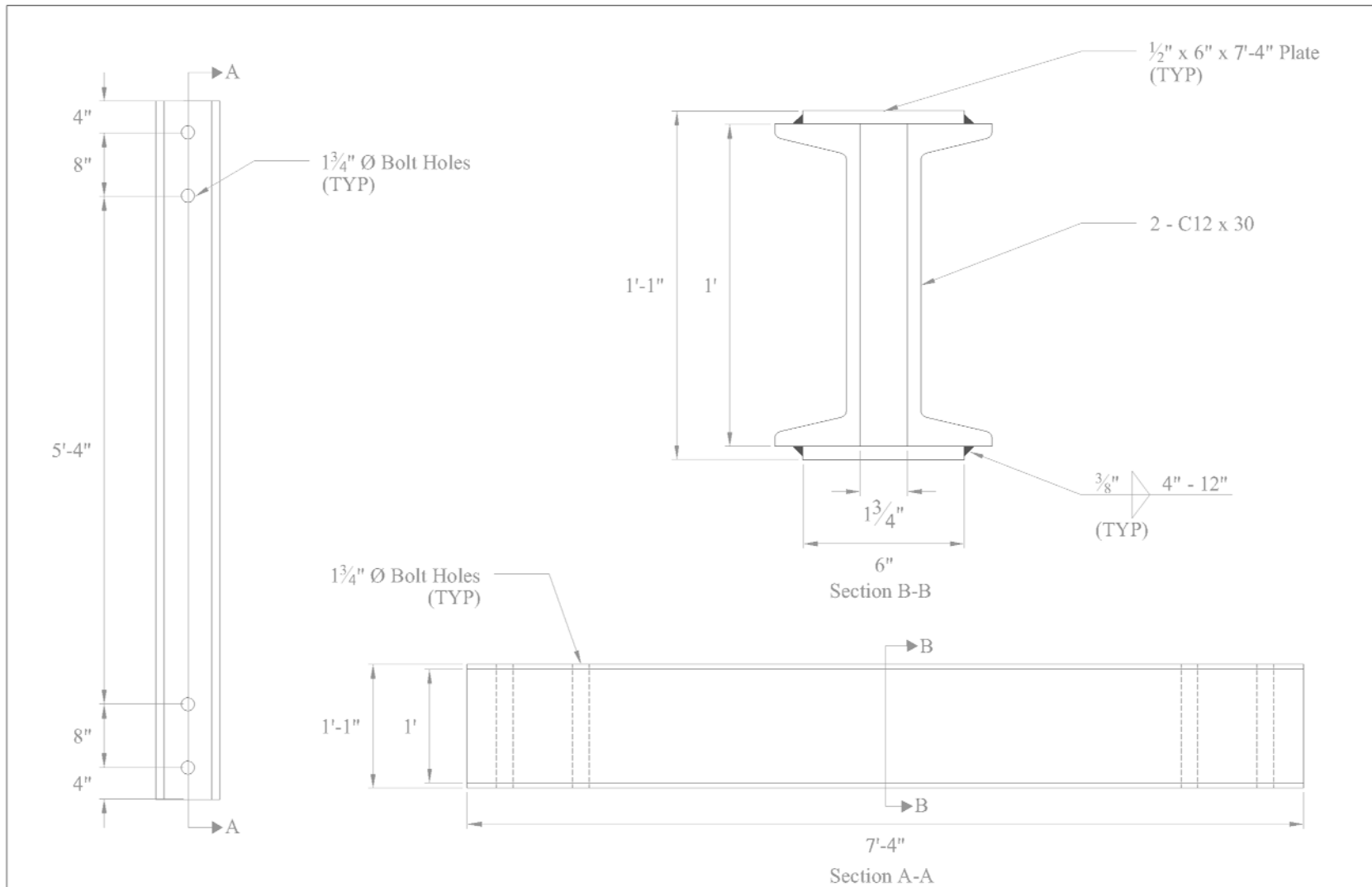


Figure B-7. Detail of the flange plate at the end of the tapered pole





	Project Investigator: R. A. Cook	<b>PART D Detail - Tie Down Assembly (previously constructed by FDOT)</b>  <b>BDK75 977-32: Base Connections for Signal/Sign Structures</b>	Date of Last Revision: 3-29-2011	
	Project Manager: A. Pavlov		Sheet Number: 8 of 8	

Figure B-8. Detail of the tie-down assembly

## APPENDIX C INSTRUMENTATION

The drawings that follow were submitted to the Florida Department of Transportation (FDOT) Marcus H. Ansley Structures Research Center in Tallahassee, Florida to indicate the type and location of instruments required for monitoring the behavior of the tapered bolted slip base connection. The dimensions of the slip joint shown are based on the actual dimensions of the assembled base connection. They differ from the originally specified dimensions of the construction drawings due to the variable nature of how the pole sections fit together.

The labeling system of the torsional strain gauges was modified from the drawings that follow to accommodate the labeling system used by the FDOT. For instance, the rosette gauge labeled TG1-3 was changed to TG1\_0, TG1\_45, and TG1\_90 where the first number indicates the location of the rosette gauge nearest the lever arm assembly and the second number indicates the angle measured from the longitudinal axis of the test pole to the longitudinal axis of the respective strain gauge in the rosette. Rosette gauges on the right side were changed to indicate location numerals 1 through 6, while rosette gauges on the left side correspond to location numerals 7 through 12. The location on each face of the slip joint is numbered in increasing order following the load path from the lever arm to the concrete pedestal.



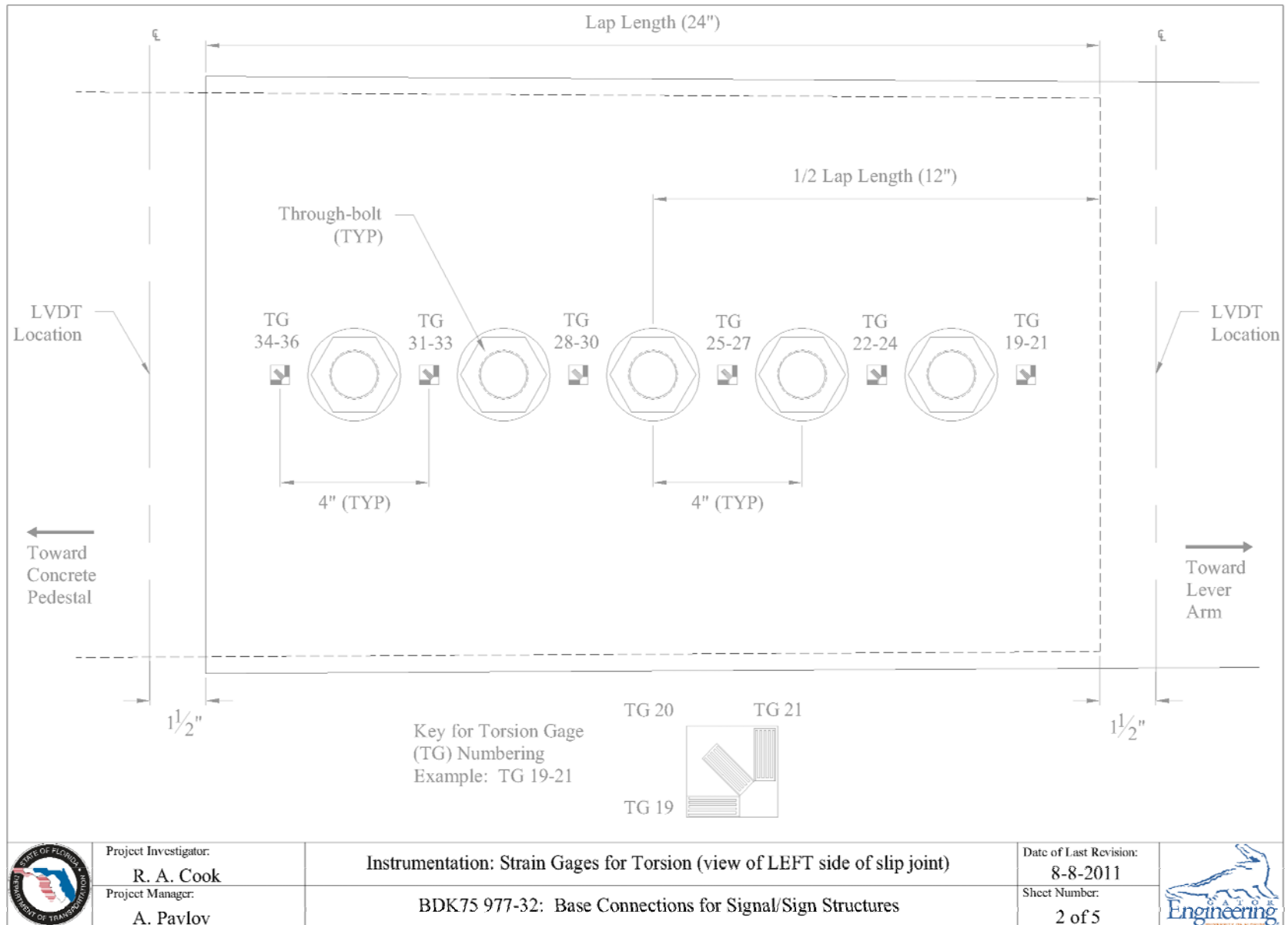


Figure C-2. Diagram of rosette strain gauges on the left face of the slip joint

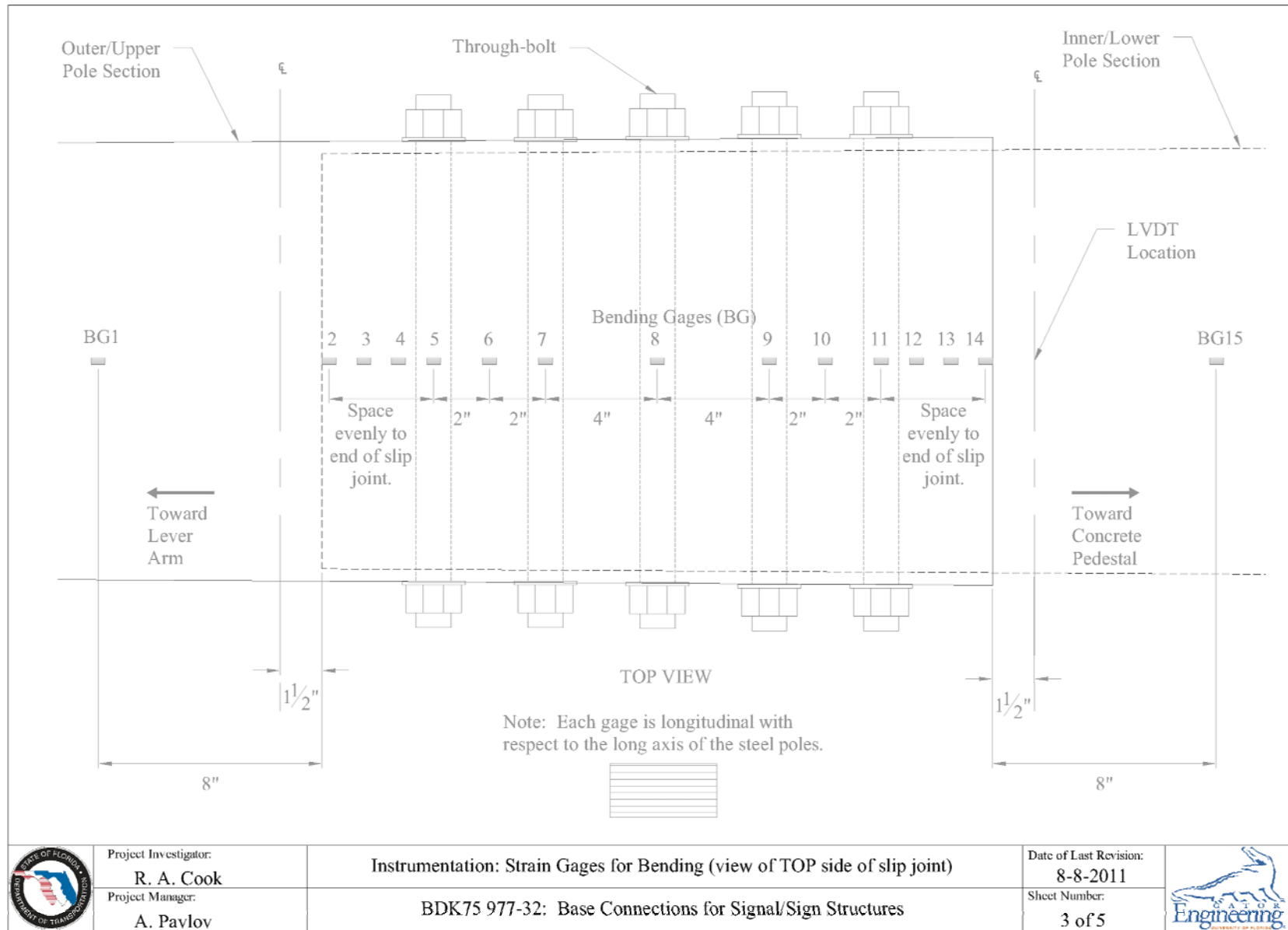


Figure C-3. Diagram of linear strain gauges on the upper face of the slip joint

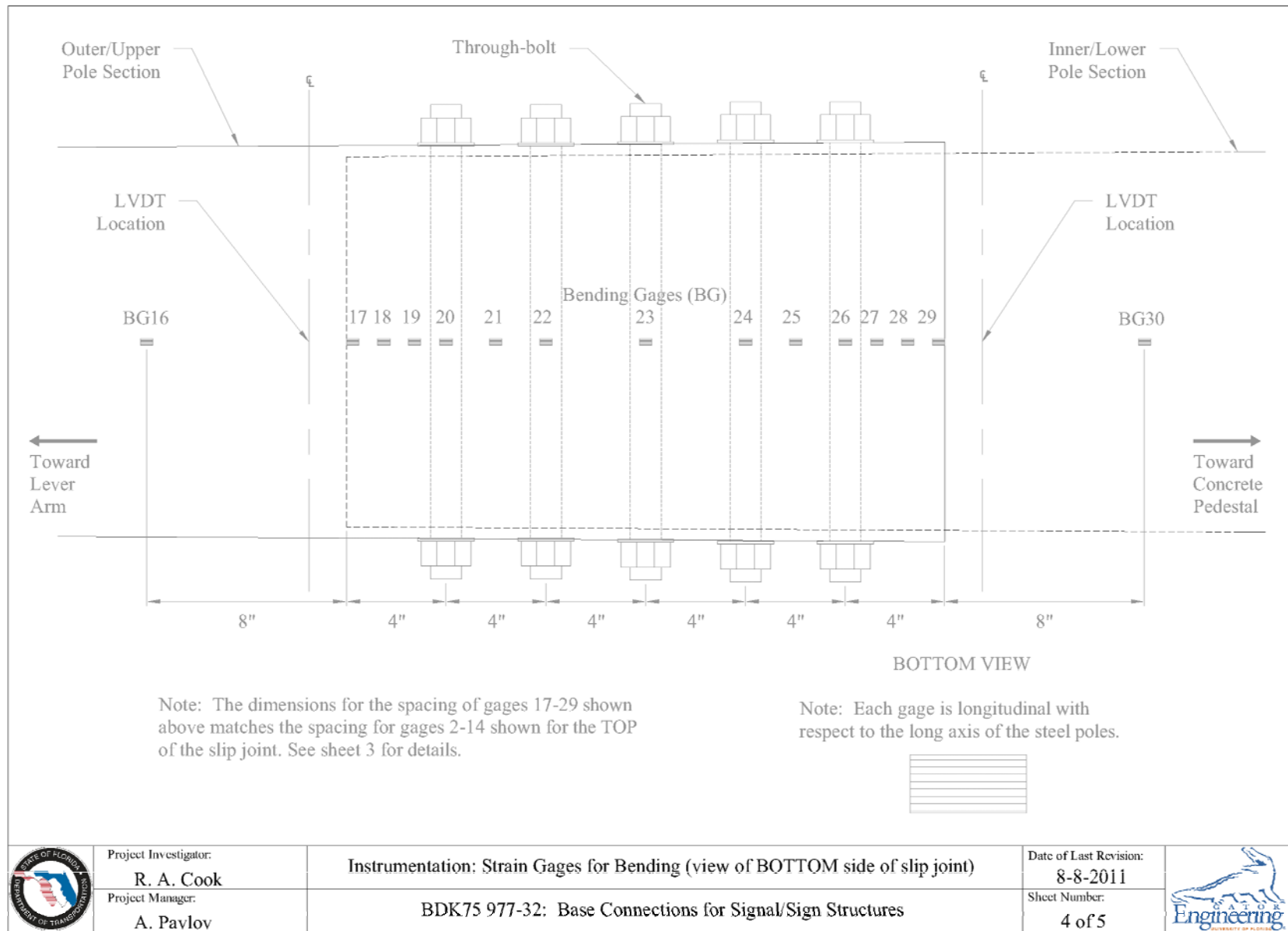


Figure C-4. Diagram of linear strain gauges on the bottom face of the slip joint

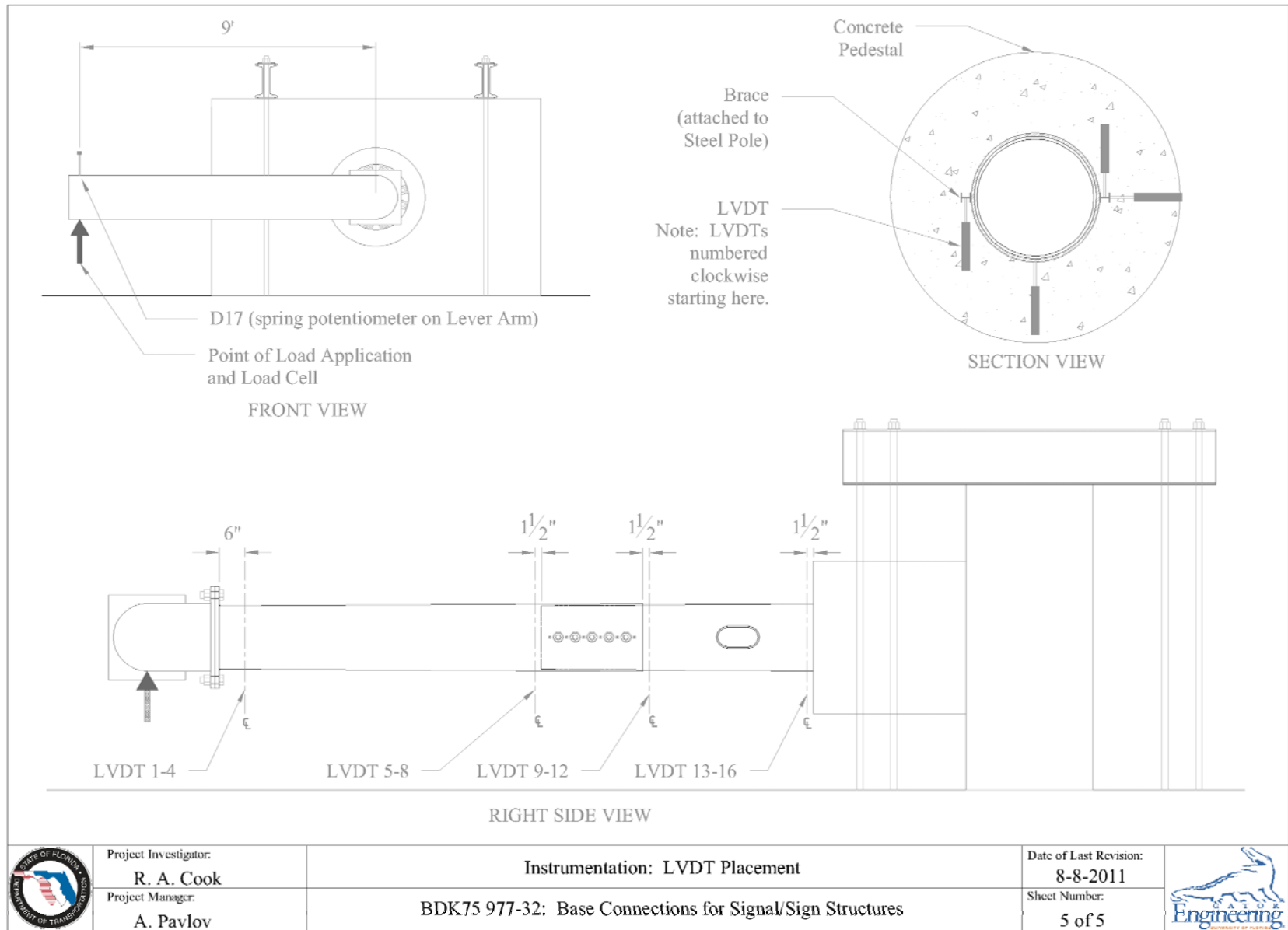


Figure C-5. Diagram of LVDT placement and orientation along test apparatus



APPENDIX D  
ACCOUNTING FOR FRICTION IN THE SLIP JOINT

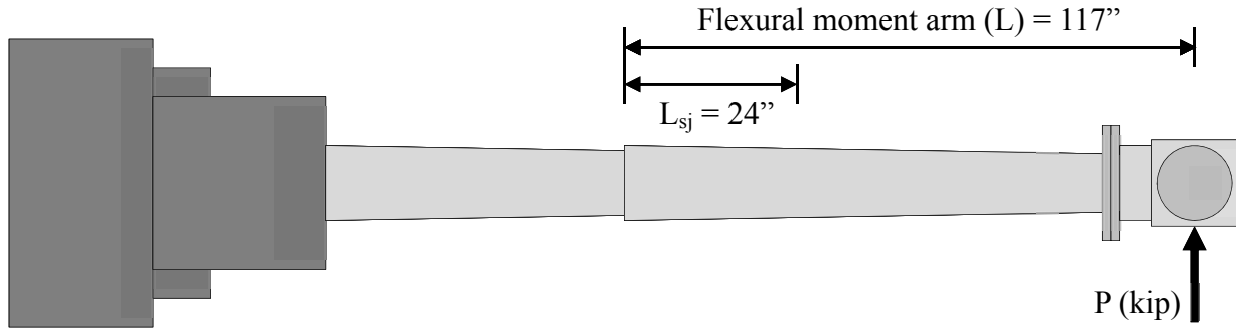


Figure D-1. Side view of test apparatus with select dimensions

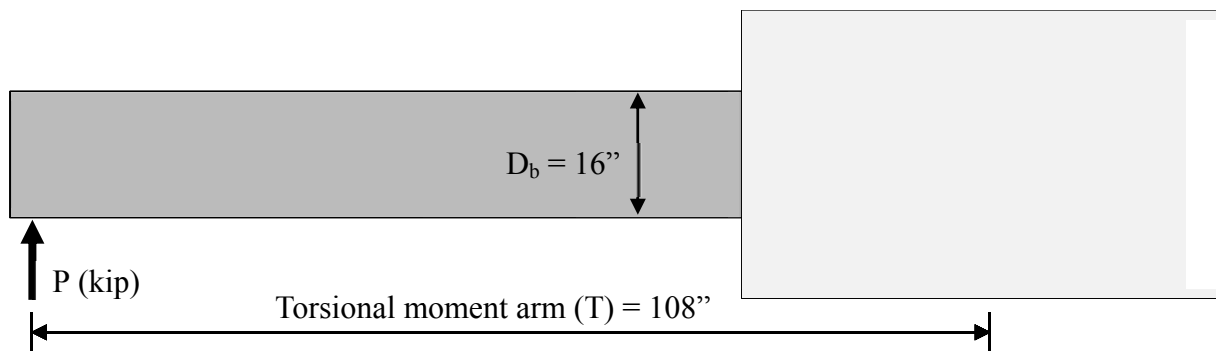


Figure D-2. Front view of test apparatus with slip joint section and dimensions

**Test Apparatus Information**

Length of torsion arm	$T := 9\text{ft}$	$T = 108\text{ in}$
Length of moment arm to base of upper pole	$L := 9.75\text{ft}$	$L = 117\text{ in}$
Length of tapered pole	$l := 100\text{in}$	
Taper of poles	$\text{Taper} := 0.14\text{in} \div \text{ft}$	
Length of slip joint	$L_{sj} := 24\text{in}$	
Base diameter of tapered pole	$D_b := 16\text{in}$	
Average diameter of shear plane in slip joint region	$D := D_b - \text{Taper} \cdot \left(1 - \frac{L_{sj}}{2}\right)$	$D = 14.973\text{ in}$

### Through-bolt Information

Ultimate tensile strength	$F_{ut} := 90.9 \text{ ksi}$
Number of through-bolts	$n_b := 3$
Diameter of through-bolts	$d_b := 1.23 \text{ in}$
Threads per inch	$n := 7 \div \text{in}$
Gross cross-sectional area	$A_g := 1.23 \text{ in}^2$
Effective tensile stress area	$A_{se} := 0.7854 \cdot \left( d_b - \frac{0.9743}{n} \right)^2 \quad A_{se} = 0.969 \text{ in}^2$

### D.1 Evaluation for Flexure

There are two ways to analyze the flexural transfer of load through the slip joint. The first method assumes the poles remain perfectly rigid and that the forces are transferred at concentrated points at either end of the slip joint. The second method assumes the poles are allowed to deform and that the forces are transferred along some length of the slip joint.

#### D.1.1 Flexural Analysis Assuming Concentrated Point Loads on Slip Joint

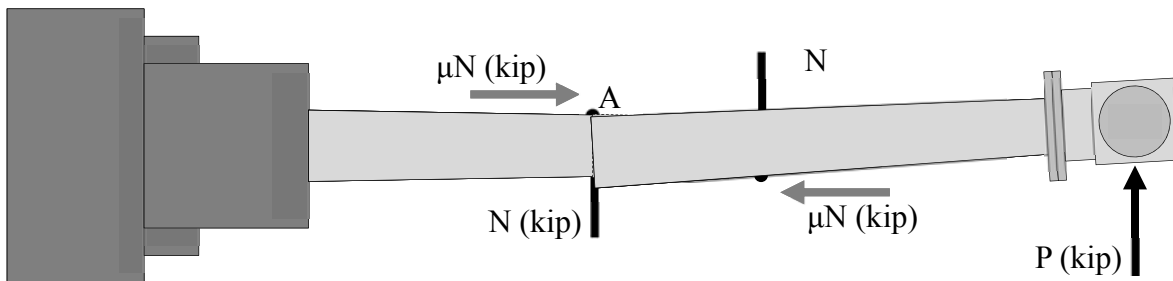


Figure D-3. Concentrated internal couple transferring applied load through slip joint

Sum moments for the outer pipe about point A:

$$P L - N L_{sj} - \mu N D = 0$$

$$N (L_{sj} + \mu D) = P L$$

$$N = P L / (L_{sj} + \mu D)$$

$$N/P = L / (L_{sj} + \mu D)$$

Solve for the ratio of  $N/P$ , denoted  $N_p$ , as a function of the coefficient of friction,  $\mu$ :

$$N_p(\mu) := \frac{L}{L_{sj} + \mu \cdot D}$$

Results for specific values of coefficient of friction:  $N_P(0) = 4.875$   
 $N_P(0.45) = 3.806$   
 $N_P(0.8) = 3.252$

### D.1.2 Flexural Analysis Assuming Distributed Loads along Slip Joint

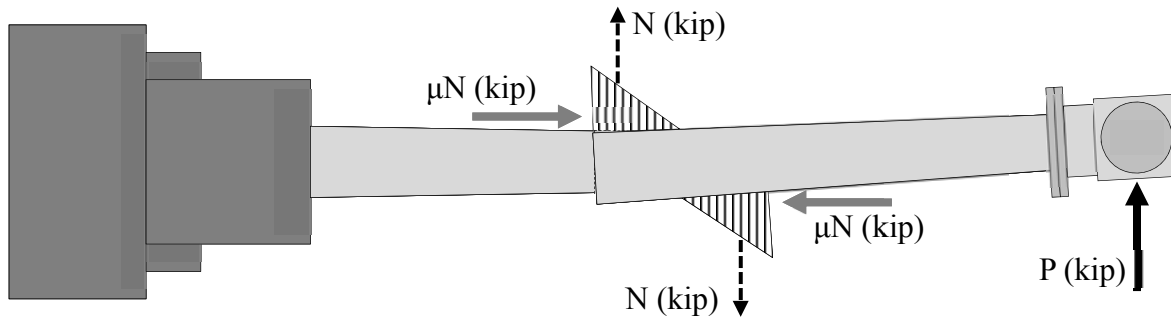


Figure D-4. Distributed internal couple transferring applied load through slip joint

#### Distributed load information

Length of triangularly distributed load:  $L_d := L_{sj} \div 2$   $L_d = 12 \text{ in}$   
Distance from maximum load to resultant force:  $d := L_d \div 3$   $d = 4 \text{ in}$

Sum moments for the outer pipe about point A:  
 $P L - N (L_{sj} - 2d) - \mu N D = 0$   
 $N (L_{sj} - 2d + \mu D) = P L$   
 $N = P L / (L_{sj} - 2d + \mu D)$   
 $N/P = L / (L_{sj} - 2d + \mu D)$

Solve for the ratio of  $N/P$ , denoted  $N_P$ , as a function of the coefficient of friction,  $\mu$ :

$$N_{Pd}(\mu) := \frac{L}{L_{sj} - 2d + \mu \cdot D}$$

Results for specific values of coefficient of friction:  $N_{Pd}(0) = 7.313$   
 $N_{Pd}(0.45) = 5.146$   
 $N_{Pd}(0.8) = 4.182$

## D.2 Evaluation for Torsion

Within the slip joint, both the through-bolts and friction resist the torsion generated by the applied load. The shear resistance of the through-bolts is determined using the AASHTO (2010) specifications for bolted connections. The torsional analysis uses the values of the resultant

forces within the slip joint region to assess the contribution of friction to the resistance of the applied load.

### D.2.1 Predicted Shear Resistance of Through-bolts

The following value represents the shear resistance provided by one bolt reaction as specified by the AASHTO (2010).

AASHTO Bolt Shear Equation:  $V_b := 0.38 \cdot A_g \cdot F_{ut}$        $V_b = 42.487 \text{ kip}$

### D.2.2 Predicted Applied Load

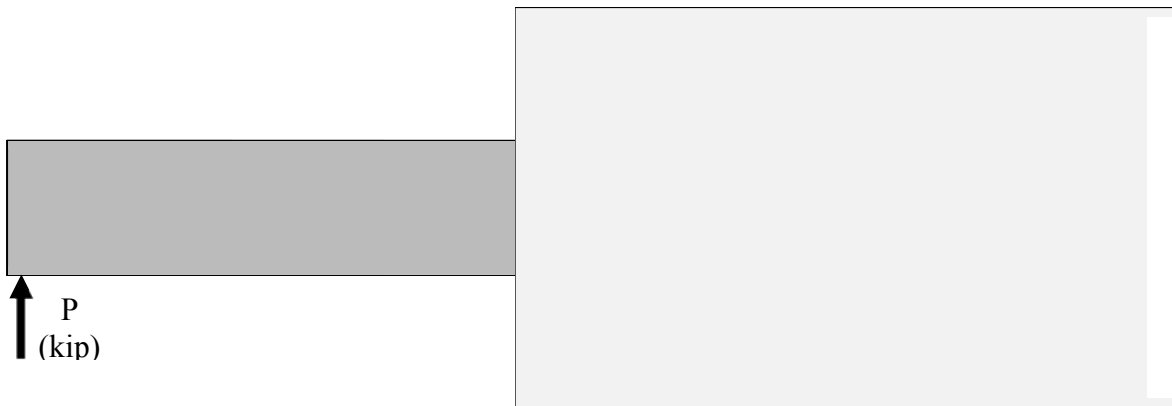


Figure D-5. Frictional and bolt shear resistance to torsion

The value of the normal force (N) is determined for a range of coefficients of friction ( $\mu$ ) based on the flexural analysis above. Depending on the type of load, whether concentrated or distributed, the appropriate expression for  $N_p$  from the flexural analysis above can be inserted below. The total number of through-bolts ( $n_b$ ) in the slip joint is incorporated into the following set of equations, because each one contributes to the total resistance of the applied load.

Sum moments about the center of the pole at point B:

$$\begin{aligned} n_b D V_b - T P + \mu N D &= 0 \\ n_b D V_b - T P + \mu(N_p P) D &= 0 \\ P(T - \mu N_p D) &= n_b D V_b \\ P &= n_b D V_b / (T - \mu N_p D) \end{aligned}$$

$$P(\mu) := \left( \frac{n_b \cdot D}{T - \mu \cdot N_p(\mu) \cdot D} \right) \cdot V_b$$

Results for specific values of coefficient of friction:

$P(0) = 17.7 \text{ kip}$   
 $P(0.45) = 23.2 \text{ kip}$   
 $P(0.8) = 27.6 \text{ kip}$

The results of the frictional analysis are summarized in the graph below. As can be determined from these results, the presence of friction in the slip joint increases the magnitude of the applied load that can be transferred through the slip joint.

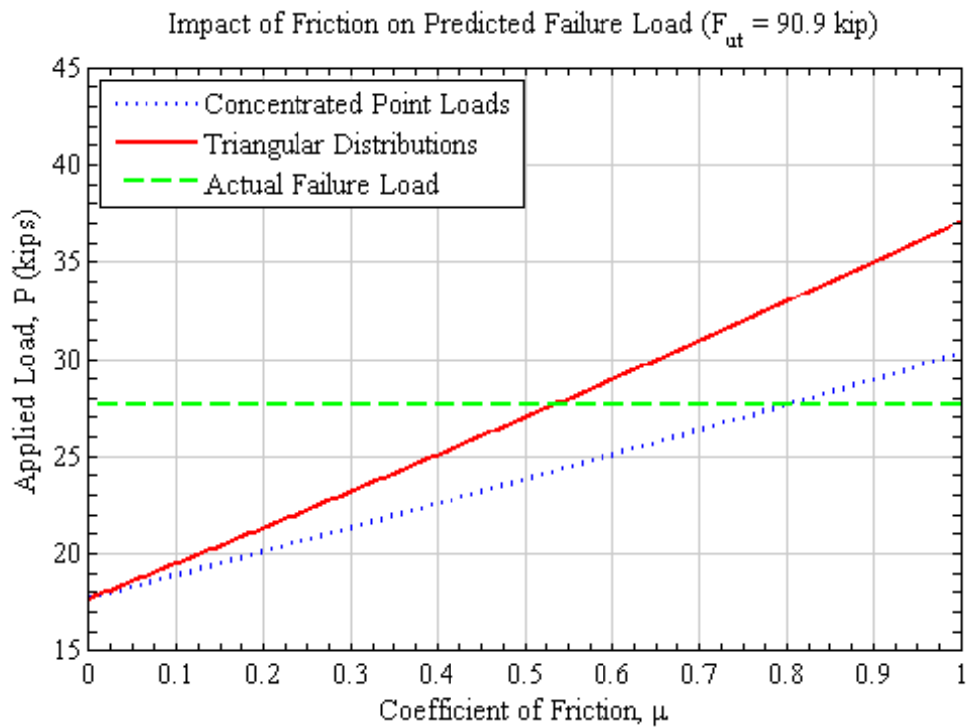


Figure D-6. Plot of the impact of friction on predicted applied load